Biophysics Reviews

REVIEW ARTICLE | MARCH 25 2025

The mechanobiology of biomolecular condensates

Special Collection: Biomolecular Phase Transitions and the Mechanochemical Control of Cells in Health & Disease

Neus Sanfeliu-Cerdán ; Michael Krieg

Biophysics Rev. 6, 011310 (2025)
https://doi.org/10.1063/5.0236610

Biophysics Reviews REVIEW pubs.aip.org/aip/bpr

The mechanobiology of biomolecular condensates

Cite as: Biophysics Rev. **6**, 011310 (2025); doi: 10.1063/5.0236610
Submitted: 1 September 2024 · Accepted: 10 February 2025 ·
Published Online: 25 March 2025

Neus Sanfeliu-Cerdán and Michael Krieg[a)]

AFFILIATIONS

ICFO - Institut de Ciències Fotòniques, Castelldefels, The Barcelona Institute of Science and Technology, Barcelona, Spain

Note: This paper is part of the BPR Special Topic on Biomolecular Phase Transitions and the Mechanochemical Control of Cells in Health & Disease.
[a)]**Author to whom correspondence should be addressed:** michael.krieg@icfo.eu

ABSTRACT

The central goal of mechanobiology is to understand how the mechanical forces and material properties of organelles, cells, and tissues influence biological processes and functions. Since the first description of biomolecular condensates, it was hypothesized that they obtain material properties that are tuned to their functions inside cells. Thus, they represent an intriguing playground for mechanobiology. The idea that biomolecular condensates exhibit diverse and adaptive material properties highlights the need to understand how different material states respond to external forces and whether these responses are linked to their physiological roles within the cell. For example, liquids buffer and dissipate, while solids store and transmit mechanical stress, and the relaxation time of a viscoelastic material can act as a mechanical frequency filter. Hence, a liquid–solid transition of a condensate in the force transmission pathway can determine how mechanical signals are transduced within and in-between cells, affecting differentiation, neuronal network dynamics, and behavior to external stimuli. Here, we first review our current understanding of the molecular drivers and how rigidity phase transitions are set forth in the complex cellular environment. We will then summarize the technical advancements that were necessary to obtain insights into the rich and fascinating mechanobiology of condensates, and finally, we will highlight recent examples of physiological liquid–solid transitions and their connection to specific cellular functions. Our goal is to provide a comprehensive summary of the field on how cells harness and regulate condensate mechanics to achieve specific functions.

TABLE OF CONTENTS

I. SIGNIFICANCE STATEMENT

Mechanobiology aims to understand how mechanical forces and the material properties of cellular structures influence biological functions. Biomolecular condensates, which exhibit varying material properties and exert forces due to capillary effects, unite various principles of mechanobiology. The ability of condensates to transition between liquid and solid states, and vice versa, suggests that they play crucial roles in processes such as force transmission, signal transduction, and cellular response to forces. Through their interactions with the cytoskeleton, condensates contribute to force generation and enable cells to sense and adapt to mechanical changes in their environment. Understanding their role in mechanobiology not only reveals fundamental aspects of cell physiology but also opens new avenues for addressing diseases influenced by mechanical stress and cellular mechanics. The principles outlined here are universal and provide a unique stepping stone into the diverse and multifaceted mechanobiology of condensates for an interdisciplinary audience. By synthesizing current knowledge, we shed light on the intricate relationship between molecular compartmentalization and mechanical forces and highlight areas of future research in this rapidly advancing field.

II. INTRODUCTION

Mechanobiology explores how cells, tissues, and animals sense and respond to mechanical forces within their microenvironment, a process that is integral to various physiological phenomena, including cell migration,[1] tissue development, and differentiation,[2,3] and the response to touch and proprioception.[4,5] Understanding how physical forces interact with biological systems is essential for advancing our knowledge of cellular functions[6] and their roles in disease.[7] Mechanotransduction is not restricted to the cell periphery but occurs anywhere in the cell, e.g., subcellular organelles, including the nucleus,[8] endoplasmic reticulum, and mitochondria,[9] but also membrane-less organelles respond to forces[10] and participate in the mechanotransduction of internal and external mechanical stress.[11]

Membrane-less organelles are cellular compartments, or biomolecular condensates, that can form through various mechanisms. These include liquid–liquid phase separation mediated by multivalent or monovalent interactions of RNA or proteins that may contain intrinsically disordered domains,[12,13] but it has also been proposed to involve ordered cooperative assembly driven by allosteric regulation,[14] site-specific interactions between highly conserved binding partners with high affinities,[15] and phase separation coupled with percolation processes.[16] In addition, active processes driven by cell contractility,[10] active fluid demixing,[17] and ATP-consuming chemical reactions may participate in phase separation.

Recent studies have shown that mechanical forces, such as shear stress, tension, and substrate stiffness, can drive or modify the phase separation of biomolecules as well as alter the fusion/fission dynamics, thereby influencing condensate function. In contrast, condensates themselves have been implicated in the regulation of cellular mechanical properties, including stiffness and adhesion, contributing to processes such as mechanotransduction and cellular adaptability to external stressors. Condensation may also indirectly affect mechanobiological functions, e.g., through the organization of membrane receptors and ion channels,[18] activation of mechanically active transcription factors through chromatin reorganization, and also the favor of cytoskeletal organization leading to actin polymerization or myosin function.[19]

Many biomolecular condensates initially exhibit liquid-like viscoelastic properties but can transition to (semi)solid hydrogels or glassy states with arrested dynamics, either reversibly or irreversibly, in both *in vitro* and *in vivo* environments.[12,16,20–23] These transitions may culminate in the formation of amyloid fibrils[11,24,25] and liquid crystalline assemblies,[26] highlighting the diverse material states condensates can adopt. For example, liquid–solid or rigidity transitions have been reported, among others, in metabolic enzymes[27] and signaling proteins,[28] ion channel complexes,[11] cell-cell junctions[29,30] and within the nucleus[31,32] in different cell types of various organisms and identities, including bacteria[33] and plants.[34] Due to the chemical complexity and structural diversity of the proteins involved in the transitions, their molecular driving force and mechanical signatures are beginning to unravel just recently.[11,22,35–40] Although rigidity transitions have been investigated primarily in disease,[41] it is plausible that the liquid- and solid-like states of biomolecular condensates have separable functions in the cell. A notable insight from previous observations is the fact that the different liquid and solid phases of the same condensate can have specialized functions.[11,42,43] Likewise, many condensates, whether liquid-like or solid-like, can modulate the cell response to forces, regulate the cell's mechanical state, and alter the mechanotransduction processes. This makes them an extremely exciting subject to study in the field of mechanobiology. For example, a liquid condensate is easily deformed, which is be important when forces need to be absorbed or buffered. In contrast, a solid condensate stores mechanical energy upon compression or extension and thus is expected to transmit and resist forces when it is in the force transmission pathway in the cell.

Even complex behaviors displayed by viscoelastic materials with their rate-dependent complex shear moduli, may be important in setting an optimal timescale for such responses and can determine if stresses at a certain velocity are transmitted or dissipated. In addition to these passive processes, wetting of the membrane or cytoskeleton by liquid-like condensates can mechanically deform or remodel their surroundings due to capillary actions,[44,45] even with forces comparable to ATP-dependent motors,[46] and droplet coarsening through fusion dynamics can reposition DNA or cytoplasmic organelles. Then, the material properties of the condensates directly influence the rate and force at which this coalescence occurs, which is approximately determined by the capillary velocity γ/η, where η represents the viscosity and γ the surface tension of the condensate.

The purpose of this review is to synthesize the field of biomolecular condensates with the principles of mechanobiology. We will explore how physical forces modulate phase transition, with particular focus on not only viscoelastic maturation and liquid–solid transitions (LST) but also how condensates, in turn, influence cellular mechanics. We will first review the molecular driving forces for liquid–solid transitions and environmental variables (Fig. 1 and Box 1), such as temperature and pressure, that influence condensate maturation. We will introduce the most common material properties (Box 2) and emerging techniques to characterize them (Figs. 2 and 3) before diving into selected case studies that revealed important physiological functions of biomolecular condensates in cell biology and neuroscience (Figs. 4–6). Our intention thereby is to focus on physiologically relevant functions and refer the reader interested in pathologies ensuing from aberrant phase transition to other excellent reviews in the field.[47]

III. CONDENSATE MATURATION AND LIQUID–SOLID TRANSITIONS

A. The molecular grammar and the driving "forces" of an LST

The formation of biomolecular condensates follows well-studied principles that can be understood by their domain architecture and specific sequence code, also known as molecular grammar.[22,40,48] Similar to condensation of soluble molecules into a dense phase, the solid transition is entropically unfavored, because of the overall reduction in molecular mobility. The entropic penalty associated with the condensation of proteins in a dense phase [Fig. 1(a)] is compensated for by the release of enthalpy through weak adhesive interactions between a set of stereotypic amino acid side chains and the increase in entropy associated with the release of water coordinated to molecules in the bulk phase.[49,50] This can occur via multivalent interactions of folded domains (e.g., SH3-proline-rich motifs,[51]) or intrinsically disordered regions (IDR), particularly within low-complexity domains, via short linear motifs (SLiMs).[52,53] These interactions can be understood with stereotypic sticker–spacer models[22,54,55]—assigning stickers as the amino acid side chains (or domains) that create physical crosslinks with each other (e.g., π-cation, $\pi-\pi$ or electrostatics[39]), while spacers are defined as the segments that connect these stickers and affect the polymer's solubility and flexibility.[55–57] The sticker residues intuitively keep the condensate connected and are separated by spacer residues consisting of stretches of glycine and serine, which are important for the hydration of the stickers. As part of a common spacer motif, glycine is important in keeping the dynamic, liquid-like properties of condensates. When glycines were systematically converted to serine in the low complexity domain of heterogeneous nuclear ribonucleoprotein A1 (hnRNPA1), the maturation of the liquid to the solid state was dramatically accelerated and it was already solid a few seconds after mixing.[22]

The way sticker–spacer systems behave is marked by a combination of phase separation and the formation of interconnected networks.[16,55,58] These systems have properties that make them both elastic and fluid-like, depending on how many connections they create, the overall network they form, and how spacers impact the movement and rearrangement of these sticker residues. Therefore, not only the content and type but also the organization of the aromatic stickers determine the viscoelastic properties of the condensates.[59,60]

For example, passive rheology measurements based on optical tweezers demonstrated that when all aromatic stickers in the low-complexity domain of hnRNPA1 were systematically converted to tryptophan (strong sticker), subsequent condensates exhibited the highest viscoelasticity, while condensates with only phenylalanines (weak sticker) displayed the lowest viscoelasticity[22] [Fig. 1(b)]. Thus, stronger stickers (TRP>TYR>PHE) lead to higher storage moduli and increased elasticity.

Apart from their sequence composition, the patterning of aromatic residues within a "sea" of spacers determines the viscoelastic transition. A strong clustering of aromatic residues was found in Velo1, the scaffold protein responsible for the solid transition of the Balbiani body in oocytes.[60] The repatterning of the aromatic stickers in Velo1 consequently leads to a lower viscosity and a higher diffusivity and a homogeneous arrangement of sticker residues (aromatic or electrostatic), resulting in the most liquid condensate.[59,60]

In summary, the exact amino acid sequence, arrangements, and strength of the spacer/sticker interactions together with heterotypic interactions (Box 1) and physical constraints determine the mechanical signature of biomolecular condensates (Box 2) and whether they respond primarily as a viscoelastic liquid, viscoelastic solid, or crystalline solid [Fig. 1(c)].

1. Aggregation hotspots, LARKS, and prion-like domains

The hardening of droplets can arise through various mechanisms, including *nonequilibrium transitions*, such as the formation of glass-like amorphous states, and *equilibrium transitions*, such as the assembly of ordered fibrous amyloids. The amorphous, glass-like states are metastable and tend to relax toward thermodynamically favorable states that may result in stable cross-links.[22] This relaxation then leads either to a nonfibrillar solid state or to an ordered fibrillar structure emerging from the disordered glass.

In *equilibrium transitions*, fibers typically form through homotypic interactions involving cross-links and cross-β sheet structures[61] [Fig. 1(d)]. Many proteins containing an intrinsically disordered region (IDR), such as FUS[23,62] and MEC-2,[11] initially form dynamically arrested condensates before transitioning into stable β-sheet-rich fibers.[63] Importantly, rigidity transitions may not percolate the entire droplet but lead to different subphases in the condensates, each with a different viscoelasticity[16,38,63] and a heterogeneous rheological response.

Similar to liquid–liquid phase separation and dynamic arrest, the emergence of an ordered phase involves a loss of entropy because of the local ordering of individual polymer chains into fibrils. This loss must be compensated for by favorable interaction energies, leading to

Glossary

Mechanotransduction: The process by which cells or organisms convert mechanical stimuli into biochemical signals that can influence cellular behavior and function.
Liquid–liquid phase separation: A supersaturated solution of proteins, RNA, or other biomolecules surpass their saturation concentration and spontaneously separate into a dense and a dilute phase that stably coexist.
Biomolecular condensate: A dynamic, membrane-less organelle, primarily composed of proteins and nucleic acids, that forms through phase separation or similar aggregation mechanisms and often exhibit liquid-like properties initially but may transition to gel-like or solid states under specific conditions. These condensates create distinct microenvironments within cells, enabling the spatial and temporal regulation of biochemical and mechanical processes.
Nematic phase: Ordered state of anisotropic molecules, such as elongated or rod-like proteins or polymers, where the molecules align parallel to a common axis but do not exhibit positional order. It gives the system orientational order while retaining fluid-like translational freedom.
Pickering agent: A substance, typically solid particles, that stabilizes emulsions by adsorbing at the interface between two immiscible liquids (e.g., the condensate and cytoplasm). Unlike traditional emulsifiers such as surfactants, Pickering agents rely on their particulate/solid nature to prevent the coalescence of droplets.
Gel: A highly connected polymer network stabilized by physical crosslinks formed between the molecular components. Gels are soft and deformable but do not flow like liquids under normal conditions due to the presence of a crosslinked or entangled network that provides mechanical stability.
Glass: A material that lacks a long-range ordered structure and instead exists in the disordered, thermodynamically frustrated (non-equilibrium) state which spontaneously evolves (aging) with time toward the closest free energy minimum, that is the corresponding metastable supercooled liquid. A glass is characterized by amorphous arrangement of its constituent atoms or molecules that lack molecular mobility over extremely long time scales and has the mechanical properties of a solid but exhibit the typical structural features of a disordered liquid.
Amyloid fiber: An insoluble, high order protein aggregate composed of cross-beta-sheet structures.
Prion-like domain: A region within a protein that shares sequence and functional features with prion proteins. These domains are typically low-complexity sequences enriched in polar amino acids such as glutamine, asparagine, serine, and glycine. They can template self-association, promote phase separation, and form amyloid fibers.
Intrinsically disordered regions: Segments of proteins that lack a stable, well-defined three-dimensional structure under physiological conditions. They are flexible and dynamic, adopting multiple conformations.
Percolation transition: A critical transformation from a disconnected to a connected state as the density or probability of connections within the system increases and shifts from a state of isolated clusters to a highly connected network. Continuous rather than catastrophic process.
Nucleation: The formation of a small, stable cluster of a new phase (e.g., droplets or crystals) within a parent phase. This occurs when a critical threshold, such as supersaturation or undercooling, is reached, enabling the growth of the new phase.
Dynamic arrest: A state where the motion of molecules or particles of the system slow or halt, leading to a transition from a fluid-like, dynamic state to a solid-like, rigid state.
Homotypic/Heterotypic buffering: A mechanism in which weak, transient interactions between identical molecules (homotypic interactions) regulate their tendency to undergo phase separation. It prevents premature, unregulated formation of phase-separated condensates by sequestering molecules in a dispersed, liquid-like state. It also ensures that the condensates can transition to a different phase, such as forming solid-like aggregates, in a controlled and spatially specific manner.
Rheology: A study of the flow and deformation of materials under applied stress, which enables the characterization of complex mechanical properties.
Elasticity: A property intrinsic to the material that describes the reversible (non-permanent) deformation behavior. It is independent from size, shape, and structure. Units of Pa.
Viscosity: A measure of a fluid's resistance to flow, it describes how much internal friction exists between the molecules of a fluid when it moves. It dissipates the energy from the applied force rather than storing it, leading to irreversible, time-dependent flow. Unit: Pa s.
Viscoelastic: A material that exhibits both viscous and elastic behavior when subjected to an applied stress. It deforms like an elastic solid in short timescales, storing energy, but flows like a viscous liquid over longer timescales, dissipating energy. It is defined as the sum of the storage and loss modulus: $G^* = G' + iG''$.
Stiffness: A structural property characterizing the material's resistance to deformation when subjected to an applied force. It quantifies how much a material resists being stretched, compressed, or bent under stress. Contrast elasticity, which is an intrinsic, material property.

a more dense, ordered phase. Using this principle, it is possible to predict and identify polymer regions that promote liquid–solid transitions. This raises a key question: What are the most frequent aggregation hot spots that drive viscoelastic phase transitions?

Condensates undergoing liquid-solid transitions often form from proteins containing prion-like domains (PrDs).[63] PrDs are generally distinguished by their low complexity sequence features, marked by an abundance of aromatic amino acids (tyrosine and phenylalanine) and

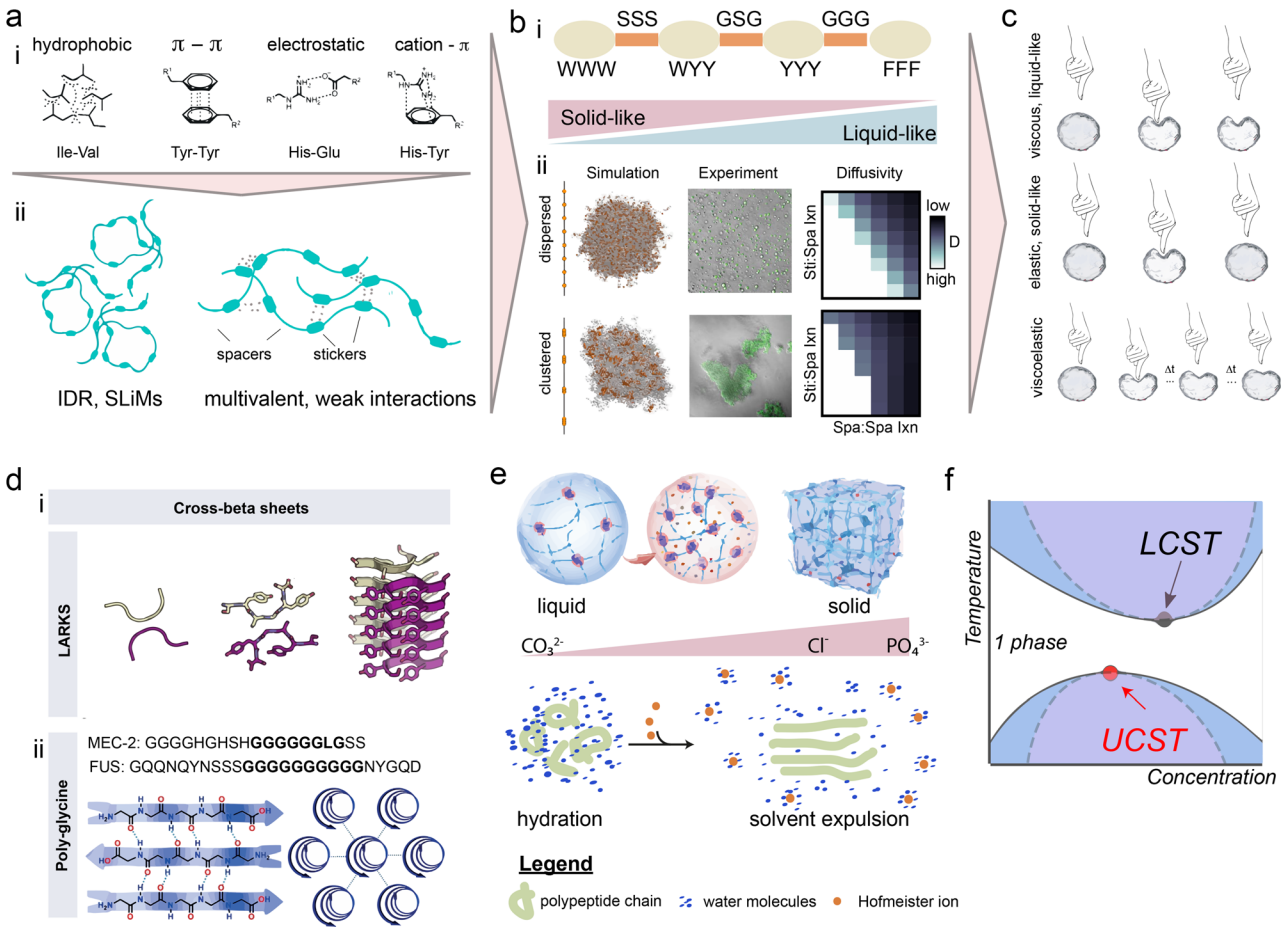

FIG. 1. Molecular signatures of liquid–solid transitions. (a) (i) Weak, noncovalent intermolecular contacts such as hydrophobic, aromatic, electrostatic, and cation-π interactions are the driving forces for liquid–liquid phase separation. (ii) The organization of these residues into stickers and spacers to maximize these contacts is key for LLPS and gives rise to a set of varying material properties. (b) (i) Spacer (Spa) and sticker (Sti) sequences and their arrangement determine the degree and timescale of liquid–solid transition. Replacing tryptophan with phenylalanine in aromatic sticker residues makes condensates more liquid-like, with reduced elasticity and viscosity, while replacing glycine with serine in spacer regions speeds up rigidity transitions but decreases condensate formation.[22] (ii) Dispersed aromatic sticker residues generally have a lower tendency to form aggregates and ensure that strong interactions among aromatic residues are weakened by the favorable solvation of the spacers. A high degree of clustering and the sticker–spacer interaction strength result in lower diffusivity. Reproduced with permission from Holehouse *et al.*, Biochemistry **60**(47), 3566–3581 (2021). Copyright 2021 authors, licensed under a Creative Commons Attribution (CC BY) license; and Reproduced with permission from Science **367**(6478), 694–699 (2020). Copyright 2020 AAAS. (c) Different mechanical signatures may arise from phase transitions, such as purely viscous, elastic, or viscoelastic condensate that behave as a fluid, solid, or gel-like material. (d) (i) Proteins with low-complexity aromatic-rich kinked segments (LARKS), SLiMs rich in [G/S]Y[G/S] tandem repeats form cross-beta sheets that drive gradual fibrillation at the high protein concentrations present within condensates. These structures are highly similar to amyloids but lack thermal and structural stability, making them amenable to cellular regulation. Reproduced with permission from Hughes *et al.*, Science **359**(6376), 698–701 (2018). Copyright 2018 AAAS. (ii) Long stretches of glycine can form poly-glycine I and II conformations with ultralow solubility and may contribute to rigidity phase transitions in condensates with poly-glycine repeats, such as MEC-2 and FUS. Reproduced with permission from Athiyarath and Sureshan, Angew. Chem., Int. Ed. **58**(2), 612–617 (2019). Copyright 2019 John Wiley and Sons. (e) Different ions have different effects on the liquid–solid transition. Their efficacy in inducing rigidification follows a modified Hofmeister series with phosphate ions as the most potent inducer. The ions with the strongest tendency to form the hydration shell compete with the corresponding amino acids in the proteins. The solvent expulsion may be accompanied by structural rearrangements and the formation of ordered structures. (f) Phase diagram for two typical proteins that are characterized by divergent phase behavior. Condensate formation through phase separation can occur by heating (characterized by a lower critical solution temperature, LCST) or cooling (characterized by an upper critical solution temperature, UCST). The dotted lines indicate the spinodal curve and the conditions under which biomolecular condensates spontaneously form, and the solid line indicates the binodal curve and the conditions under dense and lean phase coexist.

polar amino acids (glycine, serine, glutamine, and asparagine), while exhibiting a scarcity of charged residues.[64,65] As discussed above, condensate stiffening is sensitive to the composition and arrangement of these residues [Fig. 1(a)], with glycine residues stabilizing the fluid phase, while glutamine and serine residues promote solid transition.[40] A salient feature of PrD is their propensity to form ultrastable, protease-resistant "folds" composed of cross-β strands—the so-called amyloids—which are found not only in infectious prion proteins but

Box 1. Mix and Match - Heterotypic Buffering to Regulate Rigidity Transitions

Often, formation of biomolecular condensates (BMCs) and their liquid–solid transitions are driven by heterotypic interactions through protein–protein or protein–ribonucleic acid (RNA) interactions. RNA as an anionic polymer is an excellent framework for achieving multivalency and can adapt to many RNA binding proteins.[123,124] It was found that RNA influences condensate stability in a concentration-dependent manner: at high concentrations, such as those found in the nucleus, it inhibits phase transitions, while at low concentrations, like in the cytoplasm, it acts as a scaffold to promote liquid–liquid phase separation (LLPS).[125] Importantly, droplets formed through condensates of RNA and proteins are metastable and have the tendency to form irreversibly insoluble condensates through percolation transitions, dynamic arrest, or amyloids—many of those are found in disease (TAU, TDP-43, FUS, hnRNPA1, CPEB4, etc.). Stable, homotypic interactions between RNA molecules under strong base-pairing tendencies drive the percolation transition.[126] Heterotypic interactions mediated by multivalent RNA-binding proteins buffer homotypic RNA interactions, leading to an increased energetic barrier to the percolated state (see figure below)—in other words, proteins "mask" the RNA–RNA basepairing interactions and delay the transition to the solid state. This can happen passively through binding when heterotypic interactions displace the homotypic ones, or actively through energy-consuming processes (e.g., helicases).[124] Such heterotypic buffering, the ability of an interaction between two different motif to buffer against dynamic arrest,[83] can also be found in protein–protein co-condensates and ensures that condensates remain in compliant conditions until the buffering interactions are released (Fig. 6). Then, residues are exposed that can interact and cross-link with same motifs, enabling a network that percolates the whole condensate to form a stable structure in a spatio-temporally regulated manner.[83] Because the timescale of the binding and unbinding of the associated bonds, and the depth of their potential well, determines the material properties, heterotypic buffering is strongly tied to biological function.[11,70,83] Examples include UNC-89 binding to the C-terminus of MEC-2 stomatin to prevent droplet hardening and amyloid formation by disrupting an intramolecular interaction in MEC-2 c-terminus, enabling regulated transitions of MEC-2 condensates from liquid-like to solid states at sites of mechanoelectrical transduction within sensory neurites.[11] Similarly, an arginine-rich microexon of CPEB4 (me4) stabilizes CPEB4 condensates by interacting with histidine clusters, maintaining reversible condensation and regulating neurodevelopmental gene translation linked to autism spectrum disorders (ASD). Without me4, homotypic histidine interactions cause irreversible CPEB4 aggregation.[70]

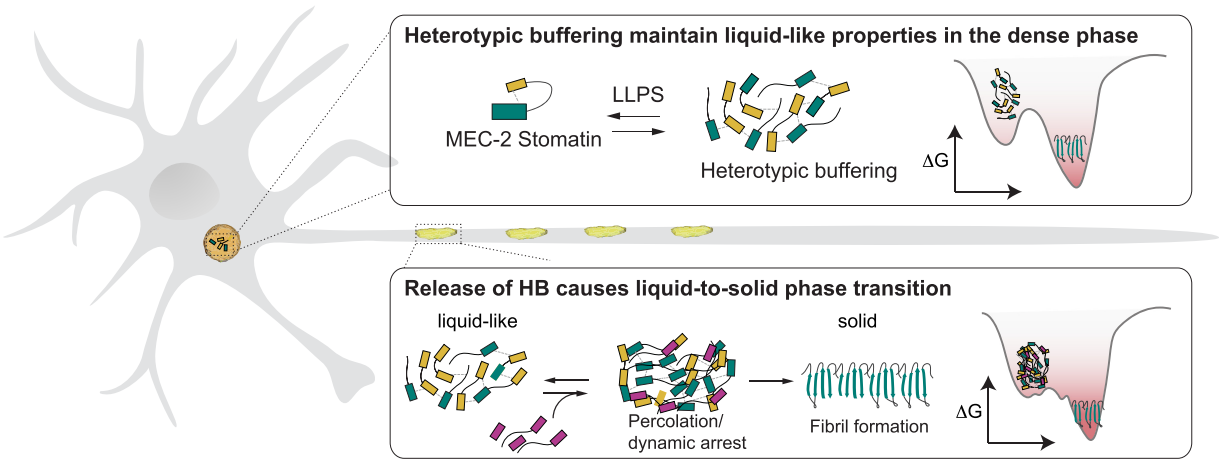

Heterotypic buffering increases the energetic barrier to a percolated state. (top) Not restricted to neurons, heterotypic buffering can maintain the liquid-like properties in a co-condensate through an interaction that masks the aggregation prone motif. This in turn will increase the energy barrier for amyloid and fiber formation. (bottom) Heterotypic buffering can be released through secondary partner (purple) that displaces the "mask" (yellow) from the aggregation prone motif (green box); or release steric constraint with an effective lowering of the energy barrier for fiber formation. Adapted from Ref. 83.

also in diseased variants of Aβ, tau, α-synuclein, SOD1 and many more aggregate-forming proteins give rise to condensates undergoing liquid-solid transitions.[66] Intriguingly, if the prion-like interaction is strong enough, the condensate may transition from an isotropic to a nematic phase, visible as long fibers.

If PrDs have such a strong propensity to form amyloids, how is the rigidity transition avoided or controlled? The transition from a dynamic to an arrested state is very dynamic and can be modulated by cellular signals (e.g., post-translational modifications,[67,68] calcium signaling,[69] pH[70]) and environmental stresses (e.g., oxidation,[71] mechanical stress[20]) rendering its properties bona fide stimulus-responsive. In the example of MEC-2 stomatin,[11] heterotypic buffering (Box 1) of a predicted PrD favored the droplet-like state, while mutations in an SH3 binding motif lead to a loss of fiber formation and a delayed maturation of the relaxation timescale. In contrast, overexpression of the SH3 domain *in vivo* promoted the amyloid-prone mode of interaction and resulted in a reduction in liquid-like MEC-2 condensates.

Similar to the extended cross-β strands found in amyloids, many proteins contain smaller motifs that do not form extended structures.

Box 2. Viscoelasticity and the rheological properties of biomolecular condensates.

Owing to the complex interaction that stabilizes the biomolecular condensates composed of multivalent and weak intermolecular bonds leading up to the liquid–solid transition, many, if not all, show frequency-dependent, viscoelastic properties.[11,23,142,149,150] A material is said to be viscoelastic, if it shows both, significant ability to store and dissipate mechanical stress upon an external deformation. Its ability to do so, depends on the deformation frequency, e.g., how fast the condensates are deformed, and characteristic timescales of the composite material. The ratio of $\frac{G''}{G'}$ is their loss tangent $\tan\delta$ and describes if the material primarily behaves dissipative ($\tan\delta > 1$) or conservative ($\tan\delta < 1$). The timescale at which the loss and storage modulus is equal ($\tan\delta = 1$) is the crossover frequency ω_c. Thus, a complete characterization of the material response requires the acquisition of the complete frequency spectrum, from ultraslow to ultrafast deformation timescales. The ideal behavior of a model material is described by a single relaxation timescale and elastic modulus in light of the classical Maxwell or Kelvin–Voigt materials, depending on if the material primarily behaves as a viscoelastic liquid or viscoelastic solid within the observed frequency window, respectively.[151] The Kelvin–Voigt model represents a firmly crosslinked polymer, in which the rate of force application is faster than the off-rate of the bonds, while the Maxwell represents an uncrosslinked polymer. These descriptions are a strong simplification, and BMCs which behave as a Maxwell material in one frequency range may behave as a Kelvin in another range. This complex behavior is described in higher order models such as the Zener (also called standard linear solid) or Jeffrey's fluid.[23] The Zener model describes a material that will fully recover after a load is removed because the spring connected in parallel to the Maxwell element will continue to move the piston of the dashpot back to its original position. It may have two crossover frequencies beyond which the material behaves elastic, but viscous in between. Importantly, during aging, condensates can remain glass-like[11,23] or "convert" from a Maxwell-fluid to a Kelvin–Voigt solid.[22] As the material is a continuous spectrum of different timescales, it can be described by a generalized form of a viscoelastic model with power law behavior. The fractional spring-pot is used to model this power-law behavior by defining the stress–strain relationship with a fractional order derivative ($\sigma(t) = C_\alpha \cdot \frac{d^\alpha \epsilon(t)}{dt^\alpha}$), which captures the material's complex time-dependent response.[151] The order of the fractional derivative in the spring-pot directly relates to the exponent in the power law. Displayed below is the common fractional Kelvin–Voigt model, which is plausible outcome if the condensate behaves as a solid on long time scales and is stabilized by several distinct interaction motifs of which each has its own force-response.[152] A continuous spectrum of relaxation timescales can also be obtained from the Rouse–Zimm theory, a microscopic framework to describe the dynamics of a polymer chain in solution, modeled as beads-on-a-spring with hydrodynamic interactions. This theory has been successful to correctly describe low frequency dynamics of condensates, which were otherwise overestimated in continuum models.[140]

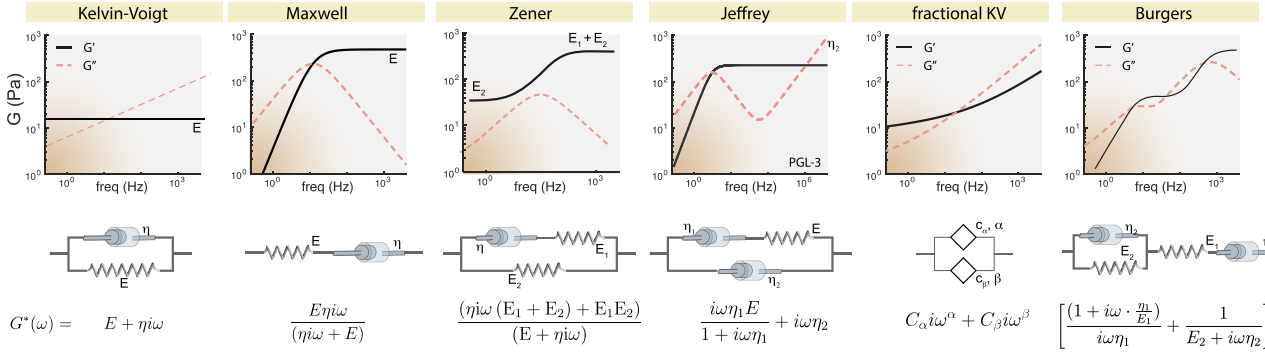

Rheological models for the study of biomolecular condensates. Five different rheological spectra for different material behavior and their frequency-dependent loss and storage moduli. In the Kelvin–Voigt material, the storage modulus dominates the loss modulus below the crossover frequencies and it is therefore elastic, whereas the Maxwell material has a higher loss modulus—it tends to flow. Higher order behavior can arise, e.g., the serial combination of the KV and the Maxwell case lead to the Burgers model.[149,153] The two timescales $\frac{\eta_n}{E_n}$ associated with the dashpots can be interpreted as conformational dynamics (fast) and transient binding/unbinding events (slow).[154]

These so-called *low complexity, aromatic rich, kinked segments*, or LARKS, establish cohesive interactions and form protein scaffolds, reminiscent of the cross-β sheet found in amyloids.[72] LARKS are surprisingly abundant and are found in approximately 400 proteins in humans, which participate in a diverse set of functions.[72] However, in contrast to amyloids, these beta sheets form reversibly and are not heat resistant. They contain the core sequence [G/S]Y[G/S], which forms kinked, instead of extended beta sheets [Fig. 1(d), panel i]. The kinks are believed to prevent side chains from interlocking across the beta-sheet interface, resulting in kinked interfaces that cover smaller surface areas compared to those in pathogenic amyloid fibrils, and likely possess lower binding energies. Consequently, LARKS can promote gel-like condensates through weak interactions instead of irreversible solid-like amyloids.[73] It was proposed that proteins with tail-located LARKS display a maturation rate much higher than those in which the LARKS are placed toward the center.[74] However, low-complexity domains containing at least two LARKS, regardless of their arrangement, can gradually form gel- or solid-like aggregates through β-sheet fibrillization.[74]

Other hotspots prone to aggregation are glycine-rich motifs, which can also become highly insoluble if the stretches exceed 7–10 residues and form fibrillar polyglycine-II-like structures.[75,76] Such

glycine-rich motifs have been found in many human proteins, and indeed, proteins containing poly-glycine/alanine stretches accumulate as inclusion bodies in the brain of patients with neurodegenerative diseases.[77] Prominent examples that can harness glycine-rich sequences are found in the PrD of FUS and in the predicted PrD of MEC-2 [Fig. 1(d), panel ii, and see below]. Polyglycine can form fibrous structures with nematic ordering, which are believed to adopt polyglycine II and extended strand-like conformations that promote intermolecular hydrogen bonding [Fig. 1(d), panel ii]. Likewise, glycine-rich sequences in FUS and nucleolin form polyproline II-like helices[78] with implications for biomolecular condensation. The helical conformation was proposed to bring the tyrosine and arginine residues close together, adding favorable interactions to the free energy budget.[79] The formation of poly-glycine assemblies is likely to occur only at the high protein concentrations present in condensates, where intermolecular interactions are promoted. At low concentrations and due to the poor water solubility of the polyglycine tracts, they form heterogeneous ensembles of collapsed conformations as individual molecules, stabilized by intramolecular amide-amide interactions.[75] Because of their poor water availability, the formation of poly-glycine-II helices may be sensitive to the ionic species and the ion's tendency to compete for the hydration shell.

Other hot spots prone to aggregation are found in poly-glutamine or poly-Q repeats.[80] Recently, it has been proposed that fragments of Huntingtin exon 1 competent for aggregation form condensates through LLPS, with longer polyQ repeats forming droplets at lower concentration.[81] Subsequently, these droplets undergo an LST and form amyloid fibers within 30–60 min after droplet formation, visible as spike-like, as well as 1,6-hexanediol-resistant protrusions *in vitro* and aggregates with lower recovery of FRAP *in vivo*. Whether this conversion from liquid to solid properties is disease-relevant is a matter of debate: Contrary to widespread belief, the length of these polyQ fragments itself (number of glutamine residues) is not related to the onset of neurodegenerative disease, while the number of CAG nucleotide repeats is causally related to the onset of the disease.[82] For an in-depth discussion of LST related to disease, we refer to other excellent reviews in the field.[83,84]

2. The effect of salt, solvation, and the hydrating water shell

It is well known that LLPS is very sensitive to salt concentrations, and, depending on the intermolecular forces that stabilize the dense phase, increases in salt will lead to a higher or lower propensity for proteins to condense through charge screening among other factors.[85] For example, MEC-2 condensates form through hydrophobic interactions and are stabilized by high salt concentrations,[11] whereas FUS, TDP-43, BRD4, SOX2, and Annexin A11 form at low concentrations.[86] Likewise, salt affects how tau condensates respond to temperature[87,88] and salt concentration affects surface tension and bulk modulus of PGL-3 droplets measured in the optical trap: higher salt causes softer condensates, ranging from 0.1 to 1 Pa at 180–75 mM NaCl, respectively.[89] However, the solvation environment of protein molecules in a condensate can be very different from that in a dilute solution. Many charged molecules, including proteins, are stabilized by a hydrated shell. Any perturbation of this shell can lead to a reorganization of the protein structure and/or condensation.[90] Thus, the addition of salt or macromolecules that compete with the hydrating water shell leads to condensation.

Condensates with liquid properties are generally more sensitive to environmental changes, as the intermolecular interactions inside liquid condensates are usually weak. The addition of salts (e.g., NaCl) or organic agents (e.g., 1,6-hexanediol) that enhance the ionic strength or hydrophobicity of the solution can lead to dissolution but also to coarsening of the liquid droplets, depending on if they are stabilized by electrostatic or hydrophobic interactions. 1,6-hexanediol, in particular, has been used to test whether condensates are stabilized by weak hydrophobic interactions,[81,91–93] and the addition of this aliphatic solvent destabilizes condensates, particularly those mediated by stacking $\pi - \pi$ or aromatic interactions.[94] In contrast, condensates formed by electrostatic interactions[87] as well as solid condensates[81,94] are less sensitive to 1,6-hexanediol. However, as it is usually applied at a relatively high concentration, it can produce unwanted stress on target cells,[95,96] affect the cytoskeleton,[97] and lead to cell death.[98]

Similarly, increases in the availability of charged ions can induce the formation of a liquid–solid transition in tau protein condensates.[99] The strength at which the ions (applied at physiological concentrations of 150 mM each) induce the LST follows the Hofmeister series, an empirical ranking of the ions based on their ability to "salt" proteins "out" of solution [Fig. 1(e)]. In this view, ions compete with the protein charges for water molecules. This draws water away and therefore destabilizes the hydration shell and reduces the protein's solubility, leading to protein aggregation. In liquid-like condensates, the loss of water that solvates and separates individual macromolecules can lead to tighter interactions and increased entanglement of monomers, potentially driving fibril formation within the condensates. Together, different functional groups of biologically active molecules may have different varying effects on the liquid–solid transition, where charged groups (PO_4^{3+}, CO_2^{2+}, NH_3^+) facilitate the liquid-to-solid transition, while hydrophobic moieties (CH_3) inhibit the transition.[99]

A key factor in condensates formed from polyanionic polymers, such as poly(ADP-ribose), RNA, and DNA, is the crucial role of divalent cations.[100] PolyrA oligomers especially have a strong tendency to phase separate even at low Mg^{2+} concentrations and undergo a rapid phase transition to a state of dynamic arrest.[101] The removal of divalent ions by chelators (e.g., EGTA), or treatment with ammonium acetate, can dissolve RNA condensates competing with divalent cations.[102]

3. Concentration dependence

All condensation mechanisms are highly dependent on the initial concentration of the participating molecules and the intrinsic properties called saturation concentration C_{sat} (for a summary of the definition, see Ref. 16). C_{sat} depends on the macromolecule–solvent interaction and the strength of the interactions in the dense phase. Thus, it is important to realize that two molecules with a similar saturation concentration will not necessarily have the same mechanical properties of the dense phase because different polymers are stabilized by different molecular interactions in the dense phase and even a subtle change can have a large stabilizing or destabilizing effect. In simple terms, if each molecule has more than three sticky regions ("stickers") and these stickers bind mainly to other molecules rather than to themselves, then more clusters will form and those clusters will also grow larger as the concentration increases.[16,103] This multivalency can lead

to "sol-gel" transition which is characterized by the percolation concentration C_{perc} and describes the valency-dependent threshold above which the whole condensate forms a viscoelastic "percolated network." C_{perc} can be lower than C_{sat}, such that a percolated gel readily forms without a prior change in phase across the system. This is rarely observed and phase separation and percolation have been proposed to be coupled, e.g., $C_{sat} < C_{perc} < C_{dense}$. Within this framework, it becomes easy to reconcile that most, if not all, condensates form viscoelastic materials.

However, the concentration of the dilute phase can also non-trivially affect the material properties of the dense phase. For example, the flux of components between the dilute and dense phases across the interface is influenced by their concentrations in the dilute phase and at the interface. The concentration of the dilute phase affects the internal dynamics and structural properties of the dense phase,[104] which can affect the exchange dynamics and stability of the dense phase. Vice versa, kinetically trapped molecules at the interface of solid condensates will limit the exchange dynamics and thus may limit condensate growth.[28]

Whereas classical LLPS has a concentration-independent partition coefficient (which describes if a molecule preferentially concentrates in the dense phase vs the dilute phase), several condensate-forming proteins have a higher partition coefficient at higher concentrations.[105] For example, a hydrophobic environment can emerge upon condensate formation[106] leading to a change in the partition coefficient. This means that the molecule preferentially enriches in the dense phase, with possible consequences in the material properties.

4. Temperature dependence

Phase separation in protein solutions can occur by cooling (characterized by an upper critical solution temperature, UCST) or heating (characterized by a lower critical solution temperature, LCST) [see Fig. 1(f)]. For components that exhibit UCST phase behavior, reducing the temperature of the system below a threshold temperature (also called a cloud point) triggers phase separation. Many native IDPs, such as hnRNPA1,[25] FUS,[107] and tau at low salt concentrations,[87] exhibit UCST phase behavior, indicating that intermolecular interactions in these IDPs are reduced relative to entropic contributions at higher temperature. This is mainly driven by electrostatic or cation-π-based interactions. The way in which temperature affects the viscoelastic properties of condensates may follow similar rules. For example, the elastic moduli of a typical amorphous polymer increase with loading rate but decrease with higher temperatures. Importantly, condensates may dissolve with an increase in temperature and gel-like condensates or those that have undergone LST may be resistant to temperature changes and do not dissolve.[108]

Less intuitively and contrary to our everyday experience, condensates can also form preferentially with an increase in temperature, such as MEC-2,[11] tau at high salt concentrations,[88] and the poly-(A)-binding protein in stress granules.[109] Here, an increase in temperature raises the entropic penalty of organizing solvent molecules around the protein backbone. To minimize this penalty, the system releases solvent molecules from the backbone, gaining entropy, triggering an LCST phase transition.[110] This is driven primarily by hydrophobic interactions, so that increasing the hydrophobicity of the protein sequence enhances phase separation by lowering the cloud point temperature.

Together, a high content of polar residues in conjunction with aromatic residues favors UCST behavior, whereas polypeptides depleted in charged amino acids and enriched with hydrophobic residues are ideal for LCST transitions.

5. Condensates maturation and the effects of the interface

The spatial position of the molecules within the condensate, e.g., if it is found on the surface or in the bulk, can also play important roles in the rigidity transition.[38,81] For example, a Pickering-like effect has been shown for FUS condensates that mature preferentially from the outside inward.[38] Using micropipette aspiration to study the mechanics of FUS condensates, it was found that these condensates gradually increased their viscosity by over 50 times within the first 24 h and became highly elastic after 72 h. Indeed, reflective confocal dynamic speckle microscopy, which measures the local dynamics of scatterers within the condensate, confirmed the presence of a highly heterogeneous droplet where liquid- and solid-like regions coexisted. Furthermore, after 24 h, a dense shell structure began to develop, propagating toward the center of the condensates until it completely solidified.[58]

Solid-like structures were also detected to develop first at the interface between the condensate and the surrounding solvent, using combination of atomic force microscopy (AFM) and vibrational spectroscopy.[111] Over time, these structures spread unevenly into the fluid core of the condensate. This process was driven by a rising density of intermolecular cation-π interactions among intrinsically disordered FUS molecules, which progressively increased the elastic properties of the system. Eventually, the amorphous solid phase extended from the interface toward the core in a non-uniform manner, resulting in a condensate with mechanical heterogeneity.[111] Simulations indicated that the interface of the liquid droplet experiences larger density fluctuations, seeding the structural transitions of the PrD from a collapsed to an extended conformation, which exposes free valencies to form cross-β sheets.[38] Thus, it is likely a common mechanism that underlies the LST of other condensates. Indeed, amyloid formation is also promoted at the interface of condensates composed of the LCD of hnRNPA1.[112] Another example comes from *Caenorhabditis elegans*. The P granules contain a stable interface composed primarily of gel-like MEG-3, which acts as a Pickering agent, surrounding and stabilizing the liquid-like condensates of PGL-3.[113] In addition, the gel-like MEG-3 act as seeds to specifically nucleate PGL-3 condensates at the posterior pole of the *C. elegans* embryo. The condensate surface can also act as a nonspecific attractor for cytoskeletal elements. In particular, microtubules have been shown to reduce the interfacial energy of various different condensates and act as a weak surfactant.[114] This may potentially serve as a microtubule nucleation platform[115] or contribute to microtubule bundling in axons.[116]

In general, the surface of condensates profoundly impacts many processes, such as the rates of biochemical reactions,[117] exchange dynamics, diffusion, and release of condensed material,[104,118] coalescence and growth of condensates, adsorption of macromolecules,[114] and nucleation of aggregates.[119]

B. Factors affecting maturation timescales and lengthscales

Having discussed the predominant sequence patterns and aggregation-prone motifs, an important outstanding question is what

determines the final size of the condensates and the rate of stiffening *in vivo*. For example, different condensates have been shown to stiffen in a few seconds or minutes[22,28,43] and up to 24 h[11,23,38] and even days or weeks.[120,121] As discussed above, the parameters involve the concentration of participating molecules relative to their saturation concentration, temperature, or salt. Given that these latter parameters are relatively constant for all different condensates in the same cell, the answer must also be found in their sequence and the steric constraint in the environment. Condensate growth is also limited by the surface reactivity, surface tension, and viscosity of the condensates. Condensates with higher viscosity grow more slowly because the diffusion of molecules into the dense phase is limited. Thus, condensates that undergo rapid maturation, fusion/fission dynamics are reduced and can become arrested and remain at a diffraction-limited size.[28] Not surprisingly, the molecular dynamics of the partitioning molecules becomes slower in the dense phase than in the dilute phase, but can remain astonishingly fast.[122] Upon further aging, reduction in molecular dynamics occurs when particles are confined by their neighbors, leading to the formation of a glassy state, but also when attractive interactions between particles result in gelation and loss of fluidity, or when the network becomes rigid due to entanglements or intermolecular crosslinks.

Condensates often consist of a mixture of proteins, RNA, and other biomolecules that interact through multivalent weak interactions (e.g., hydrophobic, electrostatic). This molecular diversity stabilizes the liquid-like state by dispersing interactions and preventing excessive clustering of specific components. Heterotypic interactions reduce the propensity of any single species to undergo aberrant condensation or aggregation (Box 1). For example, RNA or certain chaperones in stress granules can dilute and stabilize proteins with a tendency to aggregate. Regulated, or uncontrolled changes in the relative concentrations of condensate components (e.g., depletion of RNA or overexpression of aggregation-prone proteins) can destabilize the liquid-like state. The availability of the buffering component thus influences the extent and timecourse of the solid condensate growth.

C. Effects of mechanical forces and constraints

Central to understanding condensates in mechanobiology is how external forces affect their formation and thus function. As discussed above, gel-like and solid-like condensates display varying levels of resistance to disassembly in response to environmental changes, such as changes in temperature or solvent availability. Usually not a factor *in vitro*, but there has to be space in the cell for a condensate to form and grow. Therefore, a strongly viscoelastic environment and tension in the surrounding matrix (cytoskeleton or chromatin) restrict the growth of condensates.[127–129] This is due to an energetic penalty to deform the external (to the condensate) matrix, which requires a higher free energy gain to favor condensate growth. Consequently, there will typically be an increase in saturation concentration, a decrease in nucleation rate, and, contingent on the matrix properties, a thermodynamically favored droplet size.[31] In the nucleus, for example, condensates preferentially form in regions depleted of chromatin and do not coarsen as one would expect from typical equilibrium phase separation.[130] In the limit, increased tension in the matrix may lead to the dissolution of droplets already formed.[130] Mechanical forces applied to cells have been shown to remodel nuclear condensates inside living cells, determine their fusion/fission dynamics, or transduce force into chromatin organization (Refs. 10, 131, and 132 and discussion below).

Similarly, it has been shown that hydrostatic pressure destabilizes condensates,[133] while external mechanical stresses during confined cell migration promote condensation in the nucleus,[131] but it is not known how this effect may depend on the mechanical properties of the droplets themselves. Together, the mechanical properties of the droplet and the mechanical state of the environment determine the stability and dynamics of the condensate.

D. Energy-consuming processing in condensate maturation

In contrast to test tube conditions, biomolecular condensates inside the cell are exposed to metabolic activity, rapidly changing oxygen conditions, and energy-consuming processes, among others. Glycolytic enzymes (such as PFK1.1) form condensates under hypoxic conditions at presynaptic sites under energy demand,[27] which also become more viscous over time (Table I). Therefore, it is plausible that the material states of the condensates are different *in vivo* compared to the controlled environment *in vitro*. For example, helicases, which are proteins that catalyze local strand unwinding, translocation, strand annealing, RNA clamping, and displacement of bound proteins inside ribonucleoprotein complexes, can act to remodel the RNA-protein interaction in an ATP-dependent manner by dismantling these specific interactions. Helicases may also unwind RNA structures and therefore limit the long-range percolation transitions often found in RNA-containing condensates.[124] Likewise, the depletion of ATP by treating cells with carbonyl cyanide m-chlorophenyl hydrazone, or CCCP, to dissipate the mitochondrial membrane potential interfered with the formation of stress granules. It also caused accelerated stiffening of the already formed stress granules, indicating that ATP is important for both condensate formation and dynamics.[134] This may hint at the role of energy-consuming chaperones in maintaining a more liquid-like state. Indeed, Hsp104, a general anti-stress chaperone of the Hsp100 gene family from yeast but also Karyopherins in metazoans disaggregate many condensate forming proteins with prion-like domains.[135,136] The same observation has been made with condensates formed by P-body-associated DEAD-box ATPase Dhh1, which require ATP and ATPase activity to prevent dynamic arrest.[120] ATP hydrolysis by DEAD-box ATPases triggers RNA release from P-bodies and stress granules and may therefore be directly responsible for regulating the condensate material properties. ATPase activity, when stimulated by the P-body-associated factor Not1, leads to enhanced dynamics of P-bodies *in vivo* and prevents aging over time.

Other examples include the dual-specificity kinase DYRK3, which modulates the stability of P-granule-like structures. Under conditions of cellular stress, it dynamically shuttles between stress granules and the cytosol through a low-complexity domain in its N-terminus. When activated, DYRK3 facilitates the disassembly of stress granules, maintaining their dynamic nature.[137]

E. Material states, their mechanical properties, and why they matter

To understand condensates in light of mechanobiology, we aim to uncover how their mechanical properties are linked to their function in the organism. As such, different biomolecular condensates must

TABLE I. Selected examples of protein condensates and their time-dependent mechanical parameters. Abbreviations: DT-OT, dual-trap optical tweezers; PMR, passive microrheology; MPA, micropipette aspiration; FCS, fluorescence correlation spectroscopy; PPR, parallel plate rheometer; AFM, atomic force microscopy; TimSOM, time-shared optical tweezer microrheology.

Protein	Maturation	Viscosity	Elasticity	Surface tension	Technique	Ref.
MEC-2 UNC-89	0 → 24 h	3 → 20 Pa s	100 → 130 Pa	15.1 → 31.3 μN/m	DT-OT	11
FUS	0 → 45 h	3 → ∼50 Pa s	0.003 → 0.1 Pa	n.d.	PMR	23
PGL-3	0.5 → 1.5 h	0.039 → 0.39 s	56 → 50.7 Pa	4.5 → 19.3 μN/m	DT-OT	23
ProTalpha/H1	0 h	0.30 Pa s	n.d.	n.d.	FCS	122
ELF3	0 h	24 Pa s	n.d.	50 μN/m	AFM (FRAP-ID)	155
hRNPA1-LCDWT	0 h		200 Pa	n.d.	PMR	22
Chromatin	(undiff)	1.5–150 Pa s	0.8–80 Pa	n.d.	PMR	153
Chromatin	(diff)[a]	2.3–230 Pa s; 1.4–140 Pa s	E1 = 1–100 Pa, E2 = 1.8–180 Pa		PMR	153
α-synuclein	30 days	2 kPa[c]	11 kPa	n.d.	PPR	121
PSD	0.5 → 5 h	n.d.	≈5 → 15 kPa	n.d.	AFM (Hertz)	35
CPEB4	0 h	61.6 Pa	175 Pa	n.d.	TimSOM	142
PFK1.1	0 $\xrightarrow{hypoxia}$ 10 min	4.8 → 130 mPa s	n.d.	n.d.	FRAP	27
TDP-43	(?)[b]	0.1 → 0.01–3.7 Pa s	n.d.	n.d.	FRAP	156

[a]Values for differentiated chromatin were extracted from a fit of the PMR data to the Burgers model.
[b]Values for TDP-43 are associated with proximal to mid-axon transition.
[c]Loss modulus at ≈10 Hz.

show differences in mechanical properties, depending on their location and expression in the cell. This is further complicated by the fact that their material properties are subject to change with time and environmental cues—they "age" over a wide range of timescales, a process which has received attention from experimentalists and theorists alike.[138–141] Therefore, it is important to realize that the mechanical properties of the condensates are intricately related to their functions, and mutations that render the condensate soft or too stiff,[33] or simply the unchecked rigidity transition can lead to dysfunctional proteins and cellular functions.[41]

Although many condensates are formed by LLPS and appear spherical in the cell, biomolecular condensates rarely behave as perfect liquids, but can often be better described as viscoelastic materials,[16] such as gels, putties, or glasses, which may mature into crystals or hard viscoelastic solids[22] due to their degree of cross-linking, entanglement, and higher order structure (Box 2). All of these phases result in an increase in the relaxation timescale (they dissipate stresses with different rates) up until a completely elastic or plastic behavior (e.g., yield without reversibility). Thus, in addition to surface or interfacial tension, biomolecular condensates have a complex mechanical response characterized by viscous and elastic moduli and bending rigidity that determine the way these condensates respond to external forces.[142,143] Consequently, their material properties have strong implications for their reversible regulation and their ability to transmit mechanical stresses within cells. However, what are glasses and gels? A glass is typically an amorphous solid that lacks the long-range order characteristic of crystalline materials.[144] Similar to a liquid, the arrangement of its components is disordered, but, in contrast to a liquid, it is (nearly) fixed in space. The glass obtains its viscoelastic properties from the entanglement of the protein backbone and its degree slows the relaxation process.[144] In general, glasses form by cooling a liquid rapidly so that it does not crystallize and thus represents a thermodynamically frustrated material that slowly tends to relax toward equilibrium, crossing a potential barrier. The final state may be a crystalline/fibril material and thus an ordered state.[145] Therefore, a glass has a typical age-dependent relaxation time, without an increase in the elastic modulus. Many condensates display properties that can be described as aging Maxwell glasses.[23] A gel, on the other hand, is characterized by varying degrees of cross-linking between individual monomers. The more unoccupied valencies these monomers have, the more liquid-like the gel and the shorter the relaxation time. With age, these valencies may become saturated, leading to an increase in the relaxation timescale and a stiffer gel.[146] In contrast to the glass transition, gelation occurs abruptly at the gel point and is accompanied by an increase in elasticity. It is important to note that the material behavior and whether or not a condensate can be represented as a liquid or solid may change with age. For example, condensate maturation may involve a transition from a viscoelastic fluid (Maxwell-type) to a viscoelastic solid (Kelvin–Voigt type), reflecting changes in the material properties over time. (Ref. 22; see Box 2) As pointed out above, phase separation and percolation can be coupled, which leads to viscoelastic materials.[16] The network formation is governed by the multivalency and strength of the stickers that may result in pre-percolation clusters and heterogenous mechanical response of the condensate. The viscoelastic nature of the condensates requires quantitative evaluations of stress–strain relationships over time, which are essential to determine whether the biological functions attributed to a condensate at specific time point and stimulation frequency arises from its behavior as a soft viscous fluid, or a hard elastic material. For example, a condensate may respond as an elastic material when deformed quickly but continuously flows when deformed slowly. Does the crossover frequency change during age, the same slow frequency may elicit an elastic response in the same condensate type, as observed for MEC-2/UNC-89.[11] The material properties of condensates are best measured using microrheology methods,

allowing assessment of their material response in a broad frequency range.[142,147,148] Using suitable models, this approach provides insight into the frequency-dependent loss modulus (G'') and the storage modulus (G'), which reflect the ability of the condensates to absorb and transmit mechanical stresses (Box 2). In summary, whether condensates behave as liquid or solids is obviously important for how they "handle" mechanical stresses and can be important for physiology and disease.

IV. TECHNIQUES TO CHARACTERIZE MECHANICAL PROPERTIES OF BIOMOLECULAR CONDENSATES

The exact quantification of the condensate material properties, the forces they exert, and the way how they modify cell mechanical is central to understanding their mechanobiology. Often, the spherical shape of condensates or the emergence of amyloid fibers is usually taken as an indicator of their liquid and solid states, respectively. However, due to capillary forces, liquid condensates can be non-spherical and spherical condensates may turn to solids. In contrast to the amyloid formation, which is a readily visible property that can be observed in a brightfield microscope, the change in the relaxation timescale needs to be measured with sophisticated equipment. Here, we review some of the most common techniques used to characterize the material properties of condensates.

A. Optical tweezers

Optical tweezers are a popular tool for characterizing the mechanics of BMC at biologically relevant timescales and frequencies.[11,23,24,89,142,150,157,158] At the heart of the optical tweezer is a narrowly focused laser beam that can hold, or trap, microscopic particles with fN accuracy and nm precision—it can be used to record position and force acting on the trapped particle. Due to the interaction of the light with the particle, a change in momentum occurs that exerts a restoring force and keeps the particle in the center of the laser focus (principle of operation reviewed in Refs. 159 and 160) [Fig. 2(a) panels i and ii]. Due to conservation of the momentum of light, forces can be measured directly by quantifying the angular intensity distribution of light scattered by a trapped particle, even in living cells.[142,159] If all photons are collected, the force is directly proportional to the centroid position V_x of a position-sensitive device when the force sensitivity α is known. This parameter is independent of the experimental details and, when trapping inside cells, direct force sensing is especially useful, since many parameters that influence optical forces may be unknown. Because optical tweezers are 3D Hookean springs, the force and displacement of the trapped probe are proportional to back-focal-plane-interferometry detector voltages. Therefore, the force sensitivity $\alpha = k\beta$ is directly related to the stiffness of the trap k and the displacement sensitivity β and can be used to calibrate them.[159] To determine the displacement sensitivity, a known relative displacement of the particle from the trap center or a detection laser is typically used [Fig. 2(a) iii]. When using direct force measurements to perform an active rheology experiment to estimate mechanical properties, such as the complex shear modulus, probe displacements must be recorded independently. Therefore, a separate stationary detection laser or the same time-sharing laser can be used for simultaneous force/displacement measurements to determine the particle position beyond the linear detection range.

Once fully calibrated, optical tweezers have been extensively used to measure the viscoelastic properties of aging condensates and can also measure mechanics inside living cells. In one of the first applications for BMCs, optical tweezers were used to quantify the propensity of two FUS condensates to fuse, which is related to their viscoelastic properties and surface tension.[24,157] To do so, two condensates were trapped and brought into contact [Fig. 2(b)]. Upon contact, they either fused immediately or with delayed dynamics based on condensate age and whether or not they contained disease-relevant mutations.[24] The fusion of two FUS condensates was inhibited if the constituent proteins contained patient-derived mutants leading to neurodegenerative diseases, suggesting for the first time that condensate rigidity phase transitions may be linked to disease outcome. This fusion assay has since been applied to a variety of different condensates and conditions,[99,118,157,161–163] to measure capillary velocity and contact/force force of two droplets.[164] In general, rapid fusion indicates more liquid-like character, whereas slow or arrested fusion dynamics indicate more (viscoelastic) solid behavior. The fusion speed can be exactly quantified and tracked using an optical tweezer [Fig. 2(d)], allowing direct access to their fusion dynamics.[157]

To fully characterize the mechanical properties and interfacial mechanics of biomolecular condensates, the optical trap can be used to explore the frequency-dependent response of a probe particle to active or passive excitations, allowing access to a window within the complete rheological spectrum.[11,23,149] In passive microrheology, a low-power laser beam below the trapping limit is focused on the refractive particle inside the condensates and is used to record its Brownian motion.[165] It is termed passive, as the laser trap itself is not exerting any significant force on the particle, such that the fluctuations in particle position powered by thermal energy can inform about the mechanical environment—low storage and loss moduli result in large fluctuations, while small fluctuations indicate a confined motion and a stiff environment. Particle trajectories can then be analyzed to calculate their mean-squared displacement (MSD $\langle \Delta \boldsymbol{x}^2(\boldsymbol{\tau})\rangle$), which is then used to quantitatively infer the viscosity and shear modulus of the embedding microenvironment[166] [Fig. 2(c)],

$$\langle \Delta \boldsymbol{x}^2(\tau)\rangle = \left\langle \Delta \boldsymbol{x}^2\left(\frac{1}{\boldsymbol{\omega}}\right)\right\rangle [\boldsymbol{\omega t}]^{\alpha(\omega)}, \tag{1}$$

in which α is the power-law scaling exponent, directly related to the mechanical properties of the environment. Freely diffusing probe particles in Newtonian fluids have an α value of 1; in viscoelastic fluids, particles exhibit subdiffusive motion, characterized by $0 < \alpha < 1$, whereas $\alpha = 0$ indicates that particles are trapped, behaving as they would in a purely elastic material [Fig. 2(e)]. Fourier transform of the MSD by the generalized Stokes–Einstein relation yields the frequency-dependent, complex shear modulus $G^*(\omega)$ according to

$$G^*(\omega) \approx \frac{k_B T}{\pi a \left\langle \Delta x^2\left(\frac{1}{\omega}\right)\right\rangle \Gamma[1+\alpha(\omega)]}, \tag{2}$$

where a is the probe radius and Γ is the Gamma function.[166] Passive microrheology has been applied to many different types of condensates *in vivo*[153] and *in vitro*,[22,23,150] such as to determine how sequence composition of short polypeptides influences the material properties of protein-RNA condensates.[150] For example, synthetic condensates

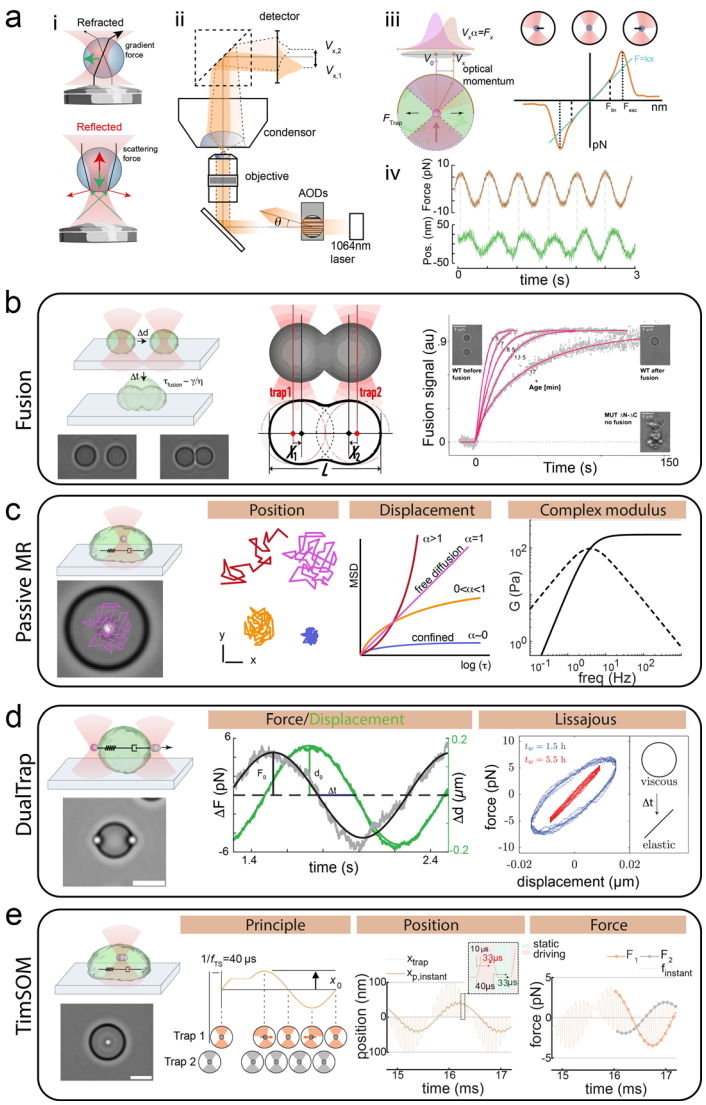

FIG. 2. Application of optical tweezers towards biomolecular condensates. (a) (i) Geometric optics to explain different forces acting on a microsphere in an optical trap. Reflected light (scattering) pushes the bead along the optical axis. The refracted light generates a spring-like gradient force that centers the microsphere within the optical axis. Any deviations from the center cause a linear restoring force back to equilibrium. (ii) Schematics of an optical tweezer apparatus equipped for direct, momentum-based force measurements. V_x = Voltage signal on the position-sensitive diode. (iii) The deflection of the beam by the trapped object causes a deviation on the photosensitive diode V_x, which is proportional to the change in momentum of the light, ergo, in the force (F) acting on the trapped object. α=instrument specific calibration factor. The resultant force displacement plot is shown to the right. (iv) Force and displacement of the trapped microsphere under the influence of an oscillating trapping potential. (b) Fusion dynamics. Two droplets can be individually captured and fused (active fusion) using dual-trap optical tweezers, which also allow real-time monitoring of the fusion dynamics. The right panel shows the timecourse of the fusion dynamics for different aged pMe31B droplets. Reproduced with permission from Sankaranarayanan *et al.*, Dev. Cell **56**(20), 2886–2901 (2021). Copyright 2021 authors, licensed under a Creative Commons Attribution (CC BY) license. (c) Passive microrheology. An optical trap with a power below the trapping limit is used to detect the position of a microsphere inside a viscoelastic matrix with high bandwidth and sub-nm accuracy. The resulting trajectory reveals the mean-squared displacement of the particle in the matrix with indication for free or constraint mobility, and the complex shear modulus. Dashed line indicates loss modulus, solid line indicates the storage modulus. (d) Dual optical tweezer active microrheology. A phase-separated droplet is periodically deformed between two traps while recording the phase angle between the force signal and the trap position. The lag between force and displacement can be visualized in the Lissajous figures and provides access to the complex shear modulus and the surface tension of the droplet. Reproduced with permission from Jawerth *et al.*, Science **370**(6522), 1317–1323 (2020). Copyright 2020 AAAS. (e) Time-shared optical tweezer microrheology (TimSOM). A time-shared laser operating at a frequency of 25 kHz is used to simultaneously drive the motion of a microsphere and measure its displacement. Trap 2 (gray) remains stationary along the optical axis and detects bead displacements using BFP interferometry, while trap 1 (orange) actively applies a sinusoidal perturbation with an amplitude x_0 at the time-sharing frequency $1/f_{TS}$. The time-shifted force/displacement measurement introduces subtle deviations compared to continuous measurements in the instantaneous position of the probe particle in water and the resulting instantaneous optical force acting onto the probe for the TimSOM method. The interleaved force values for the static and driving traps are indicated by a thin dashed line. The total force on the probe is $F_1 + F_2$. Reproduced with permission from Català-Castro *et al.*, Nat. Nanotechnol. (published online). Copyright 2025 authors, licensed under a Creative Commons Attribution (CC BY) license.

composed of polypeptides containing sequences [RGXGG]5, where X = [P, S, R, F, Y], predominantly exhibit Maxwell fluid behavior, showing a wide range of viscosities, from approximately 0.1–40 Pa s.

Not restricted to optical tweezers, the passive rheological spectrum is also accessible from the diffusive dynamics of fluorescent probes and fast time-lapse imaging. For example, fluorescent microparticles[167] or genetically encoded viral capsid proteins,[168] or even fluorescently labeled components of the dense phase can in principle be used to record trajectories with high temporal and spatial resolution in and out of condensates.[169,170] Pixel-based recordings, however, are slower and have limited resolution but offer the advantage that many particles can be recorded simultaneously, significantly speeding up data acquisition. Optical tweezers, with their back-focal plane interferometry, facilitate recordings with nm displacements up to several kHz and are therefore faster and more sensitive to small displacements than normal camera-based detection of displacement.[170] This may be important, as Brownian article motions are powered by thermal fluctuations, therefore small, and thus fall into the linear viscoelastic regime. As the thermal fluctuations of the microsphere can become confined in very stiff environments and exhibit displacements approaching the detection limit of the back-focal plane interferometry technique,[159] passive microrheology may not be able to fully characterize LST.[22]

A potential solution to overcome the limit of thermally induced displacement is active microrheology. Here, a microsphere is delivered to a condensate by co-assembly, which can then be manipulated by an optical trap to sample the properties of the condensate over various periods of time.[89,142,149] One implementation of the technique involves two trapped microspheres that sandwich the droplet [Fig. 2(d)], while one oscillates with varying frequencies and the other keeps the droplet in place and measures the transmitted stress.[11,23,89] The frequency-dependent response of the droplet can be calculated from the forces acting on the microspheres according to

$$\chi^* = \frac{\chi^*_{sys}[4k_1k_2 + i\xi\omega(k_1 + k_2)]}{2k_1(2k_2 + i\xi\omega) - 4\chi^*_{sys}(k_1 + k_2 + i\xi\omega)}, \tag{3}$$

in which ξ is the fluid drag, k_i the stiffness of each of the traps, and $\chi^*_{sys}(\omega)$ is the frequency response of the entire system composed of traps and droplet and is given by

$$\chi^*_{sys}(\omega) = \frac{\tilde{F}_2 - \tilde{F}_1}{2\Delta\tilde{x}}, \tag{4}$$

where $\tilde{F}_i$ is the Fourier transform of the force on bead i and $\Delta\tilde{x}$ is the Fourier transform of the relative position of the beads $\Delta x(t)$. This gives access to the surface tension γ of the droplet and the complex bulk shear modulus,[172]

$$\gamma \approx \frac{\chi'(\omega)}{\pi}(-\ln(\theta_0) + 0.68), \tag{5}$$

$$G^*(\omega) \approx \frac{\chi^*(\omega) - (1.25 + 4.36\theta_0^2)\gamma}{R(5.47\theta_0^5 - 29.28\theta_0^4 + 23.29\theta_0^3 - 5.08\theta_0^2 + 3.79\theta_0 - 0.02)}, \tag{6}$$

where $\chi'(\omega)$ is the real part of the complex response function, R is the radius of the spherical droplet, and $\theta_0 = r_b/R_d$ is the ratio of microsphere and protein droplet diameter.

This method was recently used to show that several types of biomolecular condensates responded like a viscoelastic liquid, or Maxwell material[11,23] (Box 2). Similar to a frustrated glass which relaxes toward a state of lower energy, these droplets were characterized by an age-independent elastic modulus but an increasing viscoelastic relaxation rate, and was succinctly coined "ageing Maxwell glass." The timescale at which these condensates mature and their final mechanical properties depend on various parameters, including molecular composition, temperature, salt concentration, and pH.[89,173] As this formalism requires two independent, calibrated optical traps, this particular implementation may be prohibitive to non-specialist labs. Furthermore, the surface tension delimits the lower frequency values such that the complex bulk modulus at the lowest frequencies becomes inaccessible.

To overcome these difficulties, direct momentum-based force measurements[159,174] have recently been used to perform active rheology of various condensates in an approach called time-shared optical tweezer microrheology (TimSOM)[142] [Fig. 2(e)]. Here, a single laser is used to measure stress and strain quasi-simultaneously over a frequency band ranging from 0.2 to 6.000 Hz and between ≈0.1 and ≈10 kPa. The method uses two traps generated by the same laser source that act simultaneously on the bead. Before starting the active micro-rheology routine, trap 1 and trap 2 are both placed in the center of the particle. Once centered, trap 1 starts to oscillate at a driving frequency ω, that is, $x_1(t) = x_0\sin(\omega t)$, while trap 2 remains fixed at $x_2(t)$=0, with x_0 as the amplitude of the oscillation and $x_1(t)$ and $x_2(t)$ as the trajectory of the driving and static trap on the laboratory frame. In general, the two traps have the same position sensitivity β and stiffness k. Because the microsphere will feel a force from both traps, the contributions from both the driving and the static traps need to be taken into account to calculate the complex response function $\hat{\chi}(\omega)$ and the complex shear modulus $\hat{G}(\omega)$,

$$\hat{\chi}(\omega) = \frac{\hat{x}(\omega)}{\hat{F}_{tot}(\omega)} = -\frac{2\hat{V}_2(\omega)}{k[\hat{V}_1(\omega) + \hat{V}_2(\omega)]}, \tag{7}$$

$$\hat{G}(\omega) = \frac{1}{6\pi a}\frac{1}{\hat{\chi}(\omega)} = -\frac{k}{12\pi a}\frac{\hat{V}_1(\omega) + \hat{V}_2(\omega)}{\hat{V}_2(\omega)}, \tag{8}$$

in which $\hat{V}_1(\omega)$ and $\hat{V}_2(\omega)$ are the Fourier-transformed trap signals recorded for the driving and the static trap for each frequency, and a is the microsphere radius. Importantly, the voltage signals V_1 and V_2 are directly proportional to the momentum change of the light interacting with the microsphere, and thus afford direct, calibration-free force measurement inside complex media.[174,175]

As can be seen, the method does not require explicit knowledge of the conversion factor β to determine $\hat{G}(\omega)$. That means that the accuracy of the proposed method is based on the ability to generate two identical traps from a single laser source and to obtain two measurements of $V_1(t)$ and $V_2(t)$ that have identical sensitivities. Consequently, the stiffness of the trap k is the single most important parameter that fixes the scale and precision of the measurement, which is adjustable by varying the power of the laser beam that controls the strength of the total stiffness of the traps. However, because the laser trap alternates between driving the microsphere deflection and measuring it with the static trap, the method does not satisfy the criterion of simultaneous measurement of stress and strain. Although this may generate deviations in the measurements from the expected ideal scenario, especially at high frequencies for Maxwell materials, a mathematical

compensation formalism was introduced to balance the measured response to obtain the expected response.[142] This method has been successfully used to measure the frequency-dependent response of MEC-2 and CPEB4.

The advantage of this implementation is that momentum-based force measurements provide a direct estimate of the force[174] and therefore do not require the elaborate calibration procedure common to optical trapping experiments. Thus, it is not affected even if the droplet changes viscosity or refractive index during LST and, in principle, can be easily applied inside cells or even animals.[142] Furthermore, it can be implemented on any inverted microscope without complicated optical alignments of multiple laser sources and detectors.

Shortcomings: Optical gradient traps apply/measure force to/at refractive interfaces; thus, the laser may interact directly with the condensate. *In vivo*, biomolecular condensates often do not display a different refractive index compared to the surrounding cytoplasm, which limits their applicability inside cells if highly refractive microspheres cannot be delivered reliably. To avoid excessive heat deposition into the sample (condensate), optical tweezers must be operated at low powers (<100 mW), which limits the maximum force it can apply. Furthermore, active and passible rheology measurements require a refractive force probe, commonly a polystyrene microsphere, which needs to be embedded into the condensate. This may alter the outcome of the measurement.

B. Atomic force microscopy (AFM)

AFM is a popular tool for quantifying the interaction force between the surface of a cantilever and a substrate.[176] AFM offers one of the largest dynamic ranges of force measurement, as it depends on a microcantilever that can be conveniently exchanged to match the expected stiffness of the sample under study and can be integrated with an optical microscope to allow multimodal observation of the sample with complementary optical techniques.[177] It was widely applied to measure the mechanobiology of single cells[178] and single molecules,[179] and more recently, it was recognized as a suitable tool to characterize the contact mechanics of biomolecular condensates.[155,180] The principle relies on a semi-flexible cantilever (with a known spring constant) that is functionalized with a small microsphere [Fig. 3(a), panel i]. The movement of the cantilever is controlled by a piezo element with nanometer precision such that the probe can be brought into contact with a surface immobilized droplet. Upon contact with the droplet surface, the cantilever bends, which is recorded and provides information about the contact force and droplet deformation directly giving access to the structural stiffness[178] [Fig. 3(a), panels ii and iii]. The appropriate models that relate force and contact area predict their material properties (such as Young's modulus E or shear modulus G). For example, the Hertz model may be used for contacts between two homogeneous, isotropic elastic spheres with diameter D_c and D_s of the condensate and microsphere respectively, and may be appropriate for solid condensates, or viscoelastic condensates that are deformed faster than their relaxation rate,

$$F \approx E^* \sqrt{K_D} \delta^{3/2}, \tag{9}$$

in which F is the contact force, E^* is the reduced Young's modulus, δ is the droplet deformation, and $K_D = \frac{D_c \cdot D_s}{D_c + D_s}$.[181] To avoid slippage, the condensate should be firmly attached to the substrate. Conveniently, the condensates can be allowed to completely wet the substrate and form a thin film, in which case the contact model reduces to the simple Hertz model of a sphere contacting an infinite half-space with $K_D = D_s$. However, the film must be thick enough to avoid that the stiffness of the substrate influences the mechanics measurements.[182] This procedure was used to characterize condensates composed of postsynaptic density proteins *in vitro*.[183]

However, if the spherical droplet behaves more as a liquid-like material with a surface tension, the cortical shell-liquid core model may be more appropriate,

$$F = \left[2\gamma \left(\frac{1}{R_c} + \frac{1}{R_s} \right) \times 2\pi R_s \right] \times \delta, \tag{10}$$

in which γ is the surface tension, R_c and R_s are the radii of the condensate and the microsphere, respectively, and δ is the indentation secondary to the contact force F. These models assume that there is no adhesion between the probe cantilever and the condensate, but often a capillary bridge may form between the two surfaces.[173,184] The interfacial tension between the coacervate phase and the coexisting aqueous phase can then be directly assessed from the cantilever retraction curves.[184]

Similarly, FRAP-ID (fluorescence recovery after probe-induced dewetting) combines AFM force spectroscopy and fluorescence measurement to characterize both surface tension and viscosity of thin condensate films wetting a glass surface, from the retraction and approach curves, respectively.[155] If a high enough contact force is applied to the thin condensate film, then a "dry" spot is created where the film dewets the surface. When the force is released by lifting the cantilever, the surface tension in the film will drive the mass flow back into the dry spot (during the rewetting process) and can yield information about the viscosity. Together with the surface tension derived from the adhesive force during cantilever withdrawal, the inverse capillary velocity can be determined.[155] As both the Hertz and cortical shell model assume pure elastic and viscous properties, they do not appropriately characterize frequency-dependent properties. Thus, like in optical tweezers, AFM can be used to record a rheological spectrum by oscillating the cantilever with varying frequencies,[173] while recording the phase lag of the cantilever response. Using this formalism, it was shown that the interfacial tension of soy protein condensates increases during a liquid-to-solid transition,[173] while the rheological properties of heterotypic poly-L-lysine–heparin condensates reveal multipathway liquid-to-gel transitions, along with the potential for rejuvenation through chemical modifications to the surrounding medium.[185] Due to its ability to measure with high forces and small deformations, AFM has been widely applied to characterize the mechanical properties of stiff amyloid fibers[186] and pathological tau assemblies.[187] Those experiments showed that Young's modulus of most amyloid fibrils is in the range of 2–4 GPa.

Shortcomings: The widespread availability and user-friendly design of commercial AFM instruments have significantly advanced research in mechanobiology. However, the technique remains restricted to measuring mechanical effects on the surface of the sample. Thus, condensates can only be probed *in vitro*, or to some extent through the interaction of the tip with the plasma membrane, inside cells. If not passivated properly, a strong interaction of the cantilever tip with the condensate will prevent complete separation during the cantilever retraction.

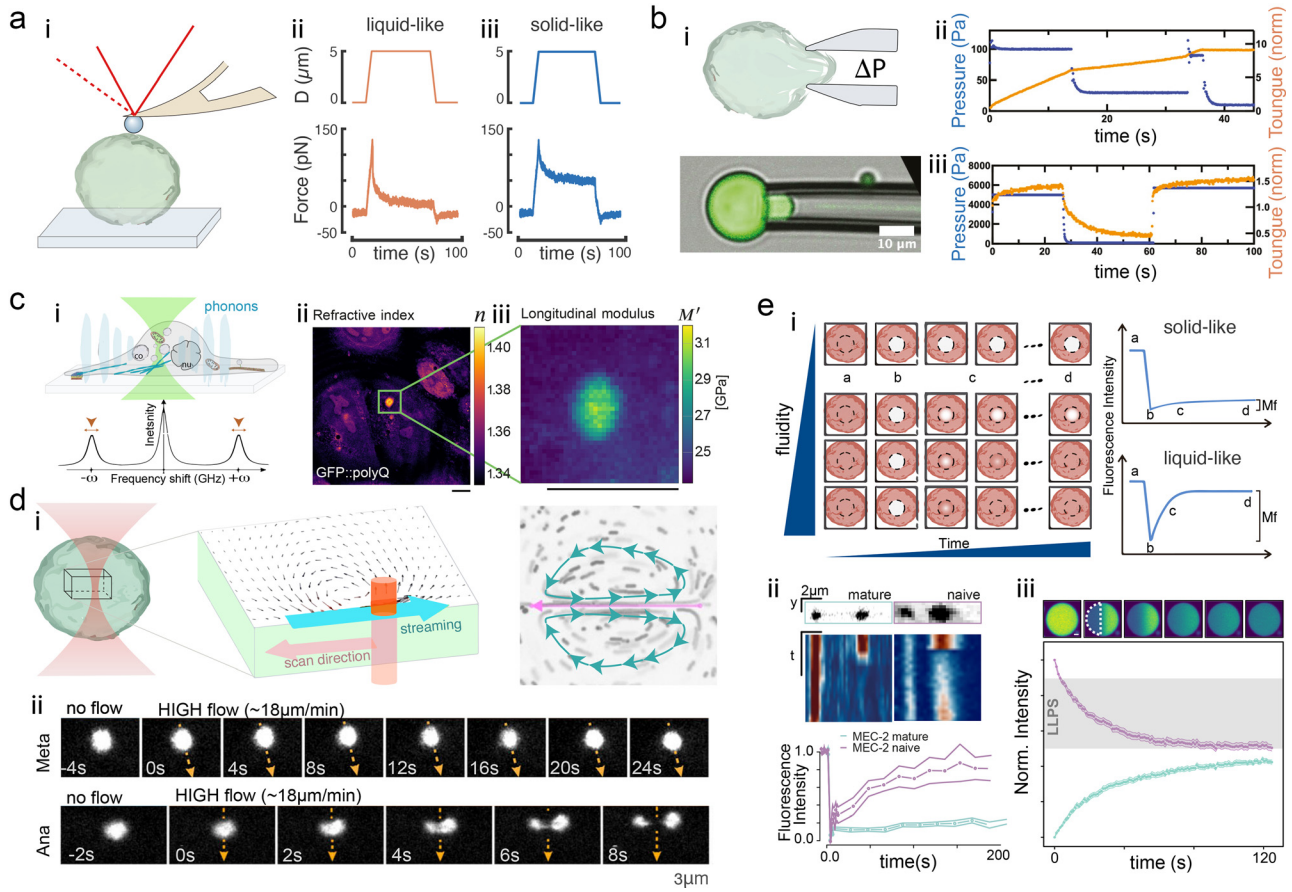

FIG. 3. Methods to infer mechanical states *in vitro* and *in vivo*. (a) AFM-based colloidal force probe microscopy leverages a small microsphere-modified cantilever to measure the contact mechanical properties. (i) Schematics of the experiment. A laser is reflected off the back of the cantilever toward a quadrant photodiode, measuring the cantilever bending and thus contact force. (ii) Indentation (D) and force, time plot of a hypothetical, liquid-like condensate and (iii) viscoelastic solid-like condensates. (b) Micropipette aspiration. (i) Schematics and photograph of the experiment in which a negative pressure is used to aspirate the BMCs. (ii) The timecourse of the aspirated part of the condensates as a function of pipette pressure visualizes the viscoelastic response before (8 h) and (iii) after the liquid–solid transition of FUS droplets (48 h). Reproduced with permission from Shen *et al.*, Proc. Natl. Acad. Sci. **120**(33), e2301366120 (2023). Copyright 2023 authors, licensed under a Creative Commons Attribution (CC BY-NC-ND) license. (c) Brillouin microscopy. (i) Schematic of the experiment. A focused laser light interacts with phonons, which causes a laser wavelength-dependent frequency shift that is proportional to the longitudinal modulus of the probed sample volume but also refractive index. (ii) Refractive index image of a cell expressing GFP::polyQ. (iii) Image showing the longitudinal modulus determined by Brillouin spectroscopy of the green ROI in (ii). Scale bars = 10 μm. Reproduced with permission from Schlüßler *et al.*, eLife **11**, e68490 (2022). Copyright 2022 authors, licensed under a Creative Commons Attribution (CC BY) license. (d) Schematic of the FLUCS (focused-light-induced cytoplasmic streaming) experiment. (i) An infrared laser is focused into a condensate and scanned along the pink line, which generates fluid convection due to heat deposition. Using fiducial fluorescent tracers, the flow field can be quantified (green arrows). (ii) Representative example of how the pericentriolar material becomes less stable during anaphase compared to the metaphase and appears to deform and eventually split during anaphase. Reproduced with permission from Mittasch *et al.*, J. Cell Biol. **219**(4), (2020). Copyright 2020 Rockefeller University Press. (e) Fluorescence recovery after photobleaching (FRAP). (i) Schematic representation of a FRAP experiment in which a region of interest (circle delimited by a dashpot line) within the condensate is bleached with a high-intensity laser spot and observed over different time points (a–d). No recovery will be observed for a perfect solid when the mobility of the labeled species is in constraint (right, upper panel), while fast and unconstraint mobility will lead to complete recovery (right, lower panel). Mf = mobile fraction of labeled molecules. (ii) Experimental data derived from naive and matured MEC-2 condensates *in vivo*, showing a representative snapshot and kymograph (top), together with the recovery curves (bottom) for the two droplet populations, naive and mature. Reproduced with permission from Sanfeliu-Cerdán *et al.*, Nat. Cell Biol. **25**(11), 1590–1599 (2023). Copyright 2023 authors, licensed under a Creative Commons Attribution (CC BY) license. (iii) Representative example of a half-FRAP experiment in which recovery is observed after bleaching half of the droplet and observing the recovery (green) and loss (purple) of fluorescence in the two hemispheres. Reproduced with permission from Muzzopappa *et al.*, Nat. Commun. **13**, 7787 (2022). Copyright 2022 authors, licensed under a Creative Commons Attribution (CC BY) license.

C. Micropipette aspiration

Micropipette aspiration (MPA) is a technique used to measure the mechanical properties of small biological samples such as cells[188] and has recently also been used to measure the mechanics of BMCs.[38,189–191] This method involves the application of a controlled negative pressure through a micropipette to aspirate a portion of the cell or condensate [Fig. 3(b), panel i], allowing for the assessment of

various biomechanical parameters such as elasticity, viscosity, and surface tension[189] [Fig. 3(b), panels ii and iii]. In this technique, a fine glass capillary tube is carefully fashioned to have an internal diameter ranging from a few micrometers to tens of micrometers, tailored to the size of the condensate being studied. This micropipette is then mounted onto a micromanipulator to control its position and movement. Once the micropipette is in contact with the sample, a controlled negative pressure is applied through the micropipette, drawing a portion of the condensate into the tube. This pressure is meticulously regulated by a microfluidic pressure controller, and informs about the condensates mechanical properties. The rate of entry into the pipette is related to the viscosity, while the critical pressure P_c informs about the surface tension. The pressure at which a hemispherical protrusion of the condensate enters the pipette can be used to determine the droplets interfacial tension γ according to

$$\gamma = \frac{P_c}{2 \times \left(\frac{1}{R_P} - \frac{1}{R_D}\right)} \tag{11}$$

with R_p and R_c as the pipette and condensates radii, respectively.[38] Excitingly, MPA has been applied to measure the mechanical properties of synapsin condensates directly in heterologous cell types and afforded measurement of viscosity and surface tension directly *in vivo*.[192] In addition, the integration of MPA with microfluidics may allow high-throughput measurements and integration with optical microscopy.[193]

Shortcomings: Although MPA has been classically applied to cells to analyze their mechanics in light of the liquid-droplet model, more sophisticated models are just emerging, which may limit the application to aging condensates. Because it requires a complete seal of the pipette entrance with the condensate, it cannot be used to probe irregular structures, such as amyloid fibers. Also, the force resolution is rather limited, rendering the technique insensitive to subtle changes—a possible reason why elasticity values derived from MPA are rather high.

D. Brillouin microscopy

In the recent years, Brillouin microscopy has emerged as a popular tool to measure the mechanical properties of biological samples in a noninvasive manner.[194] Brillouin microscopy operates on the principle of Brillouin scattering, which involves the interaction of light with a phonon which are spontaneous, thermally induced density fluctuations, or acoustic waves, to measure mechanical properties in materials. To do so, a laser beam is focused onto a sample, where the photon/phonon interaction causes the photon energy to increase or decrease [Fig. 3(c), panel i]. The scattered light is collected and analyzed for the frequency shift (ω) caused by acoustic waves [Fig. 3(c), panel i]. Specifically, the shift ν_B is influenced by the speed of sound V in the material and the wavelength of the incident laser light λ,

$$\nu_B = \sqrt{\frac{M'}{\rho}} \cdot \frac{2n}{\lambda} \sin(\theta/2) \tag{12}$$

with θ as the angle between the incident and scattered light.[194] Due to the dependence of the speed of sound, among others, on the material properties of the probed different structures, these Brillouin shifts are indicative for the local mechanical properties of the sample. These properties are recapitulated in the complex longitudinal modulus $M = M' + iM''$. The real part M' of the longitudinal modulus provides information on the elastic properties of a material (peak position), while the imaginary part iM'' is related to the longitudinal viscosity η of the medium [peak width, Fig. 3(c), panel i]. By mapping these frequency shifts across the sample, Brillouin microscopy can provide spatially resolved information about the mechanical properties of cells and their embedded organelles [Fig. 3(c), panels ii and iii]. As these shifts also depend on the refractive index n of the sample volume, there has been ongoing debate as to what the shifts correspond to, but without major changes in n, the real part of the shifts can be assigned to differences in the longitudinal elastic moduli, while the imaginary part of the linewidth reports viscoelastic properties.[195,196]

Critically, as the Brillouin shift depends on the longitudinal modulus and refractive index, correct interpretation requires independent measurements of both quantities. The refractive index can be measured using optical diffraction tomography, which is an optical measurement of the path length difference of light as it passes through the sample and undergoes diffraction and phase shifts due to variations in the sample's refractive index. These changes in the light's phase and intensity are measured using interferometric techniques. Purely optical, this modality is compatible with Brillouin microscopy and a combined setup has been designed to measure n and M in the same cell.[197] Using this approach, it was found that poly-Q aggregates have a higher refractive index and longitudinal modulus than the surrounding cytoplasm [Fig. 3(c), panels ii and iii], in contrast to other condensates, e.g., FUS stress granules which show RI and longitudinal modulus similar to the surrounding cytoplasm in HeLa cells.[199]

Brillouin microscopy was also used to assess the aging of FUS and hnRNPA1 *in vitro*,[196] as well as to study wild-type FUS (wtFUS) and mutant FUS expressed in HeLa cells.[198] The latter work represents the first documentation of the mechanical properties of biomolecular condensates (BMCs) within cells and their age-dependent liquid-to-solid transitions (LST).[198] However, due to the rapid cellular dynamics *in vivo*, recording spatiotemporally resolved mechanical maps at the cellular scale is nearly impossible without appropriate animal immobilization or anesthesia. Thus, the experiments used cells chemically fixed with 4% paraformaldehyde to "freeze" the dynamic processes of living cells during the 15-min measurement period.

Because spontaneous Brillouin is a rare process, it requires high laser intensities (tens of mW) and long acquisition times (tens of minutes).[198,199] Several recent developments offered improvements of the technique through line scanning[200] and pulsed stimulated Brillouin microscopy.[201] In particular, stimulated Brillouin techniques have the additional advantage of superior spectral resolution, increased dynamics as more photon/phonon pairs can be measured, and measurements of mass density to more accurately interpret the Brillouin shifts in terms of the sample's mechanical properties.[195,202] Operation of the pump laser in a pulsed fashion resulted in a 20-fold reduction in average laser power without negatively affecting the obtained Brillouin signal.[201] In the future, these developments may improve the ability to investigate how liquid–solid transitions are modulated directly within the cellular environment.

Shortcomings: Although Brillouin microscopy offers compelling advantages as a label-free technique providing diffraction-limited

mechanical maps, there may be considerable uncertainty as to the physical origin of the frequency shift and its interpretation.[203] Furthermore, the shift ν_B is instrument-specific and thus difficult to compare between laboratories and samples, while measurement times are long and may require high laser powers compared to other techniques.

E. Photophoresis

Focused-light-induced cytoplasmic streaming (FLUCS), also known as photophoresis, occurs upon the absorption of light energy by photosensitive molecules within the cell, leading to localized heating and consequent changes in cytoplasmic viscosity. This, in turn, induces fluid motions and directed movement of organelles and the viscous cytosol [Fig. 3(d)]. Is the focused light scanned across the sample, this causes light-induced traveling temperature fields and associated mass transport (advection). The direction and speed of cytoplasmic streaming can be controlled by altering the intensity and direction of the light source. Practically, FLUCS can be generated by scanning a low-power, infrared laser beam with a wavelength tuned to the absorption maximum of water (1550 nm).[204] Thermal expansion at the front of the beam drives these flows toward the end of the path where the flow is contracting [Fig. 3(d)].

The laser beam generates a heated spot within the fluid and is repetitively scanned along a short path, operating at approximately 2 kHz frequency. This leads to the overall movement of substances within the fluid that is typically opposite to the direction of the laser's motion, especially in proximity to the scan path. To achieve significant substance movement at physiological rates, only minor temperature adjustments, typically just a few kelvins, are necessary, thus preventing harm to the cell.[204,205] This thermoviscous-powered flow can then be used to apply a shear force to cytoplasmic organelles, including biomolecular condensates. This force is typically on the order of fN, and its precise magnitude depends on the viscosity of the cytosol and the velocity of the flow field. Because it is nearly noninvasive, it can be operated inside transparent embryos and tissue culture cells, allowing for the investigation of condensates in their native environment. With FLUCS, the molecular components and temporal events leading to a solid–liquid transition during mitosis were established [Fig. 3(d) and below]. More recently, FLUCS measurements mapped the mechanics of the nucleolus and the compartmentalization of chromatin in living nuclei, showing that these behave as viscoelastic solid-like materials[206]—a property that was also observed with active optical tweezer microrheology.[142]

Shortcomings: Photophoresis requires the sample to have a relatively low viscosity, as the induced flows occur only in viscoelastic fluids or very soft viscoelastic solids, but not in elastic materials. Photophoretic forces are generated through local heating of the sample, which can alter the mechanical properties of the cell or disrupt biological processes. Especially in tissues, variability in light absorption and scattering may lead to inconsistent results, making comparison with other systems and measurements difficult.

F. Fluorescence recovery after photobleaching (FRAP)

Owing to the simplicity and accessibility of the FRAP experiment to a wide range of users, since it can be performed without special training on any fluorescence confocal scanning microscope, it is by far the most popular technique to characterize the dynamics of biomolecular condensates. FRAP experiments have been conducted for decades on fluorescently labeled molecules inside cells, by which a portion of the labeled structure is bleached with a high laser intensity while recording a timelapse movie as labeled molecules diffuse into the bleached area. It is one of the few techniques that have been used excessively to characterize the material states *in vivo* by measuring the change in the apparent diffusion coefficient and the mobile fraction [Fig. 3(e), panels i and ii]. Often, a simple exponential is fitted to extract these parameters from the experimental measurement. If a liquid–solid transition of the condensates takes place, one would expect an increase in recovery timescale (decrease in the diffusion coefficient D), and a decrease in the mobile fraction M_f. However, the interpretation of the FRAP curves in light of the condensate mechanics is not that simple, as the diffusing species come from the unbleached portion of the condensates or the dilute phase. In addition, a change in the FRAP recovery dynamics may not be detected if maturation leads to a change in the elastic properties of the meshwork and the labeled species freely diffuse through its pores.[11,16] To overcome some of the inherent difficulties in FRAP experiments, more sophisticated models and experimental protocols have been introduced to distinguish recovery within and outside the condensates.[207,208] For example, a *mo*del-free *c*alibrated *hal*f-FRAP (MOCHA-FRAP) protocol can distinguish LLPS-driven condensation from other forms of transient binding. In this framework, bleaching half the condensate while analyzing the fluorescence recovery in the bleached domain and the fluorescence loss in the unbleached domain [Fig. 3(e), panel iii] can yield quantitative information on the mixing dynamics and the energy barrier impeding exchange of bleached and unbleached molecules with the lean phase.[208]

Shortcomings: Although FRAP is the most widely applied method for characterizing the fluidity of biomolecular condensates *in vivo*, careful interpretation of the data is required and is best suited as a complementary technique rather than as a standalone method for mapping cell mechanics in dynamic biological systems. Because FRAP measures the mobility of the labeled species, the parameters about the elasticity of the sample are usually not accessible. Thus, a FRAP experiment cannot differentiate between an increase in viscosity and an elastic network formation. Hence, FRAP results should not be used as a proxy to decide if a condensate has liquid-like or other properties. Furthermore, typical measurements reflect the mobility of labeled species at a population scale, in contrast to single-molecule tracking, and therefore cannot be used to derive scaling exponents to differentiate directed, diffusive, or constraint motion.

V. THE PHYSIOLOGY OF LIQUID–SOLID TRANSITIONS

The consequence of a liquid–solid transition in biomolecular condensates is a shift from a dynamic, fluid-like state to a more rigid, gel-like, or solid state. In the liquid state, molecules within the condensate can move freely and interact dynamically, allowing for rapid exchange and reorganization of components. This fluidity is crucial for many biological processes, such as signaling, enzymatic reactions, and the formation of transient cellular structures.

However, when a liquid–solid transition occurs, the condensate becomes more structured and less dynamic, which can affect its biological function. This solid-like state can trap molecules and reduce their mobility and reaction rates. In some cases, it can alter the normal functioning of cellular processes through the formation of pathological aggregates that lead to neurodegenerative disease. However, in other

cases, this mechanical stabilization can be beneficial, and the condensate adopts specialized properties that are tuned to fulfil certain cellular functions.

A. Buffering protein availability in a solid condensate

One of the stereotypic functions assigned to BMCs is to concentrate reactants for efficient biochemical reactions.[13] If the enzymatic reaction is dependent on a flexible protein, a higher mobility of the condensate would allow for molecular gymnastics and a rapid exchange of adducts and products.[209] Thus, a controlled and timely solidification of the condensate can guide chemical reactions, limit their availability, and, more importantly, restrict their conformational dynamics and access to transition states.[210] Likewise, solid condensates can trap RNAs and other proteins just to release them at a later time through regulated fluidification.[118] At their extreme, Balbiani bodies within oocytes form without any visible liquid-like state through a condensate-spanning amyloid network composed of Velo1 proteins,[211] with the proposed aim of trapping organelles and RNA, while excluding factors that would pose a long-term harm to oocyte health.

Viscoelastic phase transitions were also shown to be an important function of ribonucleoprotein (RNP) granules in *Drosophila* oocytes.[28] *In vivo*, assembly of *oskar* 3'UTR with the scaffold granule proteins Bruno and Hrp48 resulted in the formation of spherical condensates, thought to have formed through LLPS, but lacked discernible dynamics such as fusion and fluorescence recovery after photobleaching.[28] Because liquid-like behavior could not be detected *in vivo*, this suggested that these condensates swiftly mature into a solid state, indicating an immediate liquid-to-solid transition. This notion is further confirmed by the small size of the condensates, which are arrested as sub-micrometer particles rather than fusion into larger condensates. Importantly, the solid phase was amorphous without any detectable structural features inherent to amyloids as determined by cryoelectron tomography, suggesting a frustrated, glassy state or terminal solid material. The proposed liquid–solid transition had interesting gene regulation functions: while *oskar* mRNA was rapidly incorporated into liquid-like condensates, it was excluded from their aged, solid counterparts and was found primarily at the surface. The liquid-like state of these condensates promoted transport and delayed translation of *oskar* mRNA, while the solid-like state promoted translation and inhibited transport.[28] Disturbing the solid state of these granules *in vivo* through fusion of the mRNA to the FUS IDR rendered the condensates more liquid-like and consequently impaired the translation of *oskar* mRNA. This highlights the significance of the regulation of granule material properties for RNA post-transcriptional control and developmental processes.

B. Viscoelastic transitions at the neuronal synapse

The synapse between two neurons is an intercellular specialization rich in biomolecular condensates.[212] Synaptic structures, such as presynaptic and postsynaptic densities, rely on the liquid–solid transition for their development and stabilization and strongly affect synaptic function.[35,213] As the LST leads to increased viscosity and elasticity, the movement of components within them slows down, potentially trapping important cellular signaling molecules[214] and therefore enriching low-copy-number proteins in the small volumes of pre- and postsynaptic sites.[212] However, when these viscoelastic condensates dissolve (e.g., in a regulated solid–liquid transition), the trapped molecules can be released and become available again. For example, stiffened condensates can temporarily trap weakly bound molecules after they have been concentrated within the condensates.

In an effort to reconstitute the postsynaptic density complex, a potpourri of four different scaffold proteins from excitatory synapses (PSD-95, Shank, GKAP, and Homer3) was shown to partition into biomolecular condensates and to enrich two other factors, NMDA (NMDAR) glutamate receptor (NR2B) and GTPase-activating enzymes (SynGAP), which are naturally enriched in postsynaptic densities.[183,215] Intriguingly, this minimal PSD-95 also excluded scaffold proteins known to be restricted to inhibitory synapses, such as gephyrin. This exclusion could be due to electrostatics or simply to steric constraints.[21] AFM measurement showed that the complete reconstitution with all six components had a higher elastic modulus and an increased solidity compared to the minimal complex only composed of PSD-95 and SynGAP. Furthermore, complete PSD condensates showed considerable aging behavior as soon as 50 min after droplet formation and stiffened from 3.5 ± 1.5 kPa to approximately 16 ± 3 kPa over a period of 5 h. The solid transition of the excitatory PSD condensate may aid their segregation from inhibitory PSDs, as mixing strongly percolated PSDs generated by high-affinity interactions is energetically costly.[216] Furthermore, because PSDs were shown to condense on supported membranes and could coordinate actin polymerization and bundling, it may be speculated that the elastic phase transition helps shape postsynaptic compartments.[183] It may also stabilize synapses against mechanical stresses that act on synaptic adhesions and therefore may be essential for the clustering of neurotransmitters[217] and structural maintenance in living tissues subjected to mechanical forces through muscle[218] or vascular activity.[219] Recently, Orb2, an RNA-binding protein of the CPEB family, was shown to phase separate and undergo LST[220] at synaptic sites to form functional amyloids.[221] These solid structures play a crucial role in the formation of long-term memories by regulating the translational control of specific mRNAs at synapses. The solid amyloid-like state has been hypothesized to act as a template and facilitate the conformational transformation of existing or newly formed monomers, establishing a self-perpetuating protein "conformational memory" that persists beyond the lifetime of its individual components.[221]

Likewise, presynaptic densities undergo a maturation similar to a liquid–solid transition[213] *in vivo*. Work in *C. elegans* uncovered that the presynaptic proteins SYD-2 (Liprin-α) and ELKS-1 (ELKS/RAB6-interacting/CAST family member 1) phase separated in a heterologous cell system and formed liquid-like biomolecular condensates in developing synapses of embryonic worms, which matured into stable scaffolds in animals after hatching.[213] Similarly, the SYD-2 and ELKS-1 condensates underwent time-dependent solidification after 1 h *in vitro*. In fact, the fluid character was essential for the assembly of the active zone and the incorporation of other presynaptic components UNC-10 (worm RIM homolog) and GIT-1 (ARF GTPase activating protein GIT1), while solidification fixed the molecular composition and these auxiliary components did not enter (or left) the condensates [Fig. 4(a)]. As neurons and the synapses between them are subject to constantly changing mechanical forces,[222] pre- and postsynaptic

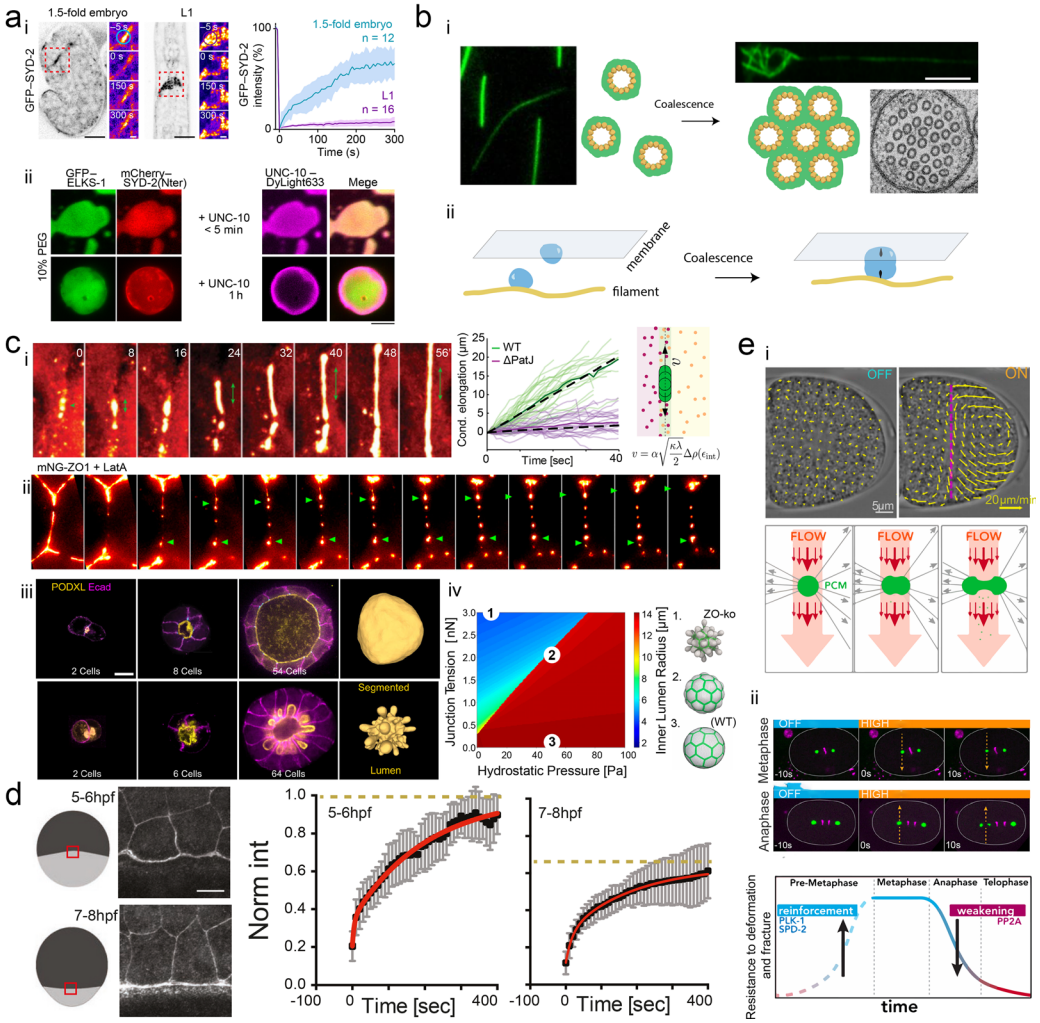

FIG. 4. Condensates and their physiological role in mechanobiology. (a) During *C. elegans* development, presynaptic active zone proteins mature from a liquid pool in 1.5-fold embryos into a non-dynamic, mature pool in L1 larval stages. (i) Representative images of a 1.5-fold embryo and L1 larva labeled with SYD-2 in the nerve-ring—the neuropil of *C. elegans* and the FRAP curves for both stages. Scalebar 5 and 1 μm. (ii) *In vitro* observations indicate that UNC-10 co-assembles with ELKS/SYD-2 naive condensates (5 min after formation), whereas UNC-10 does not co-condense when it is added 1 h after droplet formation. Scalebar = 5 μm. Reproduced with permission from McDonald *et al.*, Nature **588**, 454–458 (2020). Copyright 2020 Springer Nature. (b) Interfacial forces may drive reorganization of various intracellular complexes, including cytoskeletal filament bundles, and membrane-filament interactions, in addition to their well-studied role in membrane deformation. (i) Single microtubules decorated/wetted by tau proteins *in vitro*. Coalescence of tau liquid condensates may organize microtubules into larger bundles. Upper panel shows PTL-1 TAU decorated microtubule bundles in touch receptor neurons in *C. elegans* and their cross section. Scalebar = 5 μm. (ii) Similar coalescence may be important for capillary bridges that bring filaments close to the membrane to organize the actin cortex or ion channel activity. (c) Zonula occludens 1 (ZO-1) protein condensate tension balance luminal hydrostatic pressure. (i) Assembly of ZO condensates at the tight junction interface resembles a pre-wetting transition. A thermodynamic model predicts that the velocity v of wetting is constant and depends on molecular interactions (ϵ) with cytoplasmic scaffold protein PATJ. Reproduced with permission from Pombo-García *et al.*, Nature **632**, 647–655 (2024). Copyright 2024 authors, licensed under a Creative Commons Attribution (CC BY) license. (ii) Representative image sequence of ZO-1 condensates dewetting MDCK junctions after treatment with latrunculin A, visible as dynamic beads on a string, indicating that pre-wetting dynamics depend on actin. Reprinted with permission from Beutel *et al.*, Cell **179**(4), 923–936.e11 (2019). Copyright 2019 Elsevier. (iii) Representative images of MDCK cysts in presence and absence of ZO proteins, indicating a loss of volume due to unregulated myosin contraction. (iv) Morphological phase space with varying tight junction tension and luminal hydrostatic pressure. Snapshot of the right resemble the morphology in the regions indicated in the phase space. (d) Zonula occludens 1 (ZO-1) protein condensates undergo liquid–solid transition *in vivo*. Reproduced with permission from Mukenhirn Dev. Cell **59**, 2866–2881 (2024). Copyright 2024 authors, licensed under a Creative Commons Attribution (CC BY) license. At the right, Schematic of a zebrafish embryo at different stages of gastrulation and corresponding fluorescence photograph of labeled ZO-1b taken in the indicated ROI. FRAP curves of non-junctional ZO-1b in the yolk syncytial layer at early and late stages of gastrulation during zebrafish development. Non-junctional ZO-1b initially display properties of liquid-like condensates that might undergo a maturation process leading to their immobilization. Scalebar = 20 μm. Reprinted with permission from Schwayer *et al.*, Cell **179**, 4 (2019). Copyright 2019 Elsevier. (e) FLUCS measurements indicate solid–liquid transitions of the centrosome in the metaphase/anaphase transition during mitosis. (i) Representative flow field and force vectors acting on a PCM *in vivo*. (ii) Example of how the FLUCS-induced flow field perturbs PCM integrity in a cell-cycle dependent manner. Upper images show fission of a liquid PCM in anaphase, but not in metaphase. Reproduced with permission from Mittasch *et al.*, J. Cell Biol. **219**(4), 1–17 (2020); Copyright 2020 Rockefeller University Press.

scaffolds may also provide mechanical resistance and stability to neuronal connections and thus may be fundamental for learning and memory.

VI. MECHANOBIOLOGICAL FUNCTIONS OF BIOMOLECULAR CONDENSATES

Despite the well-documented role of biomolecular condensates in various cellular processes, their physiological functions in mechanobiology are just emerging. The realization that condensates can exert forces on the attached structure through a capillary effect but also adopt different mechanical states provided an exciting link between condensates and their functions in mechanobiology. Here, we use representative case examples to illustrate how biomolecular condensates can participate in the response to mechanical force. These include, but are not limited to, (a) organizing force-generating structures, e.g., through local nucleation and bundling of actin filaments[223,224] and microtubules;[224,226] (b) surface capillary actions of liquid condensates that participate in membrane remodeling and cell organization;[44] and (c) liquid–solid transitions and their role in mechanotransduction.

A. Regulation of the cytoskeleton and motor functions

The cytoskeleton is an important cellular component that endows most animal cells with their mechanical properties.[227] Actin and microtubule filaments not only provide resistance to mechanical force but can itself be the origin of force generations due to associated molecular motors and filament (de)-polymerization.[228] Biomolecular condensates can dynamically reposition actin or microtubule nucleating proteins by serving as localized hubs that concentrate and organize these proteins.[229] Through phase separation, condensates can sequester monomers in specific regions of the cell above their concentration threshold for polymerization, thus modulating the growth and activity of the cytoskeleton. This spatial organization enables targeted filament assembly and guides cellular processes such as migration, division, and shape maintenance. Furthermore, the material properties of condensates, such as their fluidity or viscosity, can influence the mobility and interaction dynamics of nucleating proteins, further fine-tuning the formation of cytoskeletal networks.[19]

1. The actin cytoskeleton

The coordinate assembly of biomolecular condensates by multivalent interactions involving SH3 domains and proline-rich motifs around phosphorylated membrane receptors has been shown to drive actin assembly and nucleation.[230,231] In particular, phase-separated clusters assemble actin filaments through stochiometric interactions of the adapter protein Nck, its ligand N-WASP, and the actin nucleation factor ARP2/3 in kidney cells. Thus, LLPS was shown to significantly prolong the dwell time of N-WASP on membranes, from 18 s outside clusters to 30 s inside clusters. This increased residence time correlates with enhanced actin nucleation efficiency, as longer retention allows completion of the multistep ARP2/3 activation process.[230] Protein condensates of actin-binding proteins can also mediate actin nucleation and polymerization, even without specific polymerase activity. For example, condensates formed by Lamellipodin, a non-polymerase actin-binding protein, could also polymerize and bundle actin filaments, similar to condensates formed by the actin-polymerase VASP.[225,234] Based in these observations, the idea was put forward that any condensate with actin binding capability could polymerize actin, through multivalent contacts with actin monomers. This was shown by engineering an actin binding motif to a condensate forming scaffold protein (Eps15) that normally does not bind actin. *In vitro*, these chimeras, successfully formed condensates that facilitated actin polymerization.[232] Condensates not only promote actin assembly but are also affected by actin. For example, F-actin accumulates in cortical N-WASP condensates of *C. elegans*, and *in vitro* actin filaments limit the size of the N-WASP condensate and eventually cause disassembly of N-WASP condensates,[224] closing a size control feedback loop.

Somewhat unexpected, emerging evidence suggest that the spectrin cytoskeleton also forms biomolecular condensates.[233–235] Specifically, eliminating the membrane and actin binding of β II spectrin caused the truncated fragments to form liquid-like droplets, with hypothesized roles in the assembly of the neuronal actin cytoskeleton.[233] In *C. elegans*, spectrin forms focal inclusions in the axons of old animals, which increase in size but decrease in number over time, suggesting that spectrin can form condensates that coarsen with animal age.[235]

2. The microtubule cytoskeleton

Similar principles as described for actin above also account for microtubule polymerization (reviewed in Ref. 226). The Tau dense phase, similar to centrosomes, is able to host and locally concentrate tubulin monomers above their critical threshold for polymerization, such that microtubules emerge and grow from condensates (Refs. 43 and 236; reviewed in Ref. 229). Likewise, the microtubule plus end binding proteins EB1 and EB3/CLP-170 undergo phase separation on microtubules directly influencing their growth speed while reducing catastrophe frequency.[237,238] The *T*argeting *P*rotein for *X*klp*2* (TPX2) is a microtubule binding protein that preferentially co-condenses with tubulin monomers on existing microtubules, where it nucleates new filaments. This spatially coordinated activity therefore leads to branched microtubules. Intriguingly, TPX2 condensate formation is inhibited by Importin α/β until the beginning of mitosis, suggesting a mechanism by which microtubule branching is spatiotemporally regulated in the cell.[115]

An exciting avenue consists of the development of programmable motor condensates functionalized with processive molecular motors such as kinesin and dynein.[239] In heterotypic condensates composed of RNA-binding proteins and chimeric constructs made up of a fusion of a kinesin and a multivalent scaffold (rapamycin-dependent heterodimerization of FRB and FKBP), it has been shown that they form in response to an external stimulus (rapamycin addition) and were able to perturb the spatial distribution of endogenous mRNAs from the center of the cell to the periphery.[239]

B. Reorganization of subcellular structures through interfacial forces

Similar to the active force generation of cytoskeletal filaments during polymerization, the biomolecular condensation process itself can exert mechanical forces[44,45,240] and lead to significant reshaping of associated cellular structures, such as chromatin,[46,130,241,242] cytoskeleton,[19] and intracellular and plasma membranes,[243,244] and can even lead to membrane scission events.[245] The underlying principle of force

generation is minimization of the surface energy, or interfacial tension, within the condensate inside the cell, along with the capillary forces that arise when condensates wet or dewet associated structures. They can emerge when droplets coalesce,[44] shrink,[46] but also when they spread along the surface of another compartment. It is important to note that the gain in free energy, e.g., upon droplet coalescence, is relatively low and can thus only work on soft interfaces. However, forces on the order of 0.5 pN have been measured, which are in a range similar to that generated by motor proteins.[46] Importantly, semi-flexible, cytoskeletal polymers, DNA, and membranes are compliant enough to deform under this force. For example, the coalescence of two neighboring droplet interfaces that wet the cytoskeleton can lead to the bundling and organization of these fibers [Fig. 4(b), panel i]. The actin polymerase Vasodilator Stimulated Phosphoprotein (VASP) forms condensates that promote actin nucleation and bundling.[223] Tau proteins have been shown to form liquid-like condensates that completely wet microtubules *in vitro*[246] and *in vivo*,[116] with an important role in microtubule bundling, growths,[236] and axonal mechanics.[116] For example, in the absence of the *C. elegans* tau homolog *PTL-1*, microtubules break, twist, and split, causing partial loss of neuronal function.[116] Although the cytoskeleton has been shown to deform and alter some condensates,[114] reports that condensation itself deforms microtubules are lacking, indicating that these polymers may be too stiff, as the bending energy of these filaments may not be offset by the gain in free energy resulting from droplet coalescence. The coalescence of the condensates may lead not only to the bundling of filaments but also to the recruitment of the cytoskeleton to the membrane [Fig. 4(b), panel ii], especially if the condensates form capillary bridges.[44] Such capillary bridges have also been observed between DNA strands and are involved in chromatin remodeling and gene transcription,[130,241] but also assist in DNA repair by maintaining the synapsis of two severed DNA ends.[247] Likewise, condensation at membranes is well known to cause their deformation, which in the extreme case could even lead to vesicle budding.[45,243]

C. Scaffold proteins at intercellular junctions

Tight junctions are intercellular contacts in epithelia with important functions in adhesion and as a permeability barrier, but also signaling, mechanotransduction, and morphogenesis.[248] The major scaffolding proteins, called zonula occludens 1, 2, 3 (ZO-1/ZO-2/ZO-3), have a multidomain architecture with various PDZ and SH3 domains, and provide a platform that integrates the membrane proteins with the cytoskeleton. These proteins form condensates specifically at the membrane of apical intercellular junctions.[29,30] ZO-1 and ZO-2 resident condensates are involved in tight junction assembly and shuttle between a liquid, cytoplasmic pool, and a peripheral pool that seems to completely wet the cortex.[29,30,249] Intriguingly, the condensates form at a lower concentration at the apical boundary of MDCK cells than in the cytoplasm of HEK cells, suggesting that an interaction of ZO proteins with the apical belt primes them for liquid–liquid phase separation. ZO-1 proteins transition from a dilute adsorbed state to a condensed surface layer on the apical membrane interface and form isolated condensates at the membrane interface below the critical saturation concentration for bulk phase separation through a pre-wetting transition.[250] The interaction with the PATJ protein is crucial for this transition from a diluted to a dense state and promotes the elongation of ZO-1 condensates along the apical membrane interface [Fig. 4(c), panel i]. This elongation happens at a constant velocity, driven by the binding affinity of ZO-1 to the apical interface and PATJ. As the ZO-1 condensates elongate, they fuse to form a continuous tight-junction belt that seals the epithelial tissue.[250] This process is dependent on the actin cytoskeleton and active force generations—the presence of Latrunculin A, a drug that depolymerizes the actin network, disrupted the continuous ZO-1 belt and led to the formation of regularly spaced, liquid-like droplets akin to beads on a string [Fig. 4(c), panel ii]. Interestingly, ZO-1 are mechanoresponsive proteins that undergo force-dependent unfolding and interaction events[251] and can exist in either folded or stretched conformations, depending on acto-myosin-generated tension and dimerization. In the case of tight junction assembly, a force inhibits droplet formation and causes complete wetting of the apical junctions. A similar observation was made in zebrafish, where the junctional ZO-1 recruitment increases with mechanical tension.[30] Moreover, non-junctional ZO-1b condensates within the yolk syncytial layer (YSL), initially displaying liquid-like properties, undergo a maturation process leading to their immobilization indicated by their lower fluorescence recovery after photobleaching [Fig. 4(d)]. Thus, tension generated in the actin cytoskeleton may induce and maintain a solid character and lack of tension results in fluidization. However, ZO-2/ZO-2 knockout leads to an increase in myosin II localization at the junctional interface, and a build-up of excessive tension, which leads to lumen collapse in an MDCK model of lumen formation. Intriguingly, this can be suppressed by interfering with myosin II activity (Rho kinase inhibition), and artificial increase in hydrostatic luminal pressure.[252] The data support a model in which a balance between hydrostatic pressure and junctional tension is important for tight junctions remodeling and lumen morphogenesis. How ZO-1 condensates change their material properties during tight junction assembly is, however, yet to be shown.

D. Centrosomes and the solid liquid phase transition

All previously discussed examples explain the importance of the liquid–solid transition, but the timely regulation of a solid–liquid phase transition leading to fluidification is equally important. Recent data suggest that the centrosome, specifically the pericentriolar material (PCM) composed of SPD-5 in *C. elegans*, forms condensates subject to regulated softening during the metaphase-anaphase transition.[205] *In vitro*, SPD-5 initially forms dynamic condensates that quickly mature to a solid state in 10 min.[43] These mature condensates exhibit minimal to no fluorescence recovery after photobleaching, indicating their solid-like nature. *In vivo*, no dynamic phase preceding maturation was observed,[43,253] suggesting immediate arrest after formation. During mitotic spindle assembly and chromosome segregation, the PCM must withstand microtubule-mediated pulling forces[254] as a solid-like matrix would be more effective for anchoring microtubules. In fact, SPD-5 condensates during metaphase appear to be resistant to high ($\approx 18\ \mu$m/min) cytoplasmic flow velocities generated by a FLUCS assay *in vivo* [Fig. 4(e)], indicating their high stiffness. This changes abruptly during anaphase and telophase, where even medium flow velocities ($\approx 10\ \mu$m/min) lead to a substantial deformation and even fission of these condensates. The results suggest that PCM resistance to deformation and fracture is high during metaphase and then decreases at the onset of anaphase, before full PCM disassembly in the telophase. It should be noted that cytoplasmic viscoelasticity increases during metaphase/anaphase transitions in various cell types,[253] and

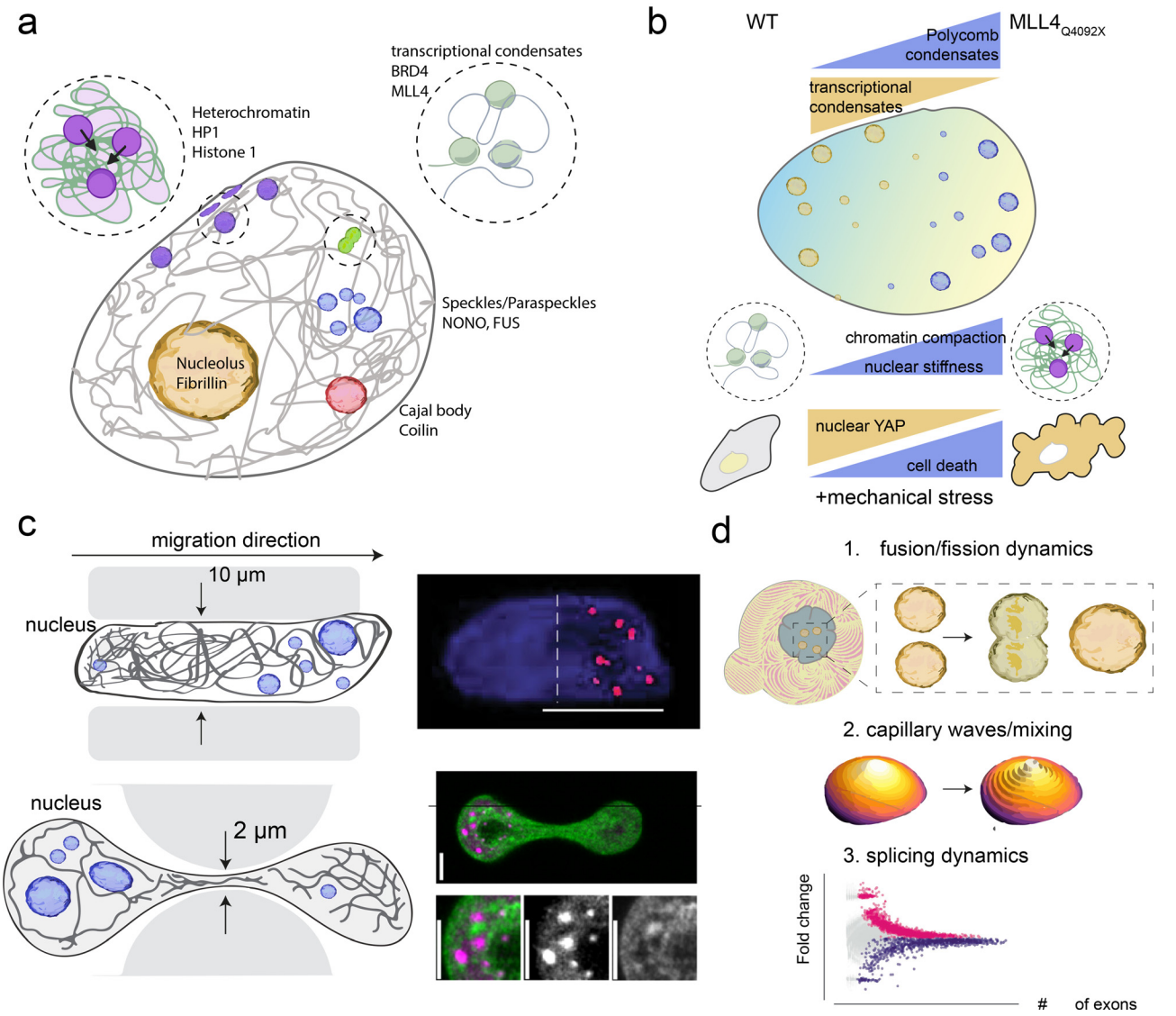

FIG. 5. Condensate dynamics and the mechanobiology of the nucleus. (a) Schematic representation of a typical nucleus with various types of nuclear condensates, including Cajal bodies, nucleoli, transcriptional and heterochromatin condensates, and the nuclear speckles/paraspeckles. Some of the major protein components are highlighted. (b) Mechanobiological implications of mutant transcriptional condensates associated with Kabuki syndrome. Expression of mutant isoform $MLL4_{Q4092X}$ leads to an increase in repressive polycomb condensates in expense of transcriptional BRD4 condensates. This leads to an increase in chromatin compaction and nuclear stiffness, loss of YAP in mutant cells and cell death under mechanical confinement. (c) Confined migration triggers mechanically activated phase separation of paraspeckles in the chromatin poor regions of the nucleus. Polarized condensation may depend on constriction size and/or geometry. Left: Schematic of the experiment; Right: representative image. Reproduced with permission from Todorovski *et al.*, Commun. Biol. **6**(145), 12 (2023). Copyright 2023 authors, licensed under a Creative Commons Attribution (CC BY) license; and Reproduced with permission from Zhao *et al.*, Nat. Commun. **15**, 9964 (2024). Copyright 2024 authors, licensed under a Creative Commons Attribution (CC BY) license. (d) Active cytoplasmic streaming in mouse oocytes influences fusion/fission dynamics of nuclear condensates, and active mixing to regulate mRNA splicing dynamics. Graph on the bottom shows overrepresented and underrepresented exons in actin deficient oocytes compared to control cells.

the resulting greater force during FLUCS-induced flow may partially confound the interpretation. Still, the dependence of condensate deformation on polo-like kinase, which reinforces SPD-5 condensates, suggests that condensate material is directly affected.

Together, a large body of work suggests that the PCM initially adopts a liquid-like state to facilitate microtubule nucleation and mobility, transitioning later to a gel-like state to resist the pulling forces exerted by these microtubules. Although maturation has been observed in reconstituted PCM *in vitro*, FLUCS measurements *in vivo* point toward a plausible mechanism involving a regulated fluidization induced by post-translational modifications through polo-like kinase.

E. Biomolecular condensates in nuclear mechanobiology

The mechanobiology of the nucleus is fundamental for understanding how mechanical forces regulate gene expression, chromatin organization, and cell behavior.[8] Many biomolecular condensates, such as nucleoli, Cajal bodies, speckles and paraspeckles, and transcriptional hubs, among others, that are embedded within the nuclear landscape are directly influenced by mechanical cues from the cytoskeleton and the external world [Fig. 5(a), reviewed in Refs. 31 and 256]. Mechanical forces can affect their formation, material properties, and dynamics, linking the physical state of the nucleus to cellular functions such as stress responses, gene regulation, and nuclear architecture.[257] This integration highlights the interaction between nuclear mechanics and condensate biology as a critical factor in maintaining cellular homeostasis and responding to mechanical cues.

1. Liquid–solid transitions and chromatin mechanics

Viscoelastic phase transitions in the nucleus have received a great deal of attention, especially for their role in transcriptional regulation and chromatin organization.[31,258] In the nucleus, DNA is organized into transcriptionally active euchromatin and inactive heterochromatin. Heterochromatin is located, among other regions, predominantly in the nuclear periphery [Fig. 5(a)], and interacts with the lamin cytoskeleton,[259] where it contributes to the mechanical resistance of the nucleus to external forces.[260] Importantly, many heterochromatin components have been shown to phase separate *in vitro*, including heterochromatin protein 1 (HP1),[261,262] Histone 1[263] and chromatin octamers composed of Histone 3 and 4.[264] In the presence of physiological salt concentrations, chromatin formed liquid-like droplets and showed complete droplet–droplet fusion dynamics that were substantially altered in the presence of Histone 1, indicative of a change in its liquid-like character.[264] Likewise, in the presence of DNA, the phase transition of HP1 was altered and compact condensates formed that were resistant to mechanical forces.[261] These observations provide a plausible basis for the hypothesis that heterochromatin formation alters mechanical resistance *in vivo* and support the exciting idea that the liquid–solid transition of the chromatin changes the way the nucleus responds to and transduces external mechanical forces. Despite the ubiquitous reports of LLPS of chromatin and LST upon the addition of heterochromatin-associated proteins (e.g., HP1, Histone 1), chromatin was found to be static over a timescale of minutes to hours *in vivo*.[32] This suggests that chromatin has a predominantly solid character across time and length scales that are relevant for biological processes, independent of its transcriptional state. On the basis of these *in vivo* observations, it was suggested that chromatin behaves as a liquid at the nanoscale because of local dissociation of histone tail-DNA interactions. However, the cumulative effect of all nucleosomal contacts in condensed chromatin leads to solid-like behavior at the mesoscale.[32] The existence of elastic chromatin condensates, which have a higher propensity to localize at the periphery of many interphase nuclei, is therefore compatible with a picture in which this dense network results in stiffer nuclei[265] and protects the genome against mechanical insults.[266] Indeed, loss of HP1 condensates resulted in softer nuclei, more prone to mechanical deformations induced by microtubule polymerization and direct forces applied by an optical trap.[267]

In addition, the material properties of chromatin also relate to stem cell differentiation and transcriptional activity. Using noninvasive passive rheology by imaging intrinsic chromatin dynamics visualized with histones H2B-GFP, it was found that undifferentiated chromatin behaves like a Maxwell fluid, while differentiated chromatin exhibits fluid-like (sol) and solid-like (gel) phases.[153] This transition corresponds to the formation of dense, transcriptionally inactive heterochromatin. Together, this suggests that chromatin undergoes a local sol-gel transition upon cell differentiation, affecting gene regulation by altering genome accessibility.[153]

Recent studies provide further evidence that chromatin is mechanosensitive. For example, transcriptional condensates have been shown to respond to mechanical signals, such as substrate stiffness and modulated chromatin compaction.[242] In mesenchymal stem cells, culturing on stiffer elastic substrates led to an increased abundance of BRD4 nuclear condensates[132] [Fig. 5(b)]. This process was found to depend on the chromatin-modifying enzyme MLL4, a factor associated with Kabuki syndrome. Intriguingly, MLL4 loss-of-function reduced the nuclear mechano-response to ECM-mediated forces and resulted in more softer nuclei on more compliant substrates and stiffer nuclei on rigid substrates compared to wildtype control nuclei. Likewise, MLL4 knockout cells were unable to maintain tension in the nuclear LINC complex, suggesting that nuclear condensates modulate and respond to external mechanical signals. Indeed, MLL4-containing condensates coalesced into larger and more abundant spherical droplets in response to direct mechanical confinement of the nucleus. Ultimately, loss of MLL4 caused substantial nuclear rupture and increased cell death in the most critical confinement[132] [Fig. 5(b)]. Important for this mechanosensing modality was the polyQ sequence naturally found in MLL4, as the deletion of this motif abrogated the coarsening of the transcriptional condensates.[242] Using molecular dynamics simulations, the authors suggested that the polyQ motif undergoes a force-dependent conformational change that may be involved in amyloid formation, possibly driving a rigidity transition. Together, the loss of functions of MLL4 found in Kabuki syndrome results in smaller, stiffer nuclei compared to healthy condition, which affects nuclear stability and cell survival to mechanical forces.[132,242]

2. Mechanical confinement and substrate stiffness alter the dynamics of nuclear condensates

Paraspeckles are a class of nuclear condensates involved in gene regulation. They form through transcription of long noncoding NEAT1 lncRNA and contain many RNA-binding proteins, such as paraspeckle component 1 (PSPC1) and non-POU domain-containing octamer binding protein (NONO). Paraspeckles are generally considered stress-responsive. Intriguingly, cancer cell lines with a higher metastatic potential show more abundant paraspeckle condensates compared to non-metastatic cells, especially on soft substrate.[268] This difference was dependent on myosin activity, suggesting that the traction forces on stiffer substrates suppressed the formation of condensate. In fact, direct application of force to paraspeckle osteoclasts increased their size, with implications for bone mechanosensing.[269] In addition, confined migration of MDA-MB-231 breast cancer cells in microchannels also increased the size and number of paraspeckles through de novo condensate formation when cells migrated through 10 μm channels, but not through 5 and 3 μm channels.[270] During this process, paraspeckles (visualized by their NEAT1 RNA content) were

formed preferentially on the leading edge side of the nucleus, where chromatin was less compact and was assumed to be softer [Fig. 5(c)]. Artificially increasing its assembly caused cells to migrate faster.[270] Because the mechanical environment was more permissive for condensate formation, this process was coined MAPS, for *mechanically activated phase separation*. However, MDA-MB-231 cells using 53BP1 as the label for nuclear condensates appeared to preferentially nucleate the condensates at the trailing edge when migrating through 2 μm wide channels[131] [Fig. 5(c)]. As condensates preferentially nucleate in softer environments where a larger interchromatin space does not limit their growth, this observation suggests that chromatin is differentially affected at the trailing and leading edges during migration through a channel with varying width. This switch of softening from the leading to the trailing edge appeared to occur when the channel width was reduced from 10 to 2 μm and the phase boundary was shifted to allow more permissive condensation.[131] In addition, mechanical deformation of the nucleus leads to an increase in the partition coefficient of various proteins (RNPS1, SART1, and SRRM1), which contributes to their local deposition.[131] However, whether these condensates have a specific mechanobiological function is speculative, but they might host and thus enrich mechanosensitive transcription factors.

Mechanical confinement was also shown to alter condensate dynamics. For example, nucleolus or speckle nuclear condensates, labeled with NPM1-mCherry and SRRM1-mCherry, respectively, undergo fusion and fission events in cells migrating through constrictions.[131] The paraspeckles were also sensitive to substrate mechanics and cell grew larger and were more abundant on soft 3 kPa poly-acrylamid gels, compared to stiff 40 kPa gels. Intriguingly, the paraspeckles may be subject to "mechano-memory," as cells first grown on 40 kPa substrates and then transferred to 3 kPa soft substrates suppressed growth of larger paraspeckle condensates. Associated with the decrease in the size of the paraspeckle, the transcription of NEAT1 RNA is reduced, providing a potential mechanism for this mechanosensitive regulation.[268] Other factors such as a higher contractility[127] and heterochromatin organization leading to altered nuclear stiffness[260] may also affect paraspeckle condensate formation and size.

3. Forces in nuclear condensate remodeling

How forces are transmitted to the nucleus is a matter of ongoing research. Forces transmitted from the substrate to the Cajal body have been shown to induce the stress-related dissociation of the coilin protein from the survival of motor neuron 1 (SMN) complexes. This dissociation was observed in cells cultured on substrates with stiffnesses of 8 and 2 kPa but not on softer substrates measuring 0.6 kPa, highlighting the mechanosensitive nature of this interaction.[271] The notion that substrate stiffness influences condensate positioning and depositioning suggests that cytoplasmic actomyosin contractility shapes their response. In mouse oocytes, forces originating from the actin cytoskeleton shaped nuclear condensates and caused nucleoli, Cajal body, nuclear speckles, and other liquid droplets to coalesce and grow.[10] The nuclei of actin-deficient oocytes with absent cytoplasmic flow had more abundant and smaller droplets, suggesting that the mechanical stirring of the cytoplasm was transduced through the nuclear envelope and affected the mobility, coarsening and internal molecular kinetics[10] [Fig. 5(d)]. Intriguingly, the presence of cytoplasmic forces led to higher mobility inside the nuclear speckles compared to nuclear speckles in cells mutant for actin cytoskeleton. This increased molecular mobility had an enhanced protein RNA interaction as a consequence—loss of cytoplasmic stirring resulted in alternative exon usage during splicing, with hundreds of isoform switches in actin mutant oocytes[10] [Fig. 5(d)]. Together, the mechanical regulation of nuclear condensates lead to more efficient splicing reactions and gene regulatory control.

F. Force transmission during touch sensing

Recently, we showed that MEC-2, a *C. elegans* stomatin homolog involved in touch sensation, forms biomolecular condensates that undergo a liquid–solid transition at sites of mechanotransduction neurons responsible for the sense of touch.[11] MEC-2 has several isoforms with varying short (MEC-2a) and long (MEC-2e) C-terminal tails that show a high degree of disorder, SLiMs, and amyloid-forming motifs [Figs. 6(a) and 6(b)] that co-assemble into the same mechanotransduction sites *in vivo*.[272] Intriguingly, the long isoform has a higher predicted phase separation score,[273] potentially participating in condensate formation. *In vivo*, condensates of both isoforms are partitioned into two pools (unpublished), one of which was found primarily close to the cell body and characterized by a directed motion of the condensates along the axons. The condensates in this pool were more spherical, visibly deformed, and experienced frequent fusion/fission events, underscoring their predominant liquid-like character. Because this liquid-like pool of MEC-2 is characterized by directed motion within the neurite indicative of motor-driven transport, these properties may allow condensates to squeeze through constriction in a neurite with varying caliper. The second pool is completely static and immobilized at distinct presumptive mechanoreceptor sites where it colocalizes with a mechanoelectrical transduction channel.[11] The picture that emerges is that the mobile, naive condensates mature into solid condensates. In contrast to pathological LST, physiological transitions occur in a regulated and possibly reversible manner in the cell. How is this maturation controlled? MEC-2 contains a stereotypic proline-rich motif (PRM) in its unstructured C-terminal tail, previously hypothesized to function in mechanotransduction by binding to an unknown protein with an SH3 domain.[274] In fact, on a CRISPR-verified cell-specific RNAi screen, we found that PRM bound weakly to the SH3 domain of UNC-89, a *C. elegans* titin homolog.[11] This interaction is critical for mechanotransduction, as animals lacking the motif were completely insensitive and those lacking UNC-89 in TRNs were partially touch insensitive. In addition, MEC-2 contains a notable glycine-rich motif, with a strong prediction to form amyloids [Fig. 6(b)]. The picture that emerged is that the SH3 domain binds to the PRM and thus can compete with an interaction responsible for heterotypic buffering [see Box 1 and Fig. 6(c)]. The residues responsible for the LST still need to be defined but may be found in the glycine-rich motif. Once this complex forms, new valencies are exposed that form homotypic interactions leading to the LST. In fact, MEC-2 formed fibrils *in vitro* in a timely manner only in the presence of the UNC-89 SH3 domain, but neither in its absence nor with mutant MEC-2 lacking a functional PRM [Fig. 6(c)]. The fibers stain positive for Thioflavin T (unpublished data), a dye that specifically intercalates with cross-beta sheets and thus likely forms amyloids. Under our experimental conditions, however, MEC-2 filaments assembled from recombinant protein differed significantly from their endogenous

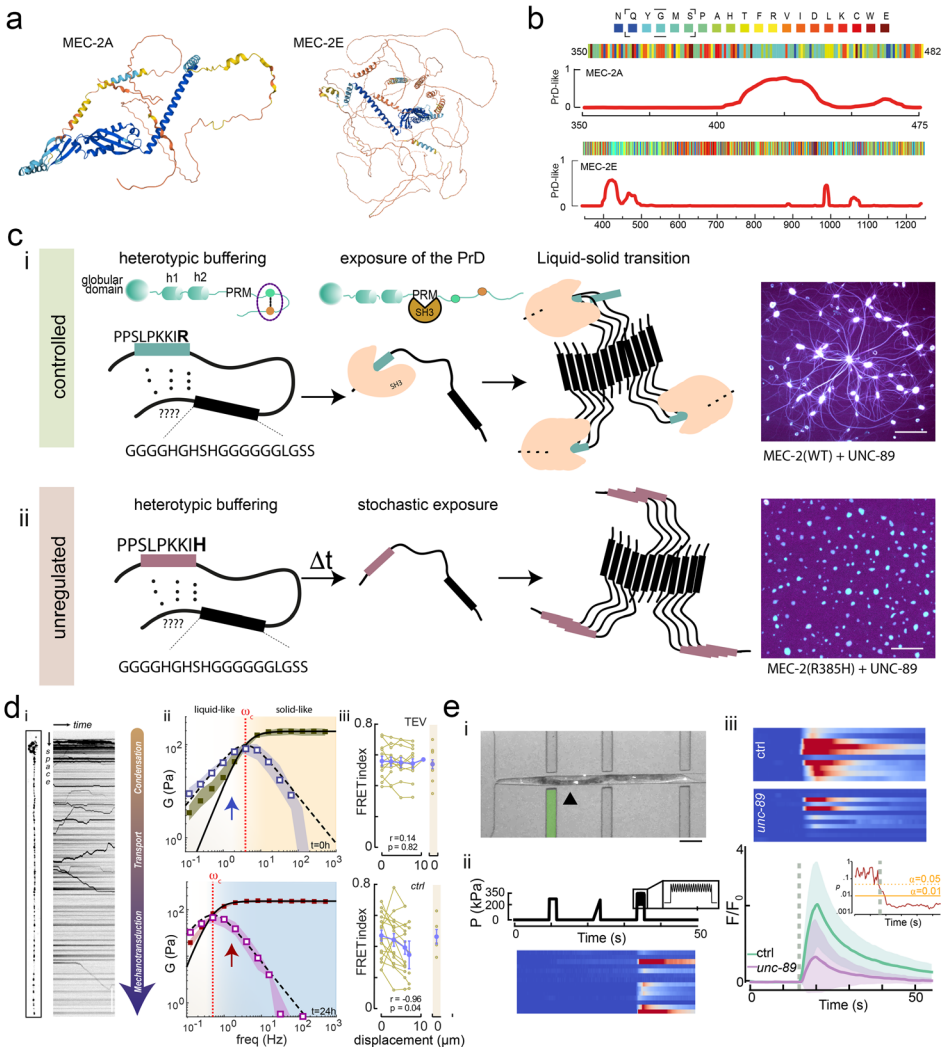

FIG. 6. Viscoelastic maturation of MEC-2 stomatin determines the response timescale during touch in *C. elegans*. (a) AlphaFold2 prediction of two isoforms of MEC-2 stomatin of *C. elegans*. (b) The sequence context of the C-terminal tail of the short and long MEC-2 isoforms highlighting a long stretch of glycines and histidines (GSEGGGGHGHSHGGGGGG) that may be involved in the amyloid formation. Plots made according to Lancaster *et al.*[292] (c) Schematic representation of a possible mechanism for the observed liquid–solid transition. (i) A heterotypic, intramolecular interaction masks the aggregation prone, amyloidogenic motif. The interaction of the PRM with its cognate SH3 domain releases the heterotypic buffering, leading to the exposure of the PrD domain, which promotes the controlled LST. (ii) In the absence of the correct SH3-binding motif, a stochastic unbinding exposure leads to a delayed and uncontrolled LST. Right images show a confocal fluorescence microscopy image of (i) wildtype MEC-2 and (ii) mutant MEC-2(R385H) in red mixed with UNC-89(SH3) in green. Scale bar = 30 μm. (d) Force transmission during sense of touch requires a controlled LST of MEC-2 stomatin. (i) Liquid-like and mobile condensates are primarily found in regions of the neurites proximal to the cell body, whereas stiff, immobile condensates are found all along the neurite. Representative fluorescence image and kymograph of a neuron expressing fluorescently labeled MEC-2::mCherry. Cell body at the top. Scale of the arrows: 20 μm (x) and 30 s (time). (ii) MEC-2 condensates respond like a viscoelastic fluid and their maturation is accompanied by a shift in crossover frequency to lower values. The arrows point to frequencies at which the condensate behaves as a liquid before and as an elastic material after the maturation. The complex shear modulus is depicted as a function of deformation frequency. Solid and dashed lines correspond to the Maxwell material model fits for the storage and loss moduli, respectively. Red dotted lines represent the fit parameters for the plateau modulus E and crossover frequency ω_c, respectively. (iii) The C-terminal domain of MEC-2 is responsible to store and transmit mechanical stress *in vivo*, as determined with a FRET-tension sensor. Quantification of FRET index vs pressure delivered to body wall of the animals, for truncated MEC-2(TEV) and control groups. Yellow and purple lines correspond to individual animals and Mean ± SE, respectively. Reproduced with permission from Sanfeliu-Cerdán *et al.*, Nat. Cell Biol. **25**(11), 1590–1599 (2023). Copyright 2023 authors, licensed under a Creative Commons Attribution (CC BY) license (e) Frequency-dependent touch response of *C. elegans*. (i) Microfluidically immobilized animal expressing GCaMP in touch receptor neurons (arrow). Scalebar = 100 μm. (ii) Touch receptor neurons do not respond to a step and a ramp stimulus (delivered below the crossover frequency), but only to a high-frequency buzz delivered through the pneumatic actuator. (i) and (ii) In the absence of the MEC-2 rigidity phase transition (*unc-89* mutant), the same high frequency stimulus does not activate TRNs as compared to control animals, indicating that the rheological properties of the condensates are important for the touch response. Reproduced with permission from Nekimken *et al.*, Lab Chip **17**, 1116–1127 (2017). Copyright 2017 authors, licensed under a Creative Commons Attribution (CC BY) license; and Reproduced with permission from Sanfeliu-Cerdán *et al.*, Nat. Cell Biol. **25**(11), 1590–1599 (2023). Copyright 2023 authors, licensed under a Creative Commons Attribution (CC BY) license.

counterparts. They were longer and had distinct morphologies, indicating that the low-complexity domain of MEC-2 can adopt different structural forms depending on whether they are formed *in vitro* or *in vivo*. This may hint toward a mechanism that ensured a spatially controlled transition and that limited the expansion of the solid state inside cells.

How is the transition spatially organized? In *C. elegans*, MEC-2 stomatin colocalizes with the pore-forming subunit of the ion channel at distinct puncta [Fig. 6(d), panel i]. We reasoned that UNC-89, localized at the presumptive transduction sites, binds to MEC-2 condensates and induces solidification as these condensates pass by. In fact, naive MEC-2 condensates had a lower mobility when encountered existing mature MEC-2 condensates, indicating a possible molecular interaction between them (unpublished observation). Likewise, the mobile, naive pool of MEC-2 did not localize with UNC-89, whereas the static, mature pool colocalized with it, which confirms the role of UNC-89 in promoting the LST. Together, these data suggest that the association of a dynamic condensate with a resident SH3 domain triggered the LST *in vivo*.

What is the consequence of this solid transition? Intriguingly, a force sensitive, FRET-based MEC-2 tension sensor reported that only the static mature pool has the ability to sustain mechanical stress delivered to the body wall through a microfluidic stimulus [Fig. 6(d), panel iii]. However, the naive, liquid-like condensate did not, emphasizing the importance of the LST in the force transduction process. Furthermore, similar to condensates composed of FUS and PGL-3,[23] MEC-2/UNC-89 co-condensates showed significant aging *in vitro* and frequency-dependent viscoelastic response[11] [Fig. 6(d), panel ii]. This means that at slow frequencies, the condensates tended to flow and dissipate mechanical energy, whereas for frequencies applied above 4 Hz, the storage modulus dominated and significant stress could be transmitted. This is particularly interesting in the context of MEC-2, as the *C. elegans* touch response is highly frequency dependent and the TRNs do not activate in response to slow stimuli delivered below 5 Hz[275,276] [Fig. 6(e), panels i]. Intriguingly, mutant animals with MEC-2 condensates that did not mature properly showed a significantly reduced calcium response to high-frequency stimulations [Fig. 6(e), panels ii]. By adjusting the mechanical properties of the condensate, the activation threshold can be modulated, and the neuron can use it during the habituation to continuous stimuli. However, it is most likely that other proteins *in vivo* further modulate the condensates and their mechanics. In the future, a detailed mechanism needs to be formulated on how the MEC-2 stomatin condensates receive the force during touch and which other clients are incorporated into these condensates.

Whether this constitutes a conserved mechanism for frequency selection remains to be shown. Interestingly though, Piezo2 ion channel sensitivity to external force also depends on functional interaction with the stomatin homolog STOML3,[277] which has also been shown to modulate membrane mechanics.[278] Likewise, Piezo2 displays IDR regions that are important in determining the activation threshold and force sensitivity.[279] Piezo2 has a preference for stimuli applied at a faster rate, making this ion channel also more selective for high-frequency stimuli than lower ones,[280] which depends on the actin cytoskeleton.[279] How actin transfers force to Piezo2 is unknown. It is interesting to speculate that these IDRs in Piezo2 may serve as a platform to direct the condensation of other proteins through multivalent interactions, for example, STOML3, such that these condensates emerge as mechanical frequency filters and set the activating force threshold by balancing the mechanotransmission pathway from the cytoskeleton to the ion channel.

VII. OPEN QUESTIONS AND FUTURE MILESTONES

A. What are the functions of LST in mechanobiology?

Undoubtedly, many pathological liquid–solid phase transitions occur inside cells,[24,25,70,81,281–283] and reports of LST in physiological processes are emerging.[11,43,213,220] An obvious question is whether a viscoelastic phase transition or hardening is tied to the physiological functions of these proteins. Many, if not all, biomolecular condensates show some degree of hardening *in vitro*.[108] Therefore, mere observation of the condensate mechanics and the changes thereof *in vitro* may not reveal its physiological role. It is critical to understand how changes in their mechanical properties affect cellular function. To assess physiological relevance, one might ask whether perturbing the LST leads to a significant loss of function at either the cellular or the organismal level. This can be achieved by mutating specific residues that involve hardening *in vitro* and investigating cellular fitness after expressing these mutant proteins in an *in vivo* system.[11] One may also specifically perturb condensate mechanics through interference with known regulators or small molecules[70,284,285] and ask if this affects the physiology. In addition, if a liquid turns into a solid, it is important to understand how the rigidity transition is regulated and whether it is reversible.

B. Pathological vs physiological LST

Much of the mechanistic insight and factors driving the liquid–solid transitions came from condensates composed of proteins associated with neuronal disorders (e.g., FUS, TAU). Thus, it remains to be seen whether the mechanism that leads to a physiological LST is the same as the one described in the context of disease. Although the pathological consequences of LST are well appreciated, their role in a physiological context is just emerging. One of the challenges is the difficulty in measuring the change in mechanical properties *in vivo* and relating this change to a physiological benefit of the cell, accounting for potential artifacts related to the method of observation.

C. Investigating the material state *in vivo*

Many proteins that form biomolecular condensates have also been shown to mature and undergo an LST *in vitro*. Because these investigations are often performed with purified proteins, the time course and final material state may be different *in vitro* compared to that of the cell. Thus, experiments within cell mimicking environments[115] and the knowledge of the complete proteome of these condensates *in vivo* will guide further investigation and possibly indicate factors that accelerate or inhibit the maturation reactions found *in vitro*. The next critical challenge is to explore the material properties of these structures and how they evolve within living organisms, cells, or tissues. Although methods for addressing this are emerging,[142,196] future efforts will require direct probing of their mechanical properties with high spatiotemporal resolution. Because BMCs are exquisitely stimulus sensitive and react to environmental challenges, these methods are at best carried out in a noninvasive manner. Furthermore, the shapes of condensates *in vitro* are often distinct from their shapes *in vivo*, due to geometric constraints,[27] environmental conditions (salt, pH), or accessory domains or client proteins that are missing

in vitro.[221] For example, some condensates mature into solid fibers *in vitro* that measure tens of micrometers, but form nm-μm arrested condensates *in vivo* during a physiological LST.[11] Thus, one may wonder what determines the timescale of the LST and the size of the functional, mature condensate. Also, condensate mixing by cytoplasmic forces has been show to modulate biochemical processes in mouse oocytes[10] and it is likely that it also affects condensate mechanics in other systems.

Although routine measurement of condensate mechanical properties *in vivo* is a formidable challenge that is on the verge of being overcome, the interpretation and correlation to *in vitro* results are nontrivial as well. The confounding fact that condensates can host additional unanticipated clients, even in a heterologous cell system, or are subjected to post-translational modifications or simply interact in the cell differently than in vitro[14] makes a direct correlation of these results difficult. Temporally resolved proximity labeling,[252] paired with *in situ* measurements and a careful top-down decomposition, will be required to link the liquid–solid transition to a specific cellular mechanism.

D. Can condensates be used to engineer mechanobiological functions?

A deeper understanding of condensate mechanobiology can help engineer specific functions within synthetic cells or replace aberrant signal transductions.[53] The principles of engineering targeted deposition,[21,286] stimulus response,[287] and controlled rigidity percolations[16,83] are beginning to be understood and poised to be applied to living cells.[239] Potential applications are manifold. For example, programmable motor condensate can form upon local enrichment of a molecular species and initiate their transport between cell compartments.[239] If the condensate participates in the transduction pathway, small molecules that modulate the mechanics of the condensate may set the threshold for mechanotransduction and render cells more or less mechanosensitive.[11,284] Or, a controlled fusion of stimulus-responsive condensates attached to the cytoskeleton can be used to bundle filaments,[223] move cargo,[239,288] or align fibers close to cellular organelles. Steps in this direction are already being taken to reposition DNA loci to facilitate DNA repair or transcriptional regulation.[46,241,247] Other approaches can harness this knowledge for molecular medical applications, for example, through a drug-induced viscoelastic rigidity transition in time, may help limit viral infections,[289] drive gene expression changes in the superenhancer,[91] curb aberrant cell dynamics in metastatic cells,[290] or build neuronal networks to combat memory loss.[221]

VIII. CONCLUSION

The formation of biomolecular condensates through LLPS of proteins from the dilute phase brings about a membrane-less "organelle" with a new set of mechanical properties, with liquid-like features. Those can then mature into a solid state, akin to a liquid–solid transition. Much remains to be learned about how LST is regulated by internal and external stimuli and, consequently, how biomolecular condensates govern mechanobiology and physiological functions. One of the challenges in our mechanistic understanding of the factors that modulate these phase transitions stems from the difficulty of measuring viscoelastic properties, interfacial tensions, and their changes *in vivo*. Although several techniques have been developed and used to measure them *in vitro*, only FRAP has been extensively used to make predictions about the changes in viscoelastic behavior *in vivo*. With the emergence of *in vivo* techniques in recent years, such as FLUCS,[204] Brillouin spectroscopy,[197] and TimSOM,[142] a surge in new information can be expected. A deeper understanding of the mechanobiology of biomolecular condensates, how they shape cell behavior and are regulated, will not only reveal key physiological processes but also pave the way for the control of severe, currently untreatable diseases related to unregulated liquid–solid transitions.[53,291]

ACKNOWLEDGMENTS

We thank Xavier Salvatella (IRB) and Frederic Català-Castro (ICFO/Impetux Optics) for fruitful discussions leading up to this work and critical comments on the manuscript. We also wish to apologize for the authors' work in this extensive and rapidly expanding field whose work we were unable to cite due to space and time constraints.

Writing and the work leading up to this manuscript was supported by the ERC (MechanoSystems, 715243), MCIN/AEI/10.13039/501100011033/FEDER "A way to make Europe" (PID2021-123812OB-I00, CNS2022-135906), "Severo Ochoa" program for Centers of Excellence in R&D (CEX2019-000910-S), from Fundació Privada Cellex, Fundació Mir-Puig, and from Generalitat de Catalunya through the CERCA and Research program. ICFO is the recipient of a Severo Ochoa Award of Excellence from MINECO (Government of Spain).

AUTHOR DECLARATIONS

Conflict of Interest

The authors have no conflicts to disclose.

Author Contributions

Neus Sanfeliu-Cerdan: Conceptualization (supporting); Writing – original draft (supporting); Writing – review & editing (supporting). **Michael Krieg:** Conceptualization (lead); Writing – original draft (lead); Writing – review & editing (lead).

DATA AVAILABILITY

Data sharing is not applicable to this article as no new data were created or analyzed in this study.

REFERENCES

[1]X. Trepat, M. R. Wasserman, T. E. Angelini, E. Millet, D. A. Weitz, J. P. Butler, and J. J. Fredberg, "Physical forces during collective cell migration," Nat. Phys. **5**, 426–430 (2009).
[2]C. P. Heisenberg and Y. Bellaïche, "Forces in tissue morphogenesis and patterning," Cell **153**, 948–962 (2013).
[3]A. J. Engler, S. Sen, H. L. Sweeney, and D. E. Discher, "Matrix elasticity directs stem cell lineage specification," Cell **126**, 677–689 (2006).
[4]S. Katta, M. Krieg, and M. B. Goodman, "Feeling force: Physical and physiological principles enabling sensory mechanotransduction," Annu. Rev. Cell Dev. Biol. **31**, 347–371 (2015).
[5]M. Krieg, A. Pidde, and R. Das, "Mechanosensitive body–brain interactions in caenorhabditis elegans," Curr. Opin. Neurobiol. **75**, 102574 (2022).
[6]B. T. Goult, M. von Essen, and V. P. Hytönen, "The mechanical cell - the role of force dependencies in synchronising protein interaction networks," J. Cell Sci. **135**, 11 (2022).
[7]N. Zuela-Sopilniak and J. Lammerding, "Can't handle the stress? Mechanobiology and disease," Trends Mol. Med. **28**(9), 710–725 (2022).

[8]V. Venturini, F. Pezzano, F. Català Castro, H. M. Häkkinen, S. Jiménez-Delgado, M. Colomer-Rosell, M. Marro, Q. Tolosa-Ramon, S. Paz-López, M. A. Valverde, J. Weghuber, P. Loza-Alvarez, M. Krieg, S. Wieser, and V. Ruprecht, "The nucleus measures shape changes for cellular proprioception to control dynamic cell behavior," Science **370**, eaba2644 (2020).
[9]Y. Song, Z. Zhao, L. Xu, P. Huang, J. Gao, J. Li, X. Wang, Y. Zhou, J. Wang, W. Zhao, L. Wang, C. Zheng, B. Gao, L. Jiang, K. Liu, Y. Guo, X. Yao, and L. Duan, "Using an ER-specific optogenetic mechanostimulator to understand the mechanosensitivity of the endoplasmic reticulum," Dev. Cell **59**, 1396–1409.e5 (2024).
[10]A. Al Jord, G. Letort, S. Chanet, F. C. Tsai, C. Antoniewski, A. Eichmuller, C. Da Silva, J. R. Huynh, N. S. Gov, R. Voituriez, M. É. Terret, and M. H. Verlhac, "Cytoplasmic forces functionally reorganize nuclear condensates in oocytes," Nat. Commun. **13**, 5070 (2022).
[11]N. Sanfeliu-Cerdán, F. Català-Castro, B. Mateos, C. Garcia-Cabau, M. Ribera, I. Ruider, M. P. de-la Riva, A. Canals-Calderón, S. Wieser, X. Salvatella, and M. Krieg, "A MEC-2/stomatin condensate liquid-to-solid phase transition controls neuronal mechanotransduction during touch sensing," Nat. Cell Biol. **25**, 1590–1599 (2023).
[12]C. P. Brangwynne, C. R. Eckmann, D. S. Courson, A. Rybarska, C. Hoege, J. Gharakhani, F. Jülicher, and A. A. Hyman, "Germline P granules are liquid droplets that localize by controlled dissolution/condensation," Science **324**, 1729 (2009).
[13]S. F. Banani, H. O. Lee, A. A. Hyman, and M. K. Rosen, "Biomolecular condensates: Organizers of cellular biochemistry," Nat. Rev. Mol. Cell Biol. **18**, 285–298 (2017).
[14]E. Korkmazhan, P. Tompa, and A. R. Dunn, "The role of ordered cooperative assembly in biomolecular condensates," Nat. Rev. Mol. Cell Biol. **22**, 647–648 (2021).
[15]A. Musacchio, "On the role of phase separation in the biogenesis of membraneless compartments," EMBO J. **41**, e109952 (2022).
[16]T. Mittag and R. V. Pappu, "A conceptual framework for understanding phase separation and addressing open questions and challenges," Mol Cell **82**(12), 2201–2214 (2022).
[17]A. M. Tayar, F. Caballero, T. Anderberg, O. A. Saleh, M. C. Marchetti, and Z. Dogic, "Controlling liquid–liquid phase behaviour with an active fluid," Nat. Mater. **22**, 1401–1408 (2023).
[18]S. Banjade and M. K. Rosen, "Phase transitions of multivalent proteins can promote clustering of membrane receptors," eLife **3**, e04123 (2014).
[19]T. Wiegand and A. A. Hyman, "Drops and fibers - how biomolecular condensates and cytoskeletal filaments influence each other," Emerging Top. Life Sci. **4**, 247–261 (2020).
[20]Y. Shen, F. S. Ruggeri, D. Vigolo, A. Kamada, S. Qamar, A. Levin, C. Iserman, S. Alberti, P. S. George-Hyslop, and T. P. J. Knowles, "Biomolecular condensates undergo a generic shear-mediated liquid-to-solid transition," Nat. Nanotechnol. **15**, 841–847 (2020).
[21]Y. Dai, L. You, and A. Chilkoti, "Engineering synthetic biomolecular condensates," Nat. Rev. Bioeng. **1**, 466–480 (2023).
[22]I. Alshareedah, W. M. Borcherds, S. R. Cohen, A. Singh, A. E. Posey, M. Farag, A. Bremer, G. W. Strout, D. T. Tomares, R. V. Pappu, T. Mittag, and P. R. Banerjee, "Sequence-specific interactions determine viscoelasticity and ageing dynamics of protein condensates," Nat. Phys. **20**(9), 1482–1491 (2024).
[23]L. Jawerth, E. Fischer-Friedrich, S. Saha, J. Wang, T. Franzmann, X. Zhang, J. Sachweh, M. Ruer, M. Ijavi, S. Saha, J. Mahamid, A. A. Hyman, and F. Jülicher, "Protein condensates as aging Maxwell fluids," Science **370**, 1317–1323 (2020).
[24]A. Patel, H. O. Lee, L. Jawerth, S. Maharana, M. Jahnel, M. Y. Hein, S. Stoynov, J. Mahamid, S. Saha, T. M. Franzmann, A. Pozniakovski, I. Poser, N. Maghelli, L. A. Royer, M. Weigert, E. W. Myers, S. Grill, D. Drechsel, A. A. Hyman, and S. Alberti, "A liquid-to-solid phase transition of the ALS protein FUS accelerated by disease mutation," Cell **162**, 1066–1077 (2015).
[25]A. Molliex, J. Temirov, J. Lee, M. Coughlin, A. P. Kanagaraj, H. J. Kim, T. Mittag, and J. P. Taylor, "Phase separation by low complexity domains promotes stress granule assembly and drives pathological fibrillization," Cell **163**, 123–133 (2015).
[26]T. P. Fraccia and G. Zanchetta, "Liquid–liquid crystalline phase separation in biomolecular solutions," Curr. Opin. Colloid Interface Sci. **56**, 101500 (2021).
[27]S. R. Jang, Z. Xuan, R. C. Lagoy, L. M. Jawerth, I. J. Gonzalez, M. Singh, S. Prashad, H. S. Kim, A. Patel, D. R. Albrecht, A. A. Hyman, and D. A. Colón-Ramos, "Phosphofructokinase relocalizes into subcellular compartments with liquid-like properties in vivo," Biophys. J. **120**, 1170–1186 (2021).
[28]M. Bose, M. Lampe, J. Mahamid, and A. Ephrussi, "Liquid-to-solid phase transition of oskar ribonucleoprotein granules is essential for their function in drosophila embryonic development," Cell **185**, 1308–1324.e23 (2022).
[29]O. Beutel, R. Maraspini, K. Pombo-García, C. Martin-Lemaitre, and A. Honigmann, "Phase separation of zonula occludens proteins drives formation of tight junctions," Cell **179**, 923–936.e11 (2019).
[30]C. Schwayer, S. Shamipour, K. Pranjic-Ferscha, A. Schauer, M. Balda, M. Tada, K. Matter, and C. P. Heisenberg, "Mechanosensation of tight junctions depends on ZO-1 phase separation and flow," Cell **179**, 937–952.e18 (2019).
[31]D. S. W. Lee, A. R. Strom, and C. P. Brangwynne, "The mechanobiology of nuclear phase separation," APL Bioeng. **6**, 021503 (2022).
[32]H. Strickfaden, T. O. Tolsma, A. Sharma, D. A. Underhill, J. C. Hansen, and M. J. Hendzel, "Condensed chromatin behaves like a solid on the mesoscale *in vitro* and in living cells," Cell **183**, 1772–1784.e13 (2020).
[33]K. Lasker, S. Boeynaems, V. Lam, D. Scholl, E. Stainton, A. Briner, M. Jacquemyn, D. Daelemans, A. Deniz, E. Villa, A. S. Holehouse, A. D. Gitler, and L. Shapiro, "The material properties of a bacterial-derived biomolecular condensate tune biological function in natural and synthetic systems," Nat. Commun. **13**, 5643 (2022).
[34]H. Kusumaatmaja, A. I. May, M. Feeney, J. F. McKenna, N. Mizushima, L. Frigerio, and R. L. Knorr, "Wetting of phase-separated droplets on plant vacuole membranes leads to a competition between tonoplast budding and nanotube formation," Proc. Natl. Acad. Sci. U. S. A. **118**, e2024109118 (2021).
[35]W.-Z. Zeng, K. L. Marshall, S. Min, I. Daou, M. W. Chapleau, F. M. Abboud, S. D. Liberles, and A. Patapoutian, "Piezos mediate neuronal sensing of blood pressure and the baroreceptor reflex," Science **362**, 464–467 (2018).
[36]A. Ali, R. Garde, O. C. Schaffer, J. A. M. Bard, K. Husain, S. K. Kik, K. A. Davis, S. Luengo-Woods, M. G. Igarashi, D. A. Drummond, A. H. Squires, and D. Pincus, "Adaptive preservation of orphan ribosomal proteins in chaperone-dispersed condensates," Nat. Cell Biol. **25**, 1691–1703 (2023).
[37]C. Garcia-Cabau and X. Salvatella, "Regulation of biomolecular condensate dynamics by signaling," Curr. Opin. Cell Biol. **69**, 111–119 (2021).
[38]Y. Shen, A. Chen, W. Wang, Y. Shen, F. S. Ruggeri, S. Aime, Z. Wang, S. Qamari, J. R. Espinosa, A. Garaizar, P. St George-Hyslop, R. Collepardo-Guevara, D. A. Weitz, D. Vigolo, and T. P. J. Knowles, "The liquid- to- solid transition of FUS is promoted by the condensate surface," Proc. Natl. Acad. Sci. U. S. A. **120**, e2301366120 (2023).
[39]G. L. Dignon, R. B. Best, and J. Mittal, "Biomolecular phase separation: From molecular driving forces to macroscopic properties," Annu. Rev. Phys. Chem. **71**, 53–75 (2020).
[40]J. Wang, J. M. Choi, A. S. Holehouse, H. O. Lee, X. Zhang, M. Jahnel, S. Maharana, R. Lemaitre, A. Pozniakovsky, D. Drechsel, I. Poser, R. V. Pappu, S. Alberti, and A. A. Hyman, "A molecular grammar governing the driving forces for phase separation of prion-like RNA binding proteins," Cell **174**, 688–699.e16 (2018).
[41]S. Alberti, A. Gladfelter, and T. Mittag, "Considerations and challenges in studying liquid-liquid phase separation and biomolecular condensates," Cell **176**, 419–434 (2019).
[42]S. Kroschwald, M. C. Munder, S. Maharana, T. M. Franzmann, D. Richter, M. Ruer, A. A. Hyman, and S. Alberti, "Different material states of Pub1 condensates define distinct modes of stress adaptation and recovery," Cell Rep. **23**, 3327–3339 (2018).
[43]J. B. Woodruff, B. Ferreira Gomes, P. O. Widlund, J. Mahamid, A. Honigmann, and A. A. Hyman, "The centrosome is a selective condensate that nucleates microtubules by concentrating tubulin," Cell **169**, 1066–1077.e10 (2017).
[44]B. Gouveia, Y. Kim, J. W. Shaevitz, S. Petry, H. A. Stone, and C. P. Brangwynne, "Capillary forces generated by biomolecular condensates," Nature **609**, 255–264 (2022).
[45]A. Mangiarotti and R. Dimova, "Biomolecular condensates in contact with membranes," Annu. Rev. Biophys. **53**, 319–341 (2024).
[46]A. R. Strom, Y. Kim, H. Zhao, A. Ko, C. Storm, and C. P. Brangwynne, "Condensate interfacial forces reposition dna loci and probe chromatin viscoelasticity," Cell **187**, 5282–5297.e20 (2024).

[47]S. Alberti and A. A. Hyman, "Biomolecular condensates at the nexus of cellular stress, protein aggregation disease and ageing," Nat. Rev. Mol. Cell Biol. **22**, 196–213 (2021).
[48]M. Vendruscolo and M. Fuxreiter, "Protein condensation diseases: Therapeutic opportunities," Nat. Commun. **13**, 5550 (2022).
[49]C. P. Brangwynne, P. Tompa, and R. V. Pappu, "Polymer physics of intracellular phase transitions," Nat. Phys. **11**, 899–904 (2015).
[50]S. S. Ribeiro, N. Samanta, S. Ebbinghaus, and J. C. Marcos, "The synergic effect of water and biomolecules in intracellular phase separation," Nat. Rev. Chem. **3**, 552–561 (2019).
[51]P. Mohanty, U. Kapoor, D. S. Devarajan, T. M. Phan, A. Rizuan, and J. Mittal, "Principles governing the phase separation of multidomain proteins," Biochemistry **61**, 2443–2455 (2022).
[52]P. Tompa, N. E. Davey, T. J. Gibson, and M. Madan Babu, "A million peptide motifs for the molecular biologist," Mol. Cell **55**, 161–169 (2014).
[53]D. M. Mitrea, M. Mittasch, B. F. Gomes, I. A. Klein, and M. A. Murcko, "Modulating biomolecular condensates: A novel approach to drug discovery," Nat. Rev. Drug Discovery **21**, 841–862 (2022).
[54]G. M. Ginell and A. S. Holehouse, "An introduction to the stickers-and-spacers framework as applied to biomolecular condensates," Methods Mol. Biol. **2563**, 95–116 (2023).
[55]J. Mo Choi, A. S. Holehouse, and R. V. Pappu, "Physical principles underlying the complex biology of intracellular phase transitions," Annu. Rev. Biophys. **49**, 107–133 (2020).
[56]T. S. Harmon, A. S. Holehouse, M. K. Rosen, and R. V. Pappu, "Intrinsically disordered linkers determine the interplay between phase separation and gelation in multivalent proteins," eLife **6**, e30294 (2017).
[57]W. Borcherds, A. Bremer, M. B. Borgia, and T. Mittag, "How do intrinsically disordered protein regions encode a driving force for liquid–liquid phase separation?" Curr. Opin. Struct. Biol. **67**, 41–50 (2021).
[58]M. Farag, S. R. Cohen, W. M. Borcherds, A. Bremer, T. Mittag, and R. V. Pappu, "Condensates formed by prion-like low-complexity domains have small-world network structures and interfaces defined by expanded conformations," Nat. Commun. **13**, 7722 (2022).
[59]E. W. Martin, A. S. Holehouse, I. Peran, M. Farag, J. J. Incicco, A. Bremer, C. R. Grace, A. Soranno, R. V. Pappu, and T. Mittag, "Valence and patterning of aromatic residues determine the phase behavior of prion-like domains," Science **367**, 694–699 (2020).
[60]A. S. Holehouse, G. M. Ginell, D. Griffith, and E. Böke, "Clustering of aromatic residues in prion-like domains can tune the formation, state, and organization of biomolecular condensates," Biochemistry **60**, 3566–3581 (2021).
[61]S. Ranganathan, J. Liu, and E. Shakhnovich, "Different states and the associated fates of biomolecular condensates," Essays Biochem. **66**, 849–862 (2022).
[62]D. T. Murray, M. Kato, Y. Lin, K. R. Thurber, I. Hung, S. L. McKnight, and R. Tycko, "Structure of FUS protein fibrils and its relevance to self-assembly and phase separation of low-complexity domains," Cell **171**, 615–627.e16 (2017).
[63]S. Ranganathan and E. Shakhnovich, "The physics of liquid-to-solid transitions in multi-domain protein condensates," Biophys. J. **121**, 2751–2766 (2022).
[64]R. Sabate, F. Rousseau, J. Schymkowitz, and S. Ventura, "What makes a protein sequence a prion?" PLoS Comput. Biol. **11**, e1004013 (2015).
[65]E. D. Ross, A. Minton, and R. B. Wickner, "Prion domains: Sequences, structures and interactions," Nat. Cell Biol. **7**, 1039–1044 (2005).
[66]D. Willbold, B. Strodel, G. F. Schröder, W. Hoyer, and H. Heise, "Amyloid-type protein aggregation and prion-like properties of amyloids," Chem. Rev. **121**, 8285–8307 (2021).
[67]M. Saito, D. Hess, J. Eglinger, A. W. Fritsch, M. Kreysing, B. T. Weinert, C. Choudhary, and P. Matthias, "Acetylation of intrinsically disordered regions regulates phase separation," Nat. Chem. Biol. **15**, 51–61 (2019).
[68]J. Li, M. Zhang, W. Ma, B. Yang, H. Lu, F. Zhou, and L. Zhang, "Post-translational modifications in liquid-liquid phase separation: A comprehensive review," Mol. Biomed. **3**, 13 (2022).
[69]S. Huang, B. Xu, and Y. Liu, "Calcium promotes α-synuclein liquid-liquid phase separation to accelerate amyloid aggregation," Biochem. Biophys. Res. Commun. **603**, 13–20 (2022).
[70]C. Garcia-Cabau, A. Bartomeu, G. Tesei, K. C. Cheung, J. Pose-Utrilla, S. Picó, A. Balaceanu, B. Duran-Arqué, M. Fernández-Alfara, J. Martín, C. De Pace, L. Ruiz-Pérez, J. García, G. Battaglia, J. J. Lucas, R. Hervás, K. Lindorff-Larsen, R. Méndez, and X. Salvatella, "Mis-splicing of a neuronal microexon promotes CPEB4 aggregation in ASD," Nature **637**, 496 (2025).
[71]M. Kato, Y. S. Yang, B. M. Sutter, Y. Wang, S. L. McKnight, and B. P. Tu, "Redox state controls phase separation of the yeast ataxin-2 protein via reversible oxidation of its methionine-rich low-complexity domain," Cell **177**, 711–721.e8 (2019).
[72]M. P. Hughes, M. R. Sawaya, D. R. Boyer, L. Goldschmidt, J. A. Rodriguez, D. Cascio, L. Chong, T. Gonen, and D. S. Eisenberg, "Atomic structures of low-complexity protein segments reveal kinked β sheets that assemble networks," Science **359**, 698–701 (2018).
[73]M. P. Hughes, L. Goldschmidt, and D. S. Eisenberg, "Prevalence and species distribution of the low-complexity, amyloid-like, reversible, kinked segment structural motif in amyloid-like fibrils," J. Biol. Chem. **297**, 101194 (2021).
[74]S. Blazquez, I. Sanchez-Burgos, J. Ramirez, T. Higginbotham, M. M. Conde, R. Collepardo-Guevara, A. R. Tejedor, and J. R. Espinosa, "Location and concentration of aromatic-rich segments dictates the percolating inter-molecular network and viscoelastic properties of ageing condensates," Adv. Sci. **10**, 1–18 (2023).
[75]M. Kar, A. E. Posey, F. Dar, A. A. Hyman, and R. V. Pappu, "Glycine-rich peptides from FUS have an intrinsic ability to self-assemble into fibers and networked fibrils," Biochemistry **60**, 3213–3222 (2021).
[76]V. Athiyarath and K. M. Sureshan, "Spontaneous single-crystal-to-single-crystal evolution of two cross-laminated polymers," Angew. Chem., Int. Ed. **58**, 612–617 (2019).
[77]M. Radwan, J. D. Lilley, C. S. Ang, G. E. Reid, and D. M. Hatters, "Immiscible inclusion bodies formed by polyglutamine and poly(glycine-alanine) are enriched with distinct proteomes but converge in proteins that are risk factors for disease and involved in protein degradation," PLoS One **15**, e0233247 (2020).
[78]M. Á. Treviño, D. Pantoja-Uceda, M. Menéndez, M. V. Gomez, M. Mompeán, and D. V. Laurents, "The singular NMR fingerprint of a polyproline II helical bundle," J. Am. Chem. Soc. **140**, 16988–17000 (2018).
[79]M. Mompeán, B. S. McAvan, S. S. Félix, M. Treviño, J. Oroz, R. López-Sánchez, D. Pantoja-Uceda, E. J. Cabrita, A. J. Doig, and D. V. Laurents, "Glycine rich segments adopt polyproline II helices: Implications for biomolecular condensate formation," Arch. Biochem. Biophys. **704**, 108867 (2021).
[80]A. P. Lieberman, V. G. Shakkottai, and R. L. Albin, "Polyglutamine repeats in neurodegenerative diseases," Annu. Rev. Pathol. Mech. Dis. **14**, 1–27 (2019).
[81]T. R. Peskett, F. Rau, J. O'Driscoll, R. Patani, A. R. Lowe, and H. R. Saibil, "A liquid to solid phase transition underlying pathological huntingtin Exon1 aggregation," Mol. Cell **70**, 588–601.e6 (2018).
[82]J. M. Lee, K. Correia, J. Loupe, K. H. Kim, D. Barker, E. P. Hong, M. J. Chao, J. D. Long, D. Lucente, J. P. G. Vonsattel, R. M. Pinto, K. Abu Elneel, E. M. Ramos, J. Srinidhi Mysore, T. Gillis, V. C. Wheeler, M. E. MacDonald, J. F. Gusella, B. McAllister, T. Massey, C. Medway, T. C. Stone, L. Hall, L. Jones, P. Holmans, S. Kwak, A. G. Ehrhardt, C. Sampaio, M. Ciosi, A. Maxwell, A. Chatzi, D. G. Monckton, M. Orth, G. B. Landwehrmeyer, J. S. Paulsen, E. R. Dorsey, I. Shoulson, and R. H. Myers, "Cag repeat not polyglutamine length determines timing of huntington's disease onset," Cell **178**, 887–900.e14 (2019).
[83]C. Mathieu, R. V. Pappu, and J. P. Taylor, "Beyond aggregation: Pathological phase transitions in neurodegenerative disease," Science **370**, 56–60 (2020).
[84]S. Elbaum-Garfinkle, "Matter over mind: Liquid phase separation and neurodegeneration," J. Biol. Chem. **294**(18), 7160–7168 (2019).
[85]H. X. Zhou and X. Pang, "Electrostatic interactions in protein structure, folding, binding, and condensation," Chem. Rev. **118**, 1691–1741 (2018).
[86]G. Krainer, T. J. Welsh, J. A. Joseph, J. R. Espinosa, S. Wittmann, E. de Csilléry, A. Sridhar, Z. Toprakcioglu, G. Gudiškytė, M. A. Czekalska, W. E. Arter, J. Guillén-Boixet, T. M. Franzmann, S. Qamar, P. S. George-Hyslop, A. A. Hyman, R. Collepardo-Guevara, S. Alberti, and T. P. J. Knowles, "Reentrant liquid condensate phase of proteins is stabilized by hydrophobic and non-ionic interactions," Nat. Commun. **12**, 1–14 (2021).
[87]S. Boyko, X. Qi, T. Hao Chen, K. Surewicz, and W. K. Surewicz, "Liquid-liquid phase separation of tau protein: The crucial role of electrostatic interactions," J. Biol. Chem. **294**, 11054–11059 (2019).
[88]Y. Lin, Y. Fichou, A. P. Longhini, L. C. Llanes, P. Yin, G. C. Bazan, K. S. Kosik, and S. Han, "Liquid-liquid phase separation of tau driven by hydrophobic interaction facilitates fibrillization of tau," J. Mol. Biol. **433**, 166731 (2021).

[89]L. M. Jawerth, M. Ijavi, M. Ruer, S. Saha, M. Jahnel, A. A. Hyman, F. Jülicher, and E. Fischer-Friedrich, "Salt-dependent rheology and surface tension of protein condensates using optical traps," Phys. Rev. Lett. **121**, 258101 (2018).
[90]J. L. Watson, E. Seinkmane, C. T. Styles, A. Mihut, L. K. Krüger, K. E. McNally, V. J. Planelles-Herrero, M. Dudek, P. M. McCall, S. Barbiero, M. Vanden Oever, S. Y. Peak-Chew, B. T. Porebski, A. Zeng, N. M. Rzechorzek, D. C. S. Wong, A. D. Beale, A. Stangherlin, M. Riggi, J. Iwasa, J. Morf, C. Miliotis, A. Guna, A. J. Inglis, J. Brugués, R. M. Voorhees, J. E. Chambers, Q. J. Meng, J. S. O'Neill, R. S. Edgar, and E. Derivery, "Macromolecular condensation buffers intracellular water potential," Nature **623**, 842–852 (2023).
[91]B. R. Sabari, A. Dall'Agnese, A. Boija, I. A. Klein, E. L. Coffey, K. Shrinivas, B. J. Abraham, N. M. Hannett, A. V. Zamudio, J. C. Manteiga, C. H. Li, Y. E. Guo, D. S. Day, J. Schuijers, E. Vasile, S. Malik, D. Hnisz, T. I. Lee, I. I. Cisse, R. G. Roeder, P. A. Sharp, A. K. Chakraborty, and R. A. Young, "Coactivator condensation at super-enhancers links phase separation and gene control," Science **361**, eaar3958 (2018).
[92]W.-K. Cho, J.-H. Spille, M. Hecht, C. Lee, C. Li, V. Grube, and I. I. Cisse, "Mediator and RNA polymerase II clusters associate in transcription-dependent condensates," Science **361**, 412–415 (2018).
[93]S. Qamar, G. Z. Wang, S. J. Randle, F. S. Ruggeri, J. A. Varela, J. Q. Lin, E. C. Phillips, A. Miyashita, D. Williams, F. Ströhl, W. Meadows, R. Ferry, V. J. Dardov, G. G. Tartaglia, L. A. Farrer, G. S. Kaminski Schierle, C. F. Kaminski, C. E. Holt, P. E. Fraser, G. Schmitt-Ulms, D. Klenerman, T. Knowles, M. Vendruscolo, and P. St George-Hyslop, "FUS phase separation is modulated by a molecular chaperone and methylation of arginine cation-π interactions," Cell **173**, 720–734.e15 (2018).
[94]S. Kroschwald, S. Maharana, and A. Simon, "Hexanediol: A chemical probe to investigate the material properties of membrane-less compartments," Matters **5**, 1–7 (2017).
[95]R. Düster, I. H. Kaltheuner, M. Schmitz, and M. Geyer, "1,6-hexanediol, commonly used to dissolve liquid-liquid phase separated condensates, directly impairs kinase and phosphatase activities," J. Biol. Chem. **296**, 100260 (2021).
[96]Y. Itoh, S. Iida, S. Tamura, R. Nagashima, K. Shiraki, T. Goto, K. Hibino, S. Ide, and K. Maeshima, "1,6-hexanediol rapidly immobilizes and condenses chromatin in living human cells," Life Sci. Alliance **4**(4), e202001005 (2021).
[97]Y. Lin, E. Mori, M. Kato, S. Xiang, L. Wu, I. Kwon, and S. L. McKnight, "Toxic PR poly-dipeptides encoded by the C9orf72 repeat expansion target LC domain polymers," Cell **167**, 789–802.e12 (2016).
[98]J. R. Wheeler, T. Matheny, S. Jain, R. Abrisch, and R. Parker, "Distinct stages in stress granule assembly and disassembly," eLife **5**, e18413 (2016).
[99]S. Jonchhe, W. Pan, P. Pokhrel, and H. Mao, "Small molecules modulate liquid-to-solid transitions in phase-separated tau condensates," Angew. Chem., Int. Ed. **61**, 1–6 (2022).
[100]N. A. Yewdall, A. A. M. André, M. H. I. van Haren, F. H. T. Nelissen, A. Jonker, and E. Spruijt, "ATP: Mg^{2+} shapes material properties of protein-RNA condensates and their partitioning of clients," Biophys. J. **121**, 3962–3974 (2022).
[101]J. K. A. Tom, P. L. Onuchic, and A. A. Deniz, "Short polya RNA homopolymers undergo Mg^{2+}-mediated kinetically arrested condensation," J. Phys. Chem. B **126**, 9715–9725 (2022).
[102]A. Jain and R. D. Vale, "RNA phase transitions in repeat expansion disorders," Nature **546**(6), 243–247 (2017).
[103]J. M. Choi, A. A. Hyman, and R. V. Pappu, "Generalized models for bond percolation transitions of associative polymers," Phys. Rev. E **102**, 042403 (2020).
[104]Y. Zhang, A. G. T. Pyo, R. Kliegman, Y. Jiang, C. P. Brangwynne, H. A. Stone, and N. S. Wingreen, "The exchange dynamics of biomolecular condensates," eLife **12**, RP91680 (2023).
[105]J. A. Riback, L. Zhu, M. C. Ferrolino, M. Tolbert, D. M. Mitrea, D. W. Sanders, M. T. Wei, R. W. Kriwacki, and C. P. Brangwynne. "Composition-dependent thermodynamics of intracellular phase separation," Nature **581**, 209–214 (2020).
[106]S. Ambadi Thody, H. D. Clements, H. Baniasadi, A. S. Lyon, M. S. Sigman, and M. K. Rosen, "Small-molecule properties define partitioning into biomolecular condensates," Nat. Chem. **16**, 1794 (2024).
[107]S. Li, T. Yoshizawa, R. Yamazaki, A. Fujiwara, T. Kameda, and R. Kitahara, "Pressure and temperature phase diagram for liquid-liquid phase separation of the RNA-binding protein fused in sarcoma," J. Phys. Chem. B **125**, 6821–6829 (2021).
[108]M. Poudyal, K. Patel, L. Gadhe, A. S. Sawner, P. Kadu, D. Datta, S. Mukherjee, S. Ray, A. Navalkar, S. Maiti, D. Chatterjee, J. Devi, R. Bera, N. Gahlot, J. Joseph, R. Padinhateeri, and S. K. Maji, "Intermolecular interactions underlie protein/peptide phase separation irrespective of sequence and structure at crowded milieu," Nat. Commun. **14**, 12 (2023).
[109]J. A. Riback, C. D. Katanski, J. L. Kear-Scott, E. V. Pilipenko, A. E. Rojek, T. R. Sosnick, and D. A. Drummond, "Stress-triggered phase separation is an adaptive, evolutionarily tuned response," Cell **168**, 1028–1040.e19 (2017).
[110]G. L. Dignon, W. Zheng, Y. C. Kim, and J. Mittal, "Temperature-controlled liquid-liquid phase separation of disordered proteins," ACS Cent. Sci. **5**(5), 821–830 (2019).
[111]A. Miller, Z. Toprakcioglu, S. Qamar, P. St. George-Hyslop, F. S. Ruggeri, T. P. J. Knowles, and M. Vendruscolo, "Nanoscale profiling of evolving intermolecular interactions in ageing FUS condensates," BioRxiv (2023).
[112]M. Linsenmeier, L. Faltova, C. Morelli, U. Capasso Palmiero, C. Seiffert, A. M. Küffner, D. Pinotsi, J. Zhou, R. Mezzenga, and P. Arosio, "The interface of condensates of the hnRNPA1 low-complexity domain promotes formation of amyloid fibrils," Nat. Chem. **15**, 1340–1349 (2023).
[113]A. Putnam, M. Cassani, J. Smith, and G. Seydoux, "A gel phase promotes condensation of liquid *P* granules in *Caenorhabditis elegans* embryos," Nat. Struct. Mol. Biol. **26**(3), 220–226 (2019).
[114]T. J. Böddeker, K. A. Rosowski, D. Berchtold, L. Emmanouilidis, Y. Han, F. H. T. Allain, R. W. Style, L. Pelkmans, and E. R. Dufresne, "Non-specific adhesive forces between filaments and membraneless organelles," Nat. Phys. **18**, 571–578 (2022).
[115]M. R. King and S. Petry, "Phase separation of TPX2 enhances and spatially coordinates microtubule nucleation," Nat. Commun. **11**, 270 (2020).
[116]M. Krieg, J. Stühmer, J. G. Cueva, R. Fetter, K. A. Spliker, D. Cremers, K. Shen, A. R. Dunn, and M. B. Goodman, "Genetic defects in β-spectrin and tau sensitize *c. elegans* axons to movement-induced damage via torque-tension coupling," eLife **6**, e20172 (2017).
[117]S. Laha, J. Bauermann, F. Jülicher, T. C. T. Michaels, and C. A. Weber, "Chemical reactions regulated by phase-separated condensates," arXiv:2403.05228 (2024).
[118]M. Sankaranarayanan, R. J. Emenecker, E. L. Wilby, M. Jahnel, I. R. Trussina, M. Wayland, S. Alberti, A. S. Holehouse, and T. T. Weil, "Adaptable P body physical states differentially regulate *bicoid* mRNA storage during early *Drosophila* development," Dev. Cell **56**, 2886–2901 (2021).
[119]C. H. Choi, D. S. W. Lee, D. W. Sanders, and C. P. Brangwynne, "Condensate interfaces can accelerate protein aggregation," Biophys. J. **123**, 1404–1413 (2024).
[120]M. Linsenmeier, M. Hondele, F. Grigolato, E. Secchi, K. Weis, and P. Arosio, "Dynamic arrest and aging of biomolecular condensates are modulated by low-complexity domains, RNA and biochemical activity," Nat. Commun. **13**, 3030 (2022).
[121]S. Ray, N. Singh, R. Kumar, K. Patel, S. Pandey, D. Datta, J. Mahato, R. Panigrahi, A. Navalkar, S. Mehra, L. Gadhe, D. Chatterjee, A. S. Sawner, S. Maiti, S. Bhatia, J. A. Gerez, A. Chowdhury, A. Kumar, R. Padinhateeri, R. Riek, G. Krishnamoorthy, and S. K. Maji, "α-synuclein aggregation nucleates through liquid–liquid phase separation," Nat. Chem. **12**(8), 705–716 (2020).
[122]N. Galvanetto, M. T. Ivanović, A. Chowdhury, A. Sottini, M. F. Nüesch, D. Nettels, R. B. Best, and B. Schuler, "Extreme dynamics in a biomolecular condensate," Nature **619**(7), 876–883 (2023).
[123]K. Rhine, V. Vidaurre, and S. Myong, "RNA droplets," Annu. Rev. Biophys. **26**, 41 (2020).
[124]G. M. Wadsworth, S. Srinivasan, L. B. Lai, M. Datta, V. Gopalan, and P. R. Banerjee, "RNA-driven phase transitions in biomolecular condensates," Mol. Cell **84**(19), 3692–3705 (2024).
[125]S. Maharana, J. Wang, D. K. Papadopoulos, D. Richter, A. Pozniakovsky, I. Poser, M. Bickle, S. Rizk, J. Guillén-Boixet, T. M. Franzmann, M. Jahnel, L. Marrone, Y.-T. Chang, J. Sterneckert, P. Tomancak, A. A. Hyman, and S. Alberti, "RNA buffers the phase separation behavior of prion-like RNA binding proteins," Science **360**, 918–921 (2018).
[126]S. Boeynaems, A. S. Holehouse, V. Weinhardt, D. Kovacs, J. Van Lindt, C. Larabell, L. Van Den Bosch, R. Das, P. S. Tompa, R. V. Pappu, and A. D.

Gitler, "Spontaneous driving forces give rise to protein−RNA condensates with coexisting phases and complex material properties," Proc. Nat. Acad. Sci. U. S. A. **116**, 7889–7898 (2019).
[127]K. A. Rosowski, T. Sai, E. Vidal-Henriquez, D. Zwicker, R. W. Style, and E. R. Dufresne, "Elastic ripening and inhibition of liquid–liquid phase separation," Nat. Phys. **16**, 422–425 (2020).
[128]R. W. Style, T. Sai, N. Fanelli, M. Ijavi, K. Smith-Mannschott, Q. Xu, L. A. Wilen, and E. R. Dufresne, "Liquid-liquid phase separation in an elastic network," Phys. Rev. X **8**, 11028 (2018).
[129]Y. Zhang, D. S. W. Lee, Y. Meir, C. P. Brangwynne, and N. S. Wingreen, "Mechanical frustration of phase separation in the cell nucleus by chromatin," Phys. Rev. Lett. **126**, 258102 (2021).
[130]Y. Shin, Y. C. Chang, D. S. W. Lee, J. Berry, D. W. Sanders, P. Ronceray, N. S. Wingreen, M. Haataja, and C. P. Brangwynne, "Liquid nuclear condensates mechanically sense and restructure the genome," Cell **175**, 1481–1491.e13 (2018).
[131]J. Z. Zhao, J. Xia, and C. P. Brangwynne, "Chromatin compaction during confined cell migration induces and reshapes nuclear condensates," Nat. Commun. **15**, 9964 (2024).
[132]S. D'Annunzio, L. Santomaso, D. Michelatti, C. Bernardis, G. Vitali, S. Lago, C. Testi, E. Pontecorvo, A. Poli, F. Pennacchio, P. Maiuri, E. Sanchez, D. Genevieve, L. Petrolli, T. Tarenzi, R. Menichetti, R. Potestio, G. Ruocco, and A. Zippo, "Chromatin condensates tune nuclear mechano-sensing in Kabuki Syndrome by constraining cGAS activation," bioRxiv (2024).
[133]H. Cinar, Z. Fetahaj, S. Cinar, R. M. Vernon, H. S. Chan, and R. H. A. Winter, "Temperature, hydrostatic pressure, and osmolyte effects on liquid–liquid phase separation in protein condensates: Physical chemistry and biological implications," Chemistry **25**, 13049–13069 (2019).
[134]S. Jain, J. R. Wheeler, R. W. Walters, A. Agrawal, A. Barsic, and R. Parker, "ATPase-modulated stress granules contain a diverse proteome and substructure," Cell **164**, 487–498 (2016).
[135]J. Shorter, "Engineering therapeutic protein disaggregases," Mol. Biol. Cell **27**(10), 1556–1560 (2016).
[136]L. Guo, H. J. Kim, H. Wang, J. Monaghan, F. Freyermuth, J. C. Sung, K. O'Donovan, C. M. Fare, Z. Diaz, N. Singh, Z. Chao Zhang, M. Coughlin, E. A. Sweeny, M. E. DeSantis, M. E. Jackrel, C. B. Rodell, J. A. Burdick, O. D. King, A. D. Gitler, C. Lagier-Tourenne, U. B. Pandey, Y. M. Chook, J. P. Taylor, and J. Shorter, "Nuclear-import receptors reverse aberrant phase transitions of RNA-binding proteins with prion-like domains," Cell **173**, 677–692.e20 (2018).
[137]F. Wippich, B. Bodenmiller, M. G. Trajkovska, S. Wanka, R. Aebersold, and L. Pelkmans, "Dual specificity kinase DYRK3 couples stress granule condensation/dissolution to mTORC1 signaling," Cell **152**, 791–805 (2013).
[138]R. Takaki, L. Jawerth, M. Popović, and F. Jülicher, "Theory of rheology and aging of protein condensates," PRX Life **1**, 1–13 (2023).
[139]W. Pönisch, T. C. T. Michaels, and C. A. Weber, "Aggregation controlled by condensate rheology," Biophys. J. **122**, 197–214 (2023).
[140]S. R. Cohen, P. R. Banerjee, and R. V. Pappu, "Direct computations of viscoelastic moduli of biomolecular condensates," J. Chem. Phys. **161**, 095103 (2024).
[141]S. Biswas and D. A. Potoyan, "Molecular drivers of aging in biomolecular condensates: Desolvation, rigidification, and sticker lifetimes," PRX Life **2**, 23011 (2024).
[142]F. Català-Castro, S. Ortiz-Vásquez, C. Martínez-Fernández, F. Pezzano, C. Garcia-Cabau, M. Fernández-Campo, N. Sanfeliu-Cerdán, S. Jiménez-Delgado, X. Salvatella, V. Ruprecht, P.-A. Frigeri, and M. Krieg, "Measuring age-dependent viscoelasticity of organelles, cells and organisms with time-shared optical tweezer microrheology," Nat. Nanotechnol. (published online).
[143]J. O. Law, C. M. Jones, T. Stevenson, T. A. Williamson, M. S. Turner, H. Kusumaatmaja, and S. N. Grellscheid, "A bending rigidity parameter for stress granule condensates," Sci. Adv. **9**, 1–11 (2023).
[144]Y. Wang, M. Tateno, and H. Tanaka, "Distinct elastic properties and their origins in glasses and gels," Nat. Phys. **20**, 1171–1179 (2024).
[145]T. P. J. Knowles, M. Vendruscolo, and C. M. Dobson, "The amyloid state and its association with protein misfolding diseases," Nat. Rev. Mol. Cell Biol. **15**, 384–396 (2014).
[146]S. Ranganathan and E. I. Shakhnovich, "Dynamic metastable long-living droplets formed by sticker-spacer proteins," eLife **9**, 1–25 (2020).
[147]R. M. Robertson-Anderson, "Optical tweezers microrheology: From the basics to advanced techniques and applications," ACS Macro Lett. **7**, 968–975 (2018).
[148]R. N. Zia, "Active and passive microrheology: Theory and simulation," Annu. Rev. Fluid Mech. **50**, 371–405 (2018).
[149]A. Ghosh, D. Kota, and H.-X. Zhou, "Shear relaxation governs fusion dynamics of biomolecular condensates," Nat. Commun. **12**, 1–10 (2021).
[150]I. Alshareedah, M. M. Moosa, M. Pham, D. A. Potoyan, and P. R. Banerjee, "Programmable viscoelasticity in protein-RNA condensates with disordered sticker-spacer polypeptides," Nat. Commun. **12**, 1–14 (2021).
[151]A. Bonfanti, J. L. Kaplan, G. Charras, and A. Kabla, "Fractional viscoelastic models for power-law materials," Soft Matter **16**, 6002–6020 (2020).
[152]E. Evans and K. Ritchie, "Dynamic strength of molecular adhesion bonds," Biophys. J. **72**, 1541–1555 (1997).
[153]I. Eshghi, J. A. Eaton, and A. Zidovska, "Interphase chromatin undergoes a local sol-gel transition upon cell differentiation," Phys. Rev. Lett. **126**, 228101 (2021).
[154]F. Tanaka and S. F. Edwards, "Viscoelastic properties of physically crosslinked networks. 1. Transient network theory," Macromolecules **25**, 1516–1523 (1992).
[155]A. Santamaria, S. Hutin, C. M. Doucet, C. Zubieta, P. E. Milhiet, and L. Costa, "Quantifying surface tension and viscosity in biomolecular condensates by FRAP-ID," Biophys. J. **123**, 3366 (2024).
[156]P. P. Gopal, J. J. Nirschl, E. Klinman, and E. L. F. Holzbaurb, "Amyotrophic lateral sclerosis-linked mutations increase the viscosity of liquid-like TDP-43 RNP granules in neurons," Proc. Nat. Acad. Sci. U. S. A. **114**, E2466–E2475 (2017).
[157]A. Ghosh and H. X. Zhou, "Determinants for fusion speed of biomolecular droplets," Angew. Chem., Int. Ed. **59**, 20837–20840 (2020).
[158]M. Ghosh, R. Misra, S. Bhattacharya, K. Majhi, K. H. Jung, and M. Sheves, "Retinal-carotenoid interactions in a sodium-ion-pumping rhodopsin: Implications on oligomerization and thermal stability," J. Phys. Chem. B **127**, 2128–2137 (2023).
[159]F. Catala-Castro, E. Schäffer, and M. Krieg, "Exploring cell and tissue mechanics with optical tweezers," J. Cell Sci. **135**, jcs259355 (2022).
[160]C. J. Bustamante, Y. R. Chemla, S. Liu, and M. D. Wang, "Optical tweezers in single-molecule biophysics," Nat. Rev. Methods Primers **1**, 1–29 (2021).
[161]X. Wang, A. Ge, L. Hu, X. Feng, W. Du, and B. F. Liu, "A microfluidic microfilter chip driven by electrotaxis and fluid flow for size-dependent c. elegans sorting with high purity and efficiency," Sens. Actuators B **260**, 311–319 (2018).
[162]T. J. Welsh, G. Krainer, J. R. Espinosa, J. A. Joseph, A. Sridhar, M. Jahnel, W. E. Arter, K. L. Saar, S. Alberti, R. Collepardo-Guevara, and T. P. J. Knowles, "Surface electrostatics govern the emulsion stability of biomolecular condensates," Nano Lett. **22**, 612–621 (2022).
[163]E. E. Boczek, J. Fürsch, M. L. Niedermeier, L. Jawerth, M. Jahnel, M. Ruer-Gruß, K. M. Kammer, P. Heid, L. Mediani, J. Wang, X. Yan, A. Pozniakovski, I. Poser, D. Mateju, L. Hubatsch, S. Carra, S. Alberti, A. A. Hyman, and F. Stengel, "HspB8 prevents aberrant phase transitions of FUS by chaperoning its folded RNA binding domain," eLife **10**, 1–27 (2021).
[164]Z. Wang, J. Lou, and H. Zhang, "Essence determines phenomenon: Assaying the material properties of biological condensates," J. Biol. Chem. **298**, 101782 (2022).
[165]T. G. Mason and D. A. Weitz, "Optical measurements of frequency-dependent linear viscoelastic moduli of complex fluids," Phys. Rev. Lett. **74**, 1250–1253 (1995).
[166]T. Mason, "Estimating the viscoelastic moduli of complex fluids using the generalized Stokes–Einstein equation," Rheol. Acta **39**, 371–378 (2000).
[167]R. S. Fisher and A. C. Obermeyer, "Viscoelasticity of globular protein-based biomolecular condensates," Chem. Sci. **15**(47), 19795–19804 (2024).
[168]M. Delarue, G. P. Brittingham, S. Pfeffer, I. V. Surovtsev, S. Pinglay, K. J. Kennedy, M. Schaffer, J. I. Gutierrez, D. Sang, G. Poterewicz, J. K. Chung, J. M. Plitzko, J. T. Groves, C. Jacobs-Wagner, B. D. Engel, and L. J. Holt, "mTORC1 controls phase separation and the biophysical properties of the cytoplasm by tuning crowding," Cell **174**, 338–349.e20 (2018).
[169]B. S. Parmar and S. C. Weber, *Single-Molecule Tracking of RNA Polymerase In and Out of Condensates in Live Bacterial Cells* (Humana Press Inc., 2023), Vol. 2563, pp. 371–381.

[170]G. Gao, E. R. Sumrall, and N. G. Walter, "Single molecule tracking reveals nanodomains in biomolecular condensates," bioRxiv (2024).
[171]F. Gittes and C. F. Schmidt, "Interference model for back-focal-plane displacement detection in optical tweezers," Opt. Lett. **23**, 7 (1998).
[172]L. M. Jawerth, M. Ijavi, M. Ruer, S. Saha, M. Jahnel, A. A. Hyman, F. Jülicher, and E. Fischer-Friedrich, "Erratum: Salt-dependent rheology and surface tension of protein condensates using optical traps," Phys. Rev. Lett. **125**, 229901 (2020).
[173]X. Li, J. van der Gucht, P. Erni, and R. de Vries, "Active microrheology of protein condensates using colloidal probe-AFM," J. Colloid Interface Sci. **632**, 357–366 (2023).
[174]A. Farré and M. Montes-Usategui, "A force detection technique for single-beam optical traps based on direct measurement of light momentum changes," Opt. Express **18**, 11955 (2010).
[175]S. B. Smith, Y. Cui, and C. Bustamante, "Optical-trap force transducer that operates by direct measurement of light momentum," Methods Enzymol. **361**, 134–162 (2003).
[176]D. J. Müller, M. Krieg, D. Alsteens, and Y. F. Dufrêne, "New frontiers in atomic force microscopy: Analyzing interactions from single-molecules to cells," Curr. Opin. Biotechnol. **20**, 4–13 (2009).
[177]P. H. Puech, K. Poole, D. Knebel, and D. J. Muller, "A new technical approach to quantify cell-cell adhesion forces by AFM," Ultramicroscopy **106**, 637–644 (2006).
[178]M. Krieg, G. Fläschner, D. Alsteens, B. M. Gaub, W. H. Roos, G. J. L. Wuite, H. E. Gaub, C. Gerber, Y. F. Dufrêne, and D. J. Müller, "Atomic force microscopy-based mechanobiology," Nat. Rev. Phys. **1**, 41–57 (2018).
[179]B. Yang, Z. Liu, H. Liu, and M. A. Nash, "Next generation methods for single-molecule force spectroscopy on polyproteins and receptor-ligand complexes," Front. Mol. Biosci. **7**, 1–19 (2020).
[180]J. Wang, J. Jiang, X. Yang, G. Zhou, L. Wang, and B. Xiao, "Tethering piezo channels to the actin cytoskeleton for mechanogating via the cadherin-β-catenin mechanotransduction complex," Cell Rep. **38**, 110342 (2022).
[181]W. C. Young and R. G. Budynas, *Roark's Formulas for Stress and Strain*, 7th ed. (McGraw-Hill, 2002), Vol. 7.
[182]E. K. Dimitriadis, F. Horkay, J. Maresca, B. Kachar, and R. S. Chadwick, "Determination of elastic moduli of thin layers of soft material using the atomic force microscope," Biophys. J. **82**, 2798–2810 (2002).
[183]M. Zeng, X. Chen, D. Guan, J. Xu, H. Wu, P. Tong, and M. Zhang, "Reconstituted postsynaptic density as a molecular platform for understanding synapse formation and plasticity," Cell **174**, 1172–1187.e16 (2018).
[184]E. Spruijt, J. Sprakel, M. A. Cohen Stuart, and J. Van Der Gucht, "Interfacial tension between a complex coacervate phase and its coexisting aqueous phase," Soft Matter **6**, 172–178 (2010).
[185]A. Naghilou, O. Armbruster, and A. Mashaghi, "Scanning probe microscopy elucidates gelation and rejuvenation of biomolecular condensates," Cell Rep. Phys. Sci. **6**(2), 102430 (2025).
[186]J. Adamcik and R. Mezzenga, "Study of amyloid fibrils via atomic force microscopy," Curr. Opin. Colloid Interface Sci. **17**(6), 369–376 (2012).
[187]S. Wegmann, I. D. Medalsy, E. Mandelkow, and D. J. Müller, "The fuzzy coat of pathological human tau fibrils is a two-layered polyelectrolyte brush," Proc. Nat. Acad. Sci. U. S. A. **110**, E313–E321 (2013).
[188]R. M. Hochmuth, "Micropipette aspiration of living cells," J. Biomech. **33**, 15–22 (2000).
[189]H. Wang, F. M. Kelley, D. Milovanovic, B. S. Schuster, and Z. Shi, "Surface tension and viscosity of protein condensates quantified by micropipette aspiration," Biophys. Rep. **1**, 100011 (2021).
[190]J. V. Roggeveen, H. Wang, Z. Shi, and H. A. Stone, "A calibration-free model of micropipette aspiration for measuring properties of protein condensates," Biophys. J. **123**, 1393–1403 (2024).
[191]I. Tunn, G. Beaune, J. Tersteegen, T. Välisalmi, J. V. I. Timonen, F. Brochard-Wyart, and M. B. Linder, "Bursting of condensates," Commun. Phys. **7**, 1–13 (2024).
[192]H. Wang, C. Hoffmann, J. V. Tromm, X. Su, J. Elliott, H. Wang, J. Baum, Z. P. Pang, D. Milovanovic, and Z. Shi, "Live-cell quantification reveals viscoelastic regulation of synapsin condensates by α-synuclein," (preprint).
[193]S. Landiech, M. Elias, P. Lapèze, H. Ajiyel, M. Plancke, B. González-Bermúdez, A. Laborde, F. Mesnilgrente, D. Bourrier, D. Berti, C. Montis, L. Mazenq, J. Baldo, C. Roux, M. Delarue, and P. Joseph, "Parallel on-chip micropipettes enabling quantitative multiplexed characterization of vesicle mechanics and cell aggregates rheology," APL Bioeng. **8**, 026122 (2024).
[194]R. Prevedel, A. Diz-Muñoz, G. Ruocco, and G. Antonacci, "Brillouin microscopy: An emerging tool for mechanobiology," Nat. Methods **16**, 969–977 (2019).
[195]G. Antonacci, T. Beck, A. Bilenca, J. Czarske, K. Elsayad, J. Guck, K. Kim, B. Krug, F. Palombo, R. Prevedel, and G. Scarcelli, "Recent progress and current opinions in brillouin microscopy for life science applications," Biophys. Rev. **12**, 615–624 (2020).
[196]T. Beck, L.-M. van der Linden, W. M. Borcherds, K. Kim, R. Schlüßler, P. Müller, T. M. Franzmann, C. Möckel, R. Goswami, M. Leaver, T. Mittag, S. Alberti, and J. Guck, "Optical characterization of molecular interaction strength in protein condensates," Mol. Biol. Cell **35**(12), ar154 (2024).
[197]R. Schlüßler, K. Kim, M. Nötzel, A. Taubenberger, S. Abuhattum, T. Beck, P. Müller, S. Maharana, G. Cojoc, S. Girardo, A. Hermann, S. Alberti, and J. Guck, "Correlative all-optical quantification of mass density and mechanics of sub-cellular compartments with fluorescence specificity," eLife **11**, e68490 (2022).
[198]G. Antonacci, V. de Turris, A. Rosa, and G. Ruocco, "Background-deflection brillouin microscopy reveals altered biomechanics of intracellular stress granules by ALS protein FUS," Commun. Biol. **1**, 139 (2018).
[199]G. Scarcelli, W. J. Polacheck, H. T. Nia, K. Patel, A. J. Grodzinsky, R. D. Kamm, and S. H. Yun, "Noncontact three-dimensional mapping of intracellular hydromechanical properties by brillouin microscopy," Nat. Methods **12**, 1132–1134 (2015).
[200]C. Bevilacqua, J. M. Gomez, U. M. Fiuza, C. J. Chan, L. Wang, S. Hambura, M. Eguren, J. Ellenberg, A. Diz-Muñoz, M. Leptin, and R. Prevedel, "High-resolution line-scan brillouin microscopy for live imaging of mechanical properties during embryo development," Nat. Methods **20**, 755–760 (2023).
[201]F. Yang, C. Bevilacqua, S. Hambura, A. Neves, A. Gopalan, K. Watanabe, M. Govendir, M. Bernabeu, J. Ellenberg, A. Diz-Muñoz, S. Köhler, G. Rapti, M. Jechlinger, and R. Prevedel, "Pulsed stimulated brillouin microscopy enables high-sensitivity mechanical imaging of live and fragile biological specimens," Nat. Methods **20**, 1971–1979 (2023).
[202]P. H. Wu, D. R. B. Aroush, A. Asnacios, W. C. Chen, M. E. Dokukin, B. L. Doss, P. Durand-Smet, A. Ekpenyong, J. Guck, N. V. Guz, P. A. Janmey, J. S. H. Lee, N. M. Moore, A. Ott, Y. C. Poh, R. Ros, M. Sander, I. Sokolov, J. R. Staunton, N. Wang, G. Whyte, and D. Wirtz, "A comparison of methods to assess cell mechanical properties," Nat. Methods **15**, 491–498 (2018).
[203]P. J. Wu, I. V. Kabakova, J. W. Ruberti, J. M. Sherwood, I. E. Dunlop, C. Paterson, P. Török, and D. R. Overby, "Water content, not stiffness, dominates brillouin spectroscopy measurements in hydrated materials," Nat. Methods **15**, 561–562 (2018).
[204]M. Mittasch, P. Gross, M. Nestler, A. W. Fritsch, C. Iserman, M. Kar, M. Munder, A. Voigt, S. Alberti, S. W. Grill, and M. Kreysing, "Non-invasive perturbations of intracellular flow reveal physical principles of cell organization," Nat. Cell Biol. **20**, 344–351 (2018).
[205]M. Mittasch, V. M. Tran, M. U. Rios, A. W. Fritsch, S. J. Enos, B. Ferreira Gomes, A. Bond, M. Kreysing, and J. B. Woodruff, "Regulated changes in material properties underlie centrosome disassembly during mitotic exit," J. Cell Biol. **219**, e201912036 (2020).
[206]B. Seelbinder, S. Wagner, M. Jain, E. Erben, S. Klykov, I. D. Stoev, V. R. Krishnaswamy, and M. Kreysing, "Probe-free optical chromatin deformation and measurement of differential mechanical properties in the nucleus," eLife **13**, e76421 (2024).
[207]N. O. Taylor, M. T. Wei, H. A. Stone, and C. P. Brangwynne, "Quantifying dynamics in phase-separated condensates using fluorescence recovery after photobleaching," Biophys. J. **117**, 1285–1300 (2019).
[208]F. Muzzopappa, J. Hummert, M. Anfossi, S. A. Tashev, D. P. Herten, and F. Erdel, "Detecting and quantifying liquid–liquid phase separation in living cells by model-free calibrated half-bleaching," Nat. Commun. **13**, 7787 (2022).
[209]W. Stroberg and S. Schnell, "Do cellular condensates accelerate biochemical reactions? Lessons from microdroplet chemistry," Biophys. J. **115**, 3–8 (2018).
[210]A. Abyzov, M. Blackledge, and M. Zweckstetter, "Conformational dynamics of intrinsically disordered proteins regulate biomolecular condensate chemistry," Chem. Rev. **122**(6), 6719–6748 (2022).

[211]E. Boke, M. Ruer, M. Wühr, M. Coughlin, R. Lemaitre, S. P. Gygi, S. Alberti, D. Drechsel, A. A. Hyman, and T. J. Mitchison, "Amyloid-like self-assembly of a cellular compartment," Cell **166**, 637–650 (2016).
[212]X. Chen, X. Wu, H. Wu, and M. Zhang, "Phase separation at the synapse," Nat. Neurosci. **23**, 301–310 (2020).
[213]N. A. McDonald, R. D. Fetter, and K. Shen, "Assembly of synaptic active zones requires phase separation of scaffold molecules," Nature **588**, 454–458 (2020).
[214]B. Belardi, T. Hamkins-Indik, A. R. Harris, J. Kim, K. Xu, and D. A. Fletcher, "A weak link with actin organizes tight junctions to control epithelial permeability," Dev. Cell **54**, 792–804.e7 (2020).
[215]M. Zeng, Y. Shang, Y. Araki, T. Guo, R. L. Huganir, and M. Zhang, "Phase transition in postsynaptic densities underlies formation of synaptic complexes and synaptic plasticity," Cell **166**, 1163–1175.e12 (2016).
[216]S. Zhu, Z. Shen, X. Wu, W. Han, B. Jia, W. Lu, and M. Zhang, "Demixing is a default process for biological condensates formed via phase separation," Science **384**, 920 (2024).
[217]S. Siechen, S. Yang, A. Chiba, and T. Saif, "Mechanical tension contributes to clustering of neurotransmitter vesicles at presynaptic terminals," Proc. Natl. Acad. Sci. U. S. A. **106**, 12611–12616 (2009).
[218]E. Bloch-Gallego, "Mechanisms controlling neuromuscular junction stability," Cell. Mol. Life Sci. **72**, 1029–1043 (2015).
[219]D. Kilinc, "The emerging role of mechanics in synapse formation and plasticity," Front. Cell. Neurosci. **12**, 1–9 (2018).
[220]K. Ashami, A. S. Falk, C. Hurd, S. Garg, S. A. Cervantes, A. Rawat, and A. B. Siemer, "Droplet and fibril formation of the functional amyloid Orb2," J. Biol. Chem. **297**(1), 100804–100807 (2021).
[221]R. Hervas, M. J. Rau, Y. Park, W. Zhang, A. G. Murzin, J. A. J. Fitzpatrick, S. H. W. Scheres, and K. Si, "Cryo-EM structure of a neuronal functional amyloid implicated in memory persistence in drosophila," Science **367**, 1230 (2020).
[222]R. Das, L. C. Lin, F. Català-Castro, N. Malaiwong, N. Sanfeliu-Cerdán, M. Porta-De la Riva, A. Pidde, and M. Krieg, "An asymmetric mechanical code ciphers curvature-dependent proprioceptor activity," Sci. Adv. **7**, 1–20 (2021).
[223]K. Graham, A. Chandrasekaran, L. Wang, A. Ladak, E. M. Lafer, P. Rangamani, and J. C. Stachowiak, "Liquid-like VASP condensates drive actin polymerization and dynamic bundling," Nat. Phys. **19**(4), 574–585 (2023).
[224]T. Wiegand, J. Liu, L. Vogeley, I. LuValle-Burke, J. Geisler, A. W. Fritsch, A. A. Hyman, S. W. Grill, and D. Weitz, "Actin polymerization counteracts prewetting of N-WASP on supported lipid bilayers," Proc. Natl. Acad. Sci. **121**, e2407497121 (2024).
[225]C. Lee-Eom, J. Jung, C. Park, and M. J. Shon, "Structuring role of tau-tubulin co-condensates in early microtubule organization," bioRxiv (2024).
[226]V. A. Volkov and A. Akhmanova, "Phase separation on microtubules: From droplet formation to cellular function?" Trends Cell Biol. **34**(1), 18–30 (2024).
[227]D. a Fletcher and R. D. Mullins, "Cell mechanics and the cytoskeleton," Nature **463**, 485–492 (2010).
[228]M. J. Footer, J. W. J. Kerssemakers, J. A. Theriot, and M. Dogterom, "Direct measurement of force generation by actin filament polymerization using an optical trap," Proc. Natl. Acad. Sci. **107**, 2181–2186 (2007).
[229]S. Mohapatra and S. Wegmann, "Biomolecular condensation involving the cytoskeleton," Brain Res. Bull. **194**, 105–117 (2023).
[230]L. B. Case, X. Zhang, J. A. Ditlev, and M. K. Rosen, "Stoichiometry controls activity of phase separated clusters of actin signaling proteins," Science **363**, 1093–1097 (2019).
[231]X. Su, J. A. Ditlev, E. Hui, W. Xing, and S. Banjade, "Phase separation of signaling molecules promotes T cell receptor signal transduction," Science **352**, 595–599 (2016).
[232]C. Walker, A. Chandrasekaran, D. Mansour, K. Graham, A. Torres, L. Wang, E. M. Lafer, P. Rangamani, and J. C. Stachowiak, "Liquid-like condensates that bind actin drive filament polymerization and bundling," bioRxiv (2024).
[233]N. P. Boyer, R. Sharma, T. Wiesner, A. Delamare, F. Pelletier, C. Leterrier, and S. Roy, "Spectrin condensates provide a nidus for assembling the periodic axonal structure," bioRxiv (2024).
[234]A. Ghisleni, C. Galli, P. Monzo, F. Ascione, M. A. Fardin, G. Scita, Q. Li, P. Maiuri, and N. C. Gauthier, "Complementary mesoscale dynamics of spectrin and acto-myosin shape membrane territories during mechanoresponse," Nat. Commun. **11**, 5108 (2020).
[235]N. Malaiwong, A.-K. Dahse, L.-C. Lin, R. Das, M. P. de-la Riva, N. Scholz, and M. Krieg, "Mechanical load conditions the spectrin network to 'runon' proteolysis and promotes early onset neurodegeneration," bioRxiv (2024).
[236]A. Hernández-Vega, M. Braun, L. Scharrel, M. Jahnel, S. Wegmann, B. T. Hyman, S. Alberti, S. Diez, and A. A. Hyman, "Local nucleation of microtubule bundles through tubulin concentration into a condensed tau phase," Cell Rep. **20**, 2304–2312 (2017).
[237]J. Miesch, R. T. Wimbish, M. C. Velluz, and C. Aumeier, "Phase separation of +TIP networks regulates microtubule dynamics," Proc. Nat. Acad. Sci. U. S. A. **120**, e2301457120 (2023).
[238]X. Song, F. Yang, T. Yang, Y. Wang, M. Ding, L. Li, P. Xu, S. Liu, M. Dai, C. Chi, S. Xiang, C. Xu, D. Li, Z. Wang, L. Li, D. L. Hill, C. Fu, K. Yuan, P. Li, J. Zang, Z. Hou, K. Jiang, Y. Shi, X. Liu, and X. Yao, "Phase separation of EB1 guides microtubule plus-end dynamics," Nat. Cell Biol. **25**(1), 79–91 (2023).
[239]A. Cochard, A. Safieddine, P. Combe, M. Benassy, D. Weil, and Z. Gueroui, "Condensate functionalization with microtubule motors directs their nucleation in space and allows manipulating RNA localization," EMBO J. **42**, 10 (2023).
[240]R. Ravindran and S. W. Michnick, "Biomolecular condensates as drivers of membrane trafficking and remodelling," Curr. Opin. Cell Biol. **89**, 102393 (2024).
[241]T. Quail, S. Golfier, M. Elsner, K. Ishihara, V. Murugesan, R. Renger, F. Jülicher, and J. Brugués, "Force generation by protein–DNA co-condensation," Nat. Phys. **17**, 1007–1012 (2021).
[242]A. Fasciani, S. D'Annunzio, V. Poli, L. Fagnocchi, S. Beyes, D. Michelatti, F. Corazza, L. Antonelli, F. Gregoretti, G. Oliva, R. Belli, D. Peroni, E. Domenici, S. Zambrano, D. Intartaglia, C. Settembre, I. Conte, C. Testi, P. Vergyris, G. Ruocco, and A. Zippo, "MLL4-associated condensates counterbalance polycomb-mediated nuclear mechanical stress in Kabuki syndrome," Nat. Genet. **52**, 1397–1411 (2020).
[243]S. Mondal and T. Baumgart, "Membrane reshaping by protein condensates," Biochim. Biophys. Acta - Biomembr. **1865**, 184121 (2023).
[244]H. Kusumaatmaja, A. I. May, and R. L. Knorr, "Intracellular wetting mediates contacts between liquid compartments and membrane-bound organelles," J. Cell Biol. **220**, 1–10 (2021).
[245]Y. Wang, S. Li, M. Mokbel, A. I. May, Z. Liang, Y. Zeng, W. Wang, H. Zhang, F. Yu, K. Sporbeck, L. Jiang, S. Aland, J. Agudo-Canalejo, R. L. Knorr, and X. Fang, "Biomolecular condensates mediate bending and scission of endosome membranes," Nature **634**, 1204 (2024).
[246]J. Hochmair, C. Exner, M. Franck, A. Dominguez-Baquero, L. Diez, H. Brognaro, M. L. Kraushar, T. Mielke, H. Radbruch, S. Kaniyappan, S. Falke, E. Mandelkow, C. Betzel, and S. Wegmann, "Molecular crowding and RNA synergize to promote phase separation, microtubule interaction, and seeding of tau condensates," EMBO J. **41**, 1–28 (2022).
[247]N. Chappidi, T. Quail, S. Doll, L. T. Vogel, R. Aleksandrov, S. Felekyan, R. Kühnemuth, S. Stoynov, C. A. M. Seidel, J. Brugués, M. Jahnel, T. M. Franzmann, and S. Alberti, "PARP1-DNA co-condensation drives DNA repair site assembly to prevent disjunction of broken DNA ends," Cell **187**, 945–961.e18 (2024).
[248]J. M. Anderson and C. M. Van Itallie, "Physiology and function of the tight junction," Cold Spring Harbor Perspect. Biol. **1**, a002584 (2009).
[249]N. Kinoshita, T. S. Yamamoto, N. Yasue, C. Takagi, T. Fujimori, and N. Ueno, "Force-dependent remodeling of cytoplasmic ZO-1 condensates contributes to cell-cell adhesion through enhancing tight junctions," iScience **25**, 103846 (2022).
[250]K. Pombo-García, O. Adame-Arana, C. Martin-Lemaitre, F. Jülicher, and A. Honigmann, "Membrane prewetting by condensates promotes tight-junction belt formation," Nature **632**(8), 647–655 (2024).
[251]D. Spadaro, S. Le, T. Laroche, I. Mean, L. Jond, J. Yan, and S. Citi, "Tension-dependent stretching activates ZO-1 to control the junctional localization of its interactors," Curr. Biol. **27**, 3783–3795.e8 (2017).
[252]M. Mukenhirn, C. H. Wang, T. Guyomar, M. J. Bovyn, M. F. Staddon, R. E. van der Veen, R. Maraspini, L. Lu, C. Martin-Lemaitre, M. Sano, M. Lehmann, T. Hiraiwa, D. Riveline, and A. Honigmann, "Tight junctions control lumen morphology via hydrostatic pressure and junctional tension," Dev. Cell **59**, 2866–2881.e8 (2024).

[253]T. Laos, G. Cabral, and A. Dammermann, "Isotropic incorporation of SPD-5 underlies centrosome assembly in *C. elegans*," Curr. Biol. **25**, R648–R649 (2015).
[254]J. B. Woodruff, "Assembly of mitotic structures through phase separation," J. Mol. Biol. **430**, 4762–4772 (2018).
[255]S. Hurst, B. E. Vos, M. Brandt, and T. Betz, "Intracellular softening and increased viscoelastic fluidity during division," Nat. Phys. **17**, 1270–1276 (2021).
[256]G. Soggia, Y. ElMaghloob, A.-K. Boromangnaeva, and A. Al Jord, "Mechanical remodeling of nuclear biomolecular condensates," Physiology **40**, 102 (2025).
[257]Y. Kalukula, A. D. Stephens, J. Lammerding, and S. Gabriele, "Mechanics and functional consequences of nuclear deformations," Nat. Rev. Mol. Cell Biol. **23**, 583–602 (2022).
[258]A. R. Strom and C. P. Brangwynne, "The liquid nucleome – phase transitions in the nucleus at a glance," J. Cell Sci. **132**, 1–7 (2019).
[259]V. E. Hoskins, K. Smith, and K. L. Reddy, "The shifting shape of genomes: Dynamics of heterochromatin interactions at the nuclear lamina," Curr. Opin. Genet. Dev. **67**, 163–173 (2021).
[260]M. M. Nava, Y. A. Miroshnikova, L. C. Biggs, D. B. Whitefield, F. Metge, J. Boucas, H. Vihinen, E. Jokitalo, X. Li, J. Manuel García Arcos, B. Hoffmann, R. Merkel, C. M. Niessen, K. N. Dahl, and S. A. Wickström, "Heterochromatin-driven nuclear softening protects the genome against mechanical stress-induced damage," Cell **181**, 800–817.e22 (2020).
[261]M. M. Keenen, D. Brown, L. D. Brennan, R. Renger, H. Khoo, C. R. Carlson, B. Huang, S. W. Grill, G. J. Narlikar, and S. Redding, "HP1 proteins compact dna into mechanically and positionally stable phase separated domains," eLife **10**, 1–38 (2021).
[262]S. Sanulli, M. J. Trnka, V. Dharmarajan, R. W. Tibble, B. D. Pascal, A. L. Burlingame, P. R. Griffin, J. D. Gross, and G. J. Narlikar, "HP1 reshapes nucleosome core to promote phase separation of heterochromatin," Nature **575**, 390–394 (2019).
[263]A. L. Turner, M. Watson, O. G. Wilkins, L. Cato, A. Travers, J. O. Thomas, and K. Stott, "Highly disordered histone H1-DNA model complexes and their condensates," Proc. Natl. Acad. Sci. U. S. A. **115**, 11964–11969 (2018).
[264]B. A. Gibson, L. K. Doolittle, M. W. G. Schneider, L. E. Jensen, N. Gamarra, L. Henry, D. W. Gerlich, S. Redding, and M. K. Rosen, "Organization of chromatin by intrinsic and regulated phase separation," Cell **179**, 470–484.e21 (2019).
[265]K. Maeshima, S. Tamura, and Y. Shimamoto, "Chromatin as a nuclear spring," Biophysics **15**, 189–195 (2018).
[266]A. D. Stephens, P. Z. Liu, V. Kandula, H. Chen, L. M. Almassalha, C. Herman, V. Backman, T. O'Halloran, S. A. Adam, R. D. Goldman, E. J. Banigan, and J. F. Marko, "Physicochemical mechanotransduction alters nuclear shape and mechanics via heterochromatin formation," Mol. Biol. Cell **30**, 2320–2330 (2019).
[267]J. F. Williams, I. V. Surovtsev, S. M. Schreiner, Z. Chen, G. Raiymbek, H. Nguyen, Y. Hu, J. S. Biteen, S. G. J. Mochrie, K. Ragunathan, and M. C. King, "The condensation of HP1α/Swi6 imparts nuclear stiffness," Cell Rep. **43**(7), 114373 (2024).
[268]V. Todorovski, A. H. Fox, and Y. S. Choi, "Matrix stiffness-sensitive long noncoding RNA NEAT1 seeded paraspeckles in cancer cells," Mol. Biol. Cell **31**, 1654–1662 (2020).
[269]C. Liu, X. Gao, Y. Li, W. Sun, Y. Xu, Y. Tan, R. Du, G. Zhong, D. Zhao, Z. Liu, X. Jin, Y. Zhao, Y. Wang, X. Yuan, J. Pan, G. Yuan, Y. Li, W. Xing, G. Kan, Y. Wang, Q. Li, X. Han, J. Li, S. Ling, and Y. Li, "The mechanosensitive lncRNA *Neat1* promotes osteoblast function through paraspeckle-dependent *Smurf1* mRNA retention," Bone Res. **10**, 12 (2022).
[270]V. Todorovski, F. McCluggage, Y. Li, A. Meid, J. P. Spatz, A. W. Holle, A. H. Fox, and Y. S. Choi, "Confined environments induce polarized paraspeckle condensates," Commun. Biol. **6**, 12 (2023).
[271]Y. C. Poh, S. P. Shevtsov, F. Chowdhury, D. C. Wu, S. Na, M. Dundr, and N. Wang, "Dynamic force-induced direct dissociation of protein complexes in a nuclear body in living cells," Nat. Commun. **3**, 866 (2012).
[272]X. Liang, C. Calovich-Benne, and A. Norris, "Sensory neuron transcriptomes reveal complex neuron-specific function and regulation of *mec*-2/stomatin splicing," Nucl. Acids Res. **50**, 2401–2416 (2022).
[273]D. Sun, X. Zhao, T. Wiegand, C. Martin-Lemaitre, T. Borianne, L. Kleinschmidt, S. W. Grill, A. A. Hyman, C. Weber, and A. Honigmann, "Assembly of tight junction belts by ZO1 surface condensation and local actin polymerization," Dev. Cell (published online).
[274]N. Kourtis and N. Tavernarakis, "Mechanosensory transduction in the nematode Caenorhabditis elegans," in *Mechanosensitive Ion Channels* (Springer, 2008), pp. 117–145.
[275]A. L. Eastwood, A. Sanzeni, B. C. Petzold, S. J. Park, B. L. Pruitt, and M. B. Goodman, "Tissue mechanics govern the rapidly adapting and symmetrical response to touch," Proc. Natl. Acad. Sci. U. S. A. **112**, E2471–E2471 (2015).
[276]A. L. Nekimken, H. Fehlauer, A. A. Kim, S. N. Manosalvas-Kjono, P. Ladpli, F. Memon, D. Gopisetty, V. Sanchez, M. B. Goodman, B. L. Pruitt, and M. Krieg, "Pneumatic stimulation of *c. elegans* mechanoreceptor neurons in a microfluidic trap," Lab Chip **17**, 1116–1127 (2017).
[277]K. Poole, M. Moroni, and G. R. Lewin, "Sensory mechanotransduction at membrane-matrix interfaces," Pflugers Arch. - Eur. J. Physiol. **467**, 121–112 (2015).
[278]Y. Qi, L. Andolfi, F. Frattini, F. Mayer, M. Lazzarino, and J. Hu, "Membrane stiffening by STOML3 facilitates mechanosensation in sensory neurons," Nat. Commun. **6**, 8512 (2015).
[279]C. Verkest, I. Schaefer, T. A. Nees, N. Wang, J. M. Jegelka, F. J. Taberner, and S. G. Lechner, "Intrinsically disordered intracellular domains control key features of the mechanically-gated ion channel PIEZO2," Nat. Commun. **13**, 1365 (2022).
[280]F. J. Taberner, V. Prato, I. Schaefer, K. Schrenk-Siemens, P. A. Heppenstall, and S. G. Lechner, "Structure-guided examination of the mechanogating mechanism of PIEZO2," Proc. Nat. Acad. Sci. U. S. A. **116**, 14260–14269 (2019).
[281]P. E. A. Ash, S. Lei, J. Shattuck, S. Boudeau, Y. Carlomagno, M. Medalla, B. L. Mashimo, G. Socorro, L. F. A. Al-Mohanna, L. Jiang, M. M. Öztürk, M. Knobel, P. Ivanov, L. Petrucelli, S. Wegmann, N. M. Kanaan, and B. Wolozin, "TIA1 potentiates tau phase separation and promotes generation of toxic oligomeric tau," Proc. Nat. Acad. Sci. U. S. A. **118**, 1–12 (2021).
[282]B. T. Hurtle, L. Xie, and C. J. Donnelly, "Disrupting pathologic phase transitions in neurodegeneration," J. Clin. Invest. **133**, e168549 (2023).
[283]T. O. Vogler, J. R. Wheeler, E. D. Nguyen, M. P. Hughes, K. A. Britson, E. Lester, B. Rao, N. D. Betta, O. N. Whitney, T. E. Ewachiw, E. Gomes, J. Shorter, T. E. Lloyd, D. S. Eisenberg, J. P. Taylor, A. M. Johnson, B. B. Olwin, and R. Parker, "TDP-43 and RNA form amyloid-like myo-granules in regenerating muscle," Nature **563**, 508–513 (2018).
[284]C. Wetzel, S. Pifferi, C. Picci, C. Gök, D. Hoffmann, K. K. Bali, A. Lampe, L. Lapatsina, R. Fleischer, E. S. J. Smith, V. Bégay, M. Moroni, L. Estebanez, J. Kühnemund, J. Walcher, E. Specker, M. Neuenschwander, J. P. Von Kries, V. Haucke, R. Kuner, J. F. A. Poulet, J. Schmoranzer, K. Poole, and G. R. Lewin, "Small-molecule inhibition of STOML3 oligomerization reverses pathological mechanical hypersensitivity," Nat. Neurosci. **20**(2), 209–218 (2017).
[285]Z. Wang, D. Chen, D. Guan, X. Liang, J. Xue, H. Zhao, G. Song, J. Lou, Y. He, and H. Zhang, "Material properties of phase-separated TFEB condensates regulate the autophagy-lysosome pathway," J. Cell Biol. **221**(5), e202112024 (2022).
[286]D. Bracha, M. T. Walls, and C. P. Brangwynne, "Probing and engineering liquid-phase organelles," Nat. Biotechnol. **37**, 1435–1445 (2019).
[287]K. M. Ruff, S. Roberts, A. Chilkoti, and R. V. Pappu, "Advances in understanding stimulus-responsive phase behavior of intrinsically disordered protein polymers," J. Mol. Biol. **430**, 4619–4635 (2018).
[288]V. S. Doan, I. Alshareedah, A. Singh, P. R. Banerjee, and S. Shin, "Diffusiophoresis promotes phase separation and transport of biomolecular condensates," Nat. Commun. **15**, 7686 (2024).
[289]J. Risso-Ballester, M. Galloux, J. Cao, R. Le Goffic, F. Hontonnou, A. Jobart-Malfait, A. Desquesnes, S. M. Sake, S. Haid, M. Du, X. Zhang, H. Zhang, Z. Wang, V. Rincheval, Y. Zhang, T. Pietschmann, J. F. Eléouët, M. A. Rameix-Welti, and R. Altmeyer, "A condensate-hardening drug blocks RSV replication in vivo," Nature **595**, 596–599 (2021).
[290]A. Boija, I. A. Klein, and R. A. Young, "Biomolecular condensates and cancer," Cancer Cell **39**, 174–192 (2021).
[291]M. Biesaga, M. Frigolé-Vivas, and X. Salvatella, "Intrinsically disordered proteins and biomolecular condensates as drug targets," Curr. Opin. Chem. Biol. **62**, 90–100 (2021).
[292]A. K. Lancaster, A. Nutter-Upham, S. Lindquist, and O. D. King, "PLAAC: A web and command-line application to identify proteins with prion-like amino acid composition," Bioinformatics **30**, 2501–2502 (2014).